

THESIS
2
2002

This is to certify that the
dissertation entitled
**The Gonadotropin Releasing Hormone (GnRH) system
in Male Syrian Hamsters (Mesocricetus Auratus):
Organization and Regulation**

presented by
Heather N. Richardson

has been accepted towards fulfillment
of the requirements for

Ph.D. degree in Neuroscience and Psychology

Cheryl J. Sisk
Major professor

Date 3/21/02

**THE GONADOTROPIN RELEASING HORMONE (GnRH) SYSTEM
IN MALE SYRIAN HAMSTERS (MESOCRICETUS AURATUS):
ORGANIZATION AND REGULATION**

By

Heather N. Richardson

A DISSERTATION

**Submitted to
Michigan State University
in partial fulfilment of the requirements
for the degree of**

DOCTOR OF PHILOSOPHY

Department of Psychology-Neuroscience Program

2002

ABSTRACT
THE GONADOTROPIN RELEASING HORMONE (GnRH) SYSTEM
IN MALE SYRIAN HAMSTERS (MESOCRICETUS AURATUS):
ORGANIZATION AND REGULATION

By
Heather N. Richardson

Neurons that synthesize and secrete the decapeptide gonadotropin releasing hormone (GnRH) are the highest order of the hypothalamic pituitary gonadal (HPG) axis, and thus, govern the entire reproductive system. Many internal (e.g., steroid hormones) and external (e.g., chemosensory cues) factors influence GnRH neuronal activity, but mechanisms underlying regulation of these cells remain elusive. GnRH neurons exist as anatomically distinct subpopulations of cells in (rostral to caudal forebrain) tenia tecta, medial septum (MS), diagonal band of Broca/organum vasculosum of the lamina terminalis (DBB/OVLT), and caudal preoptic area (cPOA). The experiments of this dissertation confirmed that a robust developmental event (puberty), an internal hormonal stimulus (testosterone), and an external sensory stimulus (female pheromones) in male Syrian hamsters all affect GnRH neurons in a brain region-dependent manner.

The most rostral cell groups were robustly affected by puberty and testosterone. These same cells groups also had a higher proportion of close appositions from GnRH fibers, suggesting more

abundant GnRH-GnRH communication within these cell groups. The most caudal cells (cPOA) may be important for generating the neuroendocrine response to female chemosensory cues, as this is the brain area that has the highest proportion of close appositions from fibers of the medial amygdala, a chemoensory processing nucleus.

In summary, there is heterogeneity within the GnRH system. GnRH cell populations respond to puberty and to internal and external stimuli differently depending on where they reside in the brain. Communication within the GnRH system and between non-GnRH and GnRH neurons also varies with brain region. Future work determining the types of connections within the GnRH system (synaptic or non-synaptic), the phenotype of neuronal or non-neuronal cells projecting to the GnRH system, and changes in receptor expression within these different GnRH subpopulations would advance understanding of how these variables are integrated by GnRH system to impact reproduction.

**This dissertation is dedicated to my parents
and to Samuel, for all of your love and support**

ACKNOWLEDGMENTS

It has been a privilege to work with the staff, students, and faculty at Michigan State University. I especially thank my graduate advisor and mentor, Dr. Cheryl Sisk. I thank you for challenging me and inspiring me to succeed. Your professional advice, guidance, and support have been invaluable to my career in science. Many thanks to my committee members, Drs. Laura Smale, Juli Wade, and Jim Galligan for your detailed comments on my research and writing. I greatly appreciate all of the advice you have provided throughout my tenure at Michigan State University.

This dissertation is the result of a great deal of work on the part of many people over the years. I would like to thank my colleague and good friend, Dr. Russell Romeo, for all of his help and support during my graduate career. Thanks also to Jane Venier, Dr. Dave Parfitt, Dr. Eman Ahmed, Dr. Yu Ping Tang, Kalynn Schulz Wilson, Kaliris Salas-Ramirez, Aaron Nelson, and Kristina Davis for all of your help along the way. This dissertation would have not been possible without you. Thanks to Drs. Heather Eisthen, Keith Lookingland, and Cindy Jordan for the use of their lab space, equipment, and expertise.

TABLE OF CONTENTS

LIST OF FIGURES	viii
LIST OF TABLES	xiv
CHAPTER 1:	
GENERAL INTRODUCTION	1
CHAPTER 2:	
DISTRIBUTION OF GnRH NEURONS AND PUBERTAL	
CHANGES IN IMMUNOREACTIVITY	13
Methods	15
Results	24
Discussion	25
CHAPTER 3:	
DOES TESTOSTERONE REGULATE GnRH mRNA?	31
Methods	36
Results	44
Discussion	54
CHAPTER 4:	
THE INFLUENCE OF TESTOSTERONE ON GNRH mRNA	
BEFORE AND AFTER PUBERTY	60
Methods	63
Results	70
Discussion	78
CHAPTER 5:	
PHEROMONES AND THE GnRH SYSTEM	83
Methods	86
Results	95
Discussion	102
CHAPTER 6:	
ANATOMICAL RELATIONSHIPS AMONG GNRH NEURONS	
AND MEDIAL AMYGDALA EFFERENTS	108
Introduction	108
Methods	111

Results	122
Discussion	135
CHAPTER 7:	
GENERAL DISCUSSION	140
REFERENCES	151

LIST OF FIGURES

Figure 1. Diagram of the hypothalamic-pituitary gonadal (HPG) axis.

Figure 2. Camera lucida line drawings depicting the three regions analyzed: DBB/OVLT, MS, and cPOA (A, dashed boxes). Asterisks represent the location of GnRH+ cells in a representative animal. *Abbreviations* : CC, corpus callosum; LV, lateral ventricle; AC, anterior commissure; II, optic nerve; 3V, 3rd ventricle; OVLT, organum vasculosum of the lamina terminalis; OC, optic chiasm. Photomicrographs depicting immunocytochemical staining of ambiguous cells (B, arrows) and GnRH cells (C, arrows) using LR-1 (1:10,000). Bar, 100 μ m.

Figure 3. Mean (\pm SEM) number of GnRH+ cells/section in the MS (A), DBB/OVLT (B), and cPOA (C) of juvenile and adult males in which brain tissue was stained with a low (1:40,000) or high (1:10,000) dilution of LR-1 antiserum. Letters in panel A indicate a significant main effect of age, with juvenile males ("a") having significantly more GnRH+ cells/section in the DBB/OVLT than adult males ("b") independent of antiserum dilution ($p \leq 0.05$). Letters in panel B indicate that juvenile males ("a") had significantly more GnRH+ cells/section than adult males ("b") only with the 1:40,000 dilution of LR-1 ($p \leq 0.05$).

Figure 4. A: Drawing of an anatomical section (adapted from Morin and Wood, 2001) delineating the location of GnRH cells in the tenia tecta. B: GnRH-immunoreactive cells and fibers in the tenia tecta (see Chapter 2 for details on GnRH immunocytochemistry methods). C: GnRH-mRNA labeled cells in the tenia tecta. Differences in section thickness (40 μ m for immunocytochemistry vs. 10 μ m for ISSH) likely account for the different number of cells in the two photomicrographs. Bar, 20 μ m.

Figure 5. Drawing of a sagittal view of the male Syrian hamster brain summarizing four GnRH subpopulations: tenia tecta (TT), medial septum (MS) diagonal band of Broca/organum vasculosum of the lamina terminalis (DBB/OVLT), and caudal preoptic area (cPOA). Red boxes delineate the boundaries of each subpopulation.

Figure 6. Camera lucida drawings of the most anterior and posterior sections of the four brain regions analyzed: tenia tecta, medial septum (MS), diagonal band of Broca/organum vasculosum of the lamina terminalis (DBB/OVLT), and caudal preoptic area (cPOA). The area within which the GnRH cells reside is indicated by shading.

Abbreviations: II, optic nerve; 3V, 3rd ventricle; AC, anterior commissure; CC, corpus callosum; LV, lateral ventricle; OC, optic chiasm.

Figure 7. Plasma testosterone (top panel) and LH (bottom panel) levels in juvenile and adult males following castration and treatment with 0 or 2.5 mg testosterone. Asterisk and bars indicate a main effect of testosterone treatment on plasma testosterone and LH ($p \leq 0.05$) and no interaction within age. Thus, hamsters treated with 2.5 mg testosterone had significantly higher plasma testosterone than hamsters treated with 0 mg testosterone (top panel). Hamsters treated with 2.5 mg testosterone had significantly lower plasma LH than hamsters treated with 0 mg testosterone (bottom panel).

Figure 8. Photomicrographs of labeled cells in the tenia tecta from castrated adults treated with 0 mg testosterone (A) or 2.5 mg testosterone (B). Only silver grains over the Nissl stain were measured (dark grains in plane of focus), providing a conservative estimate of the total silver grain staining associated with each cell. Bar, 20 μm .

Figure 9. Mean grain area (μm^2) in the tenia tecta, DBB/OVLT, MS, and cPOA in castrates (collapsed across age) treated with 0 or 2.5 mg of testosterone. Asterisk indicates a significant effect of treatment only in the tenia tecta ($p \leq 0.05$). Testosterone treatment significantly reduced GnRH mRNA mean grain area within this group of GnRH neurons.

Figure 10. Frequency distribution of the percentage of GnRH neurons within the tenia tecta, DBB/OVLT, MS, and cPOA in each category of GnRH mRNA grain area (μm^2). Mean grain area for each analyzed cell was rounded to the nearest whole number and the cells were categorized into bins ranging from 1 μm^2 -36 μm^2 . The total number of cells for each treatment group determined n . Data from both juveniles and adults were included in the treatment groups. Frequency

distributions for castrates and testosterone-treated males were significantly different ($P \leq .001$) only in the tenia tecta and MS.

Figure 11. Simple regression analyses of GnRH mRNA mean grain area (μm^2) and plasma LH for the tenia tecta, DBB/OVLT, MS, and cPOA. All age and treatment groups are represented in these analyses and each dot represents data from an individual animal. There was a significant correlation ($P \leq .05$) between plasma LH and GnRH mRNA mean grain area only within the tenia tecta.

Figure 12. Camera lucida drawings of the tissue dissection procedure. Asterisks mark the three tissue blocks collected for the RNase protection assay: tenia tecta and medial septum (TT/MS), DBB/OVLT, and cPOA. *Abbreviations:* II, optic nerve; 3V, 3rd ventricle; AC, anterior commissure; CC, corpus callosum; LV, lateral ventricle; OC, optic chiasm; ME, median eminence.

Figure 13. GnRH mRNA RNase protection assay reference standards (A) and standard curve (B).

Figure 14. Plasma testosterone levels following testosterone treatment. Treatment significantly increased plasma testosterone in a dose dependent manner ($p \leq 0.05$). Juveniles and adults did not differ in plasma testosterone levels with any dose.

Figure 15. Plasma LH levels following treatment with different doses of testosterone. Plasma LH was significantly reduced by testosterone treatment in a dose dependent manner ($p \leq 0.05$). Adults had significantly higher plasma LH than juveniles ($p \leq 0.05$).

Figure 16. Representative examples of GnRH mRNA levels in the TT/MS, DBB/OVLT, and cPOA of gonadectomized juvenile and adult males exposed to 0, 0.5, 1.5, or 2.5 mg testosterone pellets.

Figure 17. Mean GnRH mRNA levels in the TT/MS, DBB/OVLT, and cPOA following treatment with testosterone. Age and treatment effects were significant only in the TT/MS ($p \leq 0.05$). Within the TT/MS adults had higher mean levels of GnRH mRNA and testosterone treatment reduced mean levels of GnRH mRNA in a dose dependent manner.

Figure 18. Representative example plasma LH profiles following exposure to a cotton swab containing pheromone (A) or a control swab (B). The arrows indicate delivery of the swab (pheromone=black arrow, blank=clear arrow).

Figure 19. Time response curves of mean (\pm SEM) plasma LH (% change from baseline) following exposure to pheromone or blank swabs. There was a significant increase in plasma LH only after exposure to pheromone ($p \leq 0.05$).

Figure 20. Mean (\pm SEM) plasma LH levels (ng/ml) 0, 60, and 120 min following exposure to swabs containing pheromone. There was not a significant effect of pheromone on LH across time ($p > 0.05$).

Figure 21. Mean (\pm SEM) plasma testosterone levels (ng/ml) 0, 60, and 120 min following exposure to swabs containing pheromone. Testosterone was significantly elevated 60 min after exposure ($p \leq 0.05$).

Figure 22. Mean area of silver grains (μm^2) as measured within the boundary of the cell body (left graphs) and within and surrounding the cell body (right graphs) in the tenia tecta, MS, DBB/OVLT, and cPOA of pheromone exposed males. Pheromones did not affect GnRH mRNA, as measured by either index, at any time point following exposure ($p > 0.05$).

Figure 23. Photomicrographs showing medial amygdala BDA injection sites in representative animals killed 2, 4, 7, and 14 days after surgery. Survival times of 2 and 4 days resulted in diffuse spread of BDA. The injection sites were more distinct 7 and 14 days after surgery.

Figure 24. Schematic representations of animals with BDA injections into the medial amygdala (A, #806; B, #809) and substantia innominata (C, #810). Animal #806, #812, and #810 had BDA-GnRH ratios of 1.0, 0.9, and 0, respectively, in the cPOA ipsilateral to the injection. *Abbreviations:* ACo, anterior cortical nucleus of the amygdala; AHA, amygdalohippocampal area; BM, basolateral nucleus of the amygdala; Ce, central nucleus of the amygdala; IM, intercalated mass cell; MeA, anterior medial

amygdala; MeP, posterior medial amygdala group; oc, optic chiasm; ot, optic tract; PMCo, posteromedial cortical nucleus of the amygdala; PLCo, posterolateral cortical nucleus of the amygdala, si; substantia innominata.

Figure 25. GnRH and BDA fibers in the stria terminalis. Bar, 20 μ m.

Figure 26. GnRH (gray arrows) and BDA (black arrows) double labeled fiber. Bar, 20 μ m.

Figure 27. Photomicrographs of a GnRH cell in the cPOA viewed in different focal planes. The black arrow indicates a BDA close apposition and gray arrows indicate GnRH close appositions onto the same cell. Bar, 10 μ m.

Figure 28. Photomicrograph of a GnRH neuron in the tenia tecta with a BDA apposition onto the axon. Also note the second GnRH cell body in close apposition to this GnRH neuron. Bar, 10 μ m.

Figure 29. Ratio of the number of GnRH cells with BDA appositions to the total number of GnRH cells within the tenia tecta, MS, DBB/OVLT, and cPOA on the side of the brain ipsi- or contralateral to the BDA injection into the medial amygdala. Independent of brain region there was a significantly higher proportion of BDA appositions onto GnRH neurons on the side ipsilateral to the injection (asterisk, $p \leq 0.05$. On the ipsilateral side, cPOA had a higher BDA-GnRH ratio compared to the tenia tecta, MS, and DBB/OVLT (b is different from a, ($p \leq 0.05$)).

Figure 30. Four GnRH close appositions (gray arrows) onto a single GnRH neuron in the tenia tecta. Bar, 10 μ m.

Figure 31. Mean GnRH-GnRH ratios (both ipsi - and contralateral sides combined) in the tenia tecta, MS, DBB/OVLT, and cPOA. The proportion of GnRH cells with one or more GnRH appositions was significantly greater in the tenia tecta and MS as compared to the DBB/OVLT and cPOA (a is different from b, $p \leq 0.05$).

Figure 32. Three closely apposed GnRH cell bodies (gray arrows) within the tenia tecta. Bar, 10 μ m.

Figure 33. Drawing of a sagittal view of the Syrian hamster brain (adapted from Morin and Wood, 2001) summarizing differences in pubertal, testosterone, or chemosensory regulation of GnRH protein (detectable cell #), GnRH mRNA in, or neuronal projections (appositions) to the various GnRH subpopulations.

LIST OF TABLES

Table 1. Mean (\pm SEM) number of GnRH mRNA expressing cells.

Table 2. Mean body weight \pm SEM and mean seminal vesicle weight \pm SEM of juveniles and adults treated with different doses of testosterone. Within each physiological measure, identical letters indicate no differences between groups, whereas different letters indicate significant differences between groups.

Table 3. Sampling periods and swab exposure treatments of animals used to generate time response curves.

Table 4. Mean (\pm SEM) number of GnRH mRNA expressing cells 0, 60, and 120 minutes after exposure to a swab containing pheromone.

Table 5. Summarized data from the experiments described in this dissertation and in Parfitt, Thompson, Richardson, Romeo, and Sisk, 1999, asterisks). Arrows indicate the direction of change in GnRH protein or mRNA (\leftrightarrow represents no change). Checks indicate appositions from the medial amygdala or GnRH fibers onto GnRH neurons. A higher number of checks reflects a higher proportion of appositions.

KEY TO ABBREVIATIONS:

<u>Abbreviation</u>	<u>Turn or Phrase</u>
3V	third ventricle
ACo	anterior cortical nucleus of the amygdala
AHA	amygdalohippocampal area
ANOVA	analysis of variance
BDA	biotinylated dextran amine
BM	basolateral nucleus of the amygdala
BNST	bed nucleus of the stria terminalis
BNSTpm	posteriomedial subdivision of the bed nucleus of the stria terminalis
CC	corpus callosum
Ce	central amygdala
CPM	counts per minute
CV	coefficient of variance
cPOA	caudal preoptic area
DBB	diagonal band of Broca
FSH	follicle stimulating hormone
GABA	gamma-aminobutyric acid
GnRH	gonadotropin releasing hormone
GnRH+	GnRH-immunopositive (-immunoreactive)
HPG axis	hypothalamic-pituitary-gonadal axis
HRP	horseradish peroxidase
<i>icv</i>	intracerebroventricular injection
IM	intercalated mass cell group
ICC	immunocytochemistry
<i>ip</i>	intrapertitoneal injection
ISSH	<i>in situ</i> hybridization histochemistry
LV	lateral ventricle
LH	luteinizing hormone
NMDA	N-methyl-D,L-aspartate
MeA	anterior medial amygdala
MeP	posterior medial amygdala
MPN	medial preoptic nucleus
MS	medial septum

oc	optic chiasm
ot	optic tract
OVL	organum vasculosum of the lamina terminalis
PBS	phosphate buffered saline
PBS-TX	PBS containing 0.2% Triton-X
pir	piriform cortex
PLCo	posterolateral cortical amygdaloid nucleus
PMCo	posteromedial cortical amygdaloid nucleus
PVP	polyvinyl pyrrolidone with heparin
RIA	radioimmunoassay
RPA	RNAse protection assay
sc	subcutaneous injection
si	substantia innominata
SEM	standard error of the mean
SSC	Na/Cl/Na citrate
TT	tenia tecta
TBS	tris buffered saline

CHAPTER 1:

GENERAL INTRODUCTION

Gonadotropin releasing hormone (GnRH, also known as luteinizing releasing hormone, or LHRH) is the primary endocrine regulator of the reproductive system in mammalian species. Despite their small number (less than 2000 in mammals) and scattered distribution within the forebrain, GnRH-producing neurons are critical to reproductive health. They ultimately determine not only the level of gonadal steroids circulating in the blood but also whether sperm is produced in males or ovulation occurs in females. Clinical conditions in which the GnRH system develops abnormally, such as Kallmann's syndrome (reviewed in Rugarli, 1999), result in failure to undergo puberty and complete reproductive shutdown.

Hypothalamic-Pituitary-Gonadal Axis

GnRH cells govern reproductive status through the hypothalamic-pituitary-gonadal (HPG) axis (Figure 1). GnRH is released in a pulsatile manner into the median eminence of the hypothalamus and travels through a portal system to the anterior pituitary, where it induces pulsatile release of the gonadotropins,

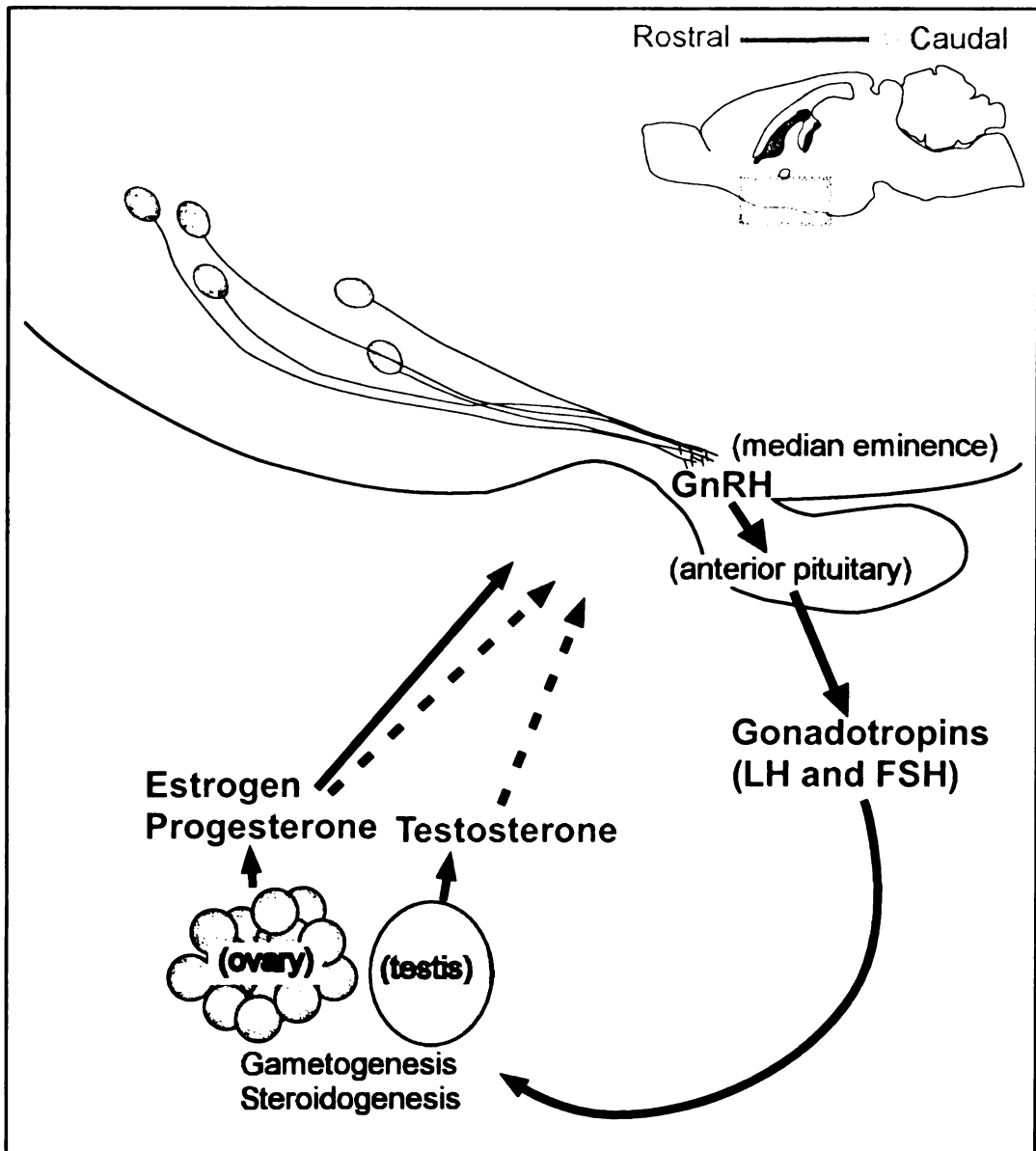


Figure 1. Diagram of the hypothalamic-pituitary gonadal (HPG) axis. follicle stimulating hormone (FSH) and luteinizing hormone (LH). FSH and LH stimulate gamete production and maturation and steroid hormone production and release.

Circulating gonadal steroid hormones, in turn, regulate the HPG axis by negative feedback in males and by both negative and positive steroid hormone feedback in females (Kalra and Kalra, 1989;Freeman, 1994). In males, high levels of testosterone resulting from increased activation of the HPG-axis inhibit GnRH and LH secretion by action at both the hypothalamic and pituitary levels. In females, both estrogen and progesterone serve to inhibit HPG axis activity during the luteal phase of the estrous (rodents) or menstrual (primates) cycle. However, the high levels of estrogen present in the late follicular phase exert positive feedback to induce the LH surge and subsequent ovulation.

Development and Distribution of the GnRH system

The ontogeny of the GnRH neuronal system is unique from most other cellular systems of the brain in that these cells originally arise in the nasal placode (Schwanzel-Fukuda and Pfaff, 1989;Wray, Nieburgs, and Elkabes, 1989;Daikoku-Ishido, Okamura, Yanaihara, and Daikoku, 1990;Ronnekleiv and Resko, 1990;Silverman, Livne, and Witkin, 1994). As gestational development ensues, GnRH cells migrate along the nervus terminalis, enter the brain, and eventually come to reside in a number of different locations throughout the forebrain and

diencephalon. In rodent species the majority of cells are situated in the more rostral regions such as the medial septum (MS) diagonal band of Broca (DBB), and organum vasculosum of the lamina terminalis (OVLT), whereas in carnivores and primates GnRH cells are more numerous caudal to the optic chiasm (preoptic area, hypothalamus, arcuate nucleus). The majority of GnRH neurons project caudally to the median eminence of the hypothalamus (Jennes and Stumpf, 1980; Silverman *et al.*, 1994). Thus, the hormonal signal received by the anterior pituitary reflects integrated neurosecretory activity of spatially and possibly functionally diverse populations of cells.

GnRH and Puberty

By early postnatal life, GnRH cells have come to reside in their permanent anatomical location, their axons have innervated the median eminence, and their cellular machinery is fully capable of producing the mature decapeptide form of GnRH, yet these cells remain relatively quiescent in terms of neurosecretory activity until puberty onset (reviewed in Plant, 1994; Ojeda and Urbanski, 1994; Foster, 1994). Increased secretion of GnRH at puberty, through its regulation of the HPG axis, begins a cascade of events that

ultimately lead to maturation of the endocrine and nervous system.

Factors Impacting the GnRH System

Puberty onset results in a dramatic change in GnRH secretion, but this developmental step is not the only factor that influences GnRH activity. As mentioned previously, gonadal steroids are strong internal regulators of the GnRH system. Other internal and external (environmental) cues also provide meaningful information about whether conditions are optimal for reproductive success. Because the GnRH system ultimately governs reproductive status, these cells must respond to all of these signaling systems. For example, *photoperiod* (Sisk and Turek, 1983a; Ronchi, Krey, and Pfaff, 1992b; Porkka-Heiskanen, Khoshaba, Scarbrough, Urban, Vitaterna, Levine, Turek, and Horton, 1997; Bernard, Abuav-Nussbaum, Horton, and Turek, 1999; Terasawa and Fernandez, 2001), *pheromones* (Meredith, 1991; Wysocki and Lepri, 1991; Romeo, Parfitt, Richardson, and Sisk, 1998), and *nutritional cues* (Foster and Olster, 1985; Berriman, Wade, and Blaustein, 1992; I'Anson, Terry, Lehman, and Foster, 1997) all influence the GnRH system. Details on how these different stimuli regulate GnRH cells remain largely unknown.

Understanding how GnRH cells are regulated poses an

interesting neurobiological problem. The GnRH system is comprised of a relatively small number of neurons that have a widespread distribution. While these cells are regulated by many variables and neurosecretory activity changes with development, investigations are limited by the intractability of the system. Many of the standard techniques of neuroscience (e.g., lesions, microinjections of pharmacological agents, electrophysiology) cannot be readily used to investigate the GnRH system, given its diffuse distribution and small number of cells. These methodological limitations have left neuroendocrinologists with many unanswered questions, despite years of research.

One approach to understanding the GnRH system is to use its unique characteristics as tools, rather than limitations, in study design. By studying the various subpopulations of the GnRH system, one might gain information and insight into the functional organization of the entire system. Questions include how the different subpopulations of GnRH neurons are regulated by so many factors and how is information integrated within the system? Are all GnRH cells regulated by all endogenous and exogenous signals? Or does their responsiveness to different regulators depend on where they are

located in the brain? The local environment in which different subpopulations of GnRH cells reside varies with neuroanatomical location, suggesting that specialization among the different populations is probable. More empirical evidence is needed, however, to validate whether these different GnRH subpopulations are functionally specialized. The following set of experiments investigates how the GnRH system is organized, i.e., do various populations respond differently to developmental changes such as puberty, or to regulation by internal stimuli (e.g., steroids) or external stimuli (e.g., pheromones)? These experiments will determine whether testosterone or female chemosensory stimuli impact expression of GnRH mRNA or protein in a brain region-dependent manner. Tract tracing is also used to address whether neurons in the medial amygdala, a chemosensory integrating nucleus, project to GnRH neurons and, if so, whether this neuronal input is unique to certain populations of GnRH cells.

Animal Model

The male Syrian hamster (*Mesocricetus auratus*) is an ideal model species for addressing questions about GnRH subpopulation organization and regulation for several reasons: 1) the neuroendocrine

and behavioral components of puberty have been well-established in this animal model (Romeo, Richardson, and Sisk, 2002); 2) distribution of the GnRH system has been described (Jennes *et al.*, 1980; Lehman and Silverman, 1988); 3) steroid hormones are less potent inhibitors of LH secretion in adult male than in juvenile male hamsters (Sisk *et al.*, 1983a), which suggests a differential response of the GnRH system to steroid negative feedback before and after puberty. Therefore, we can use pubertal status as tool to investigate testosterone regulation of GnRH neurons; and 4) GnRH is known to play a critical role in the display of male sexual behavior, and female chemosensory cues elicit an elevation in testosterone in male Syrian hamsters (Meredith, 1998). Investigating how pheromones affect the GnRH system will aid in the understanding of how information about the external environment is transduced within the nervous system to impact reproductive hormone secretion and behavior. Therefore, this animal model can be used to investigate differential regulation of GnRH subpopulations during puberty and by internal (steroid hormones) and external (chemosensory) stimuli.

Overview of Chapters

The experiment described in Chapter 2 was designed to identify

which populations of GnRH cells likely contribute to the increased LH release associated with pubertal maturation. To address this, immunocytochemistry was used to identify and map out GnRH containing cells before and after puberty and to investigate whether particular subpopulations were associated with the onset of puberty. This experiment is published in *Brain Research* (Richardson, Romeo, and Sisk, 1999).

The experiments described in Chapter 3 and 4 were designed to investigate testosterone negative feedback upon the different subpopulations of the GnRH system. In these experiments, pubertal status was included as a variable to explore whether pubertal change in responsiveness of the HPG axis to steroid negative feedback involves differential regulation of GnRH mRNA by testosterone before and after puberty. In the experiment described in Chapter 3, *in situ* hybridization histochemistry was used to investigate these questions. This experiment is *in press* in *Journal of Neuroendocrinology* (Richardson, Parfitt, Thompson, and Sisk, 2002). As a follow up to the experiment described in Chapter 3, an experiment (Chapter 4) was designed to address similar questions using a more quantitative approach to mRNA analysis, RNase protection assay (RPA). GnRH

mRNA and plasma LH dose-response curves to testosterone were determined in pre- and postpubertal males to assess whether there was differential regulation of GnRH mRNA and plasma LH between juveniles and adults. These data will soon be submitted to *Endocrinology* for publication.

Chapters 5 and 6 present experiments designed to investigate how chemosensory information impacts the GnRH system in adults. Female pheromones are essential chemosensory stimuli for the expression of reproductive behavior in the male Syrian hamster. If processing of this sensory information is curtailed, for example by removing the vomeronasal organ or olfactory bulbs in the male, he will not engage in mating behavior. At least part of this chemosensory processing is thought to involve the GnRH system. Exposure to chemosensory information causes a rise in plasma LH (Graham and Desjardins, 1980; Coquelin, Clancy, Macrides, Noble, and Gorski, 1984) and testosterone (Macrides, Bartke, Fernandez, and D'Angelo, 1974; Wirsig-Wiechmann, 1993; Romeo *et al.*, 1998). Furthermore, *icv* administration of GnRH reinstates behavior in vomeronasalectomized males (Meredith and Howard, 1992; Fernandez-Fewell and Meredith, 1995). Thus, pheromonal information must reach and impact the

GnRH system through some mechanism. Experiments in Chapters 5 and 6 investigated how this external sensory stimulus impacts GnRH cells. The first experiment in Chapter 5 was conducted to generate a time course for the plasma LH response to pheromone exposure in adult animals, which has not been well-documented in the literature. The second experiment in this chapter investigated whether female pheromones affect GnRH mRNA in a brain region-dependent manner, using *in situ* hybridization to measure GnRH mRNA.

The experiment in Chapter 6 addressed whether a chemosensory processing region of the amygdala directly projects to GnRH cells in any of the various subpopulations. The neural circuitry underlying chemosensory processing and male sexual behavior has been well-documented (Gomez and Newman, 1992; Wood and Coolen, 1997; Coolen and Wood, 1998). The medial amygdala is important for chemosensory and processing and has been shown to project to some of the regions in which GnRH neurons reside (Coolen *et al.*, 1998). Based on this knowledge, the experiment presented in Chapter 6 was designed to investigate whether the medial amygdala projects to the GnRH system, and if so, whether projections are specific to particular populations of GnRH neurons. Anterograde tract tracing was utilized

to answer this question.

Chapter 7 is a general discussion of the questions and various outcomes of these experiments. Data are briefly summarized, and this is succeeded by a discussion encompassing this entire body of work.

CHAPTER 2:
DISTRIBUTION OF GnRH NEURONS AND PUBERTAL
CHANGES IN IMMUNOREACTIVITY

Introduction

Puberty onset is associated with increased activity of the GnRH system (reviewed in (Plant, 1994;Ojeda *et al.*, 1994;Foster, 1994). The neural events underlying puberty activation of the GnRH system are still being elucidated, and probably involve both decreased inhibition and increased excitation of the GnRH system to become active at puberty. The importance of activation occurring at this point in development cannot be stressed enough. These maturational processes not only induce reproductive fertility through activation of the HPG axis, but the steroid hormonal events associated with this increased activity are critical to pubertal maturation of the nervous system.

With respect to the various subpopulations of GnRH cells, it is not known if puberty arises from activation of the entire GnRH system as a whole, or if there is some regional specificity to this developmental change in activity. Immunocytochemical studies

provide evidence for a division of labor among the spatially diverse subpopulations of GnRH cell bodies. There are several reports of brain region-specific reductions in GnRH immunopositive (GnRH+) cell number under conditions in which GnRH secretion is increased (Shivers, Harlan, Morrel, and Pfaff, 1983; King, Kugel, Zahniser, Woledge, Damassa, and Alexsavich, 1987; Tang and Sisk, 1992; Ronchi, Aoki, Krey, and Pfaff, 1992a; Rubin and King, 1994; I'Anson *et al.*, 1997). In general, these results have been interpreted as evidence for involvement of specific subpopulations of GnRH neurons in which somal stores of GnRH become undetectable when secretory activity is high. For example, I'Anson *et al.* (I'Anson *et al.*, 1997) demonstrated a higher number of GnRH+ cells within the medial basal hypothalamus in diet-restricted prepubertal female lambs compared with well-fed prepubertal female lambs. The lower GnRH+ cell number in the medial basal hypothalamus of normal growing lambs suggests that the increase in LH pulse frequency characteristic of these lambs (Foster *et al.*, 1985) is mediated by this particular population of cells. Similarly, there is a brain region-specific change in GnRH+ cell number in the arcuate nucleus of adult male ferrets compared with prepubertal males (Tang, Kashon, and Sisk, 1997),

suggesting that in this species the pubertal increase in GnRH may be primarily mediated by GnRH cells located in the arcuate nucleus.

The purpose of this experiment was to test the hypothesis that specific populations of GnRH cells mediate the pubertal increase in gonadotropin secretion in male Syrian hamsters.

Immunocytochemistry was used to identify GnRH cells in the brains of adult and prepubertal males. Two different concentrations of primary antiserum were used that were expected to result in detection of different numbers of GnRH+ cells, depending on the somal level of GnRH within these cells. This hypothesis predicted that when the tissue was run with the lower (less sensitive) concentration of primary antiserum, a reduced number of GnRH+ neurons in the adult males in subpopulations contributing to the pubertal increase in GnRH release.

Methods

Animals

The male Syrian hamsters (*Mesocricetus auratus*) used in this study were bred at Michigan State University (E. Lansing, MI) and treated in accordance with the NIH Guide for the Care and Use of Laboratory Animals. Protocols were approved by the MSU All-

University Committee for Animal Use and Care. Following weaning, they were singly housed in a 14 hr light/10 hr dark schedule in a temperature-controlled ($21 \pm 2^\circ \text{C}$) room with *ad libitum* access to rodent chow (Teklad Rodent Diet No. 8640, Harlan, Madison, WI) and water.

Study Design

At either 28 (juvenile; n=5) or 49 (adult; n=5) days of age animals were weighed and given an overdose of Equithesin anesthetic (80 mg/kg, *ip*). A cardiac blood sample was taken and plasma was stored at -20°C until the radioimmunoassay was performed. Paired testis and seminal vesicle weights were obtained. Animals were then perfused intracardially with buffered saline followed by 0.4% glutaraldehyde in 2% paraformaldehyde. The brains were stored in 20% sucrose before sectioning into consecutive sets of 40 μm thick coronal sections. Brain sections were stored in cryoprotectant at -20°C until the immunocytochemistry was performed.

Testosterone Radioimmunoassay

Plasma concentrations of testosterone were measured using the Coat-A-Count Total Testosterone Kit (Diagnostic Products, Los Angeles, CA). This assay has been validated in our laboratory for the Syrian

hamster. The lower limit of detectability was 0.1 ng/ml. The intra-assay coefficient of variation (CV) was 14%.

GnRH Immunocytochemistry

Dilution Trials:

Several different dilutions (concentrations ranging from 1:7,000-1:80,000) of LR-1 anti-GnRH antiserum (obtained from R. Benoit, Montreal General Hospital) were used in pilot trials to determine the conditions under which the experimental tissue was run. LR-1 binds to amino acid residues 2-4 and 7-10 of GnRH, and recognizes both the mature decapeptide and the preprohormone forms of GnRH. A concentration of 1:40,000 resulted in a range of GnRH+ staining intensities within a single brain and was therefore chosen for the low concentration set of experimental tissue. Concentrations lower than 1:40,000 resulted in extremely light staining, which made accurate microscopic analyses difficult. A concentration of 1:10,000 was chosen for the high concentration set of experimental tissue because it resulted in darker cell body staining than with the 1:40,000 concentration, without significantly increased background staining. Concentrations higher than 1:10,000 produced elevated background levels, which made accurate cell counting difficult.

Experimental Tissue:

Every fourth section from each experimental brain was processed with LR-1 at a concentration of 1:10,000 and an adjacent set of sections was processed with LR-1 at 1:40,000, in two separate ICC runs. Within a concentration, all tissue from both age groups was processed simultaneously. Sections were rinsed five times in 0.1 M phosphate buffered saline (PBS), followed by five rinses in PBS containing 0.2% Triton-X (PBS-TX). The sections were then placed in 0.3% H₂O₂/MeOH at room temperature for 30 min to reduce endogenous peroxidase activity, followed by three rinses in PBS-TX and a 30 min incubation in normal horse serum (room temperature, Vectastain ABC Rabbit Kit, Burlingame, CA). This incubation was followed by 3 rinses in PBS-TX and a 24 hr incubation at 4° C in LR-1 (at either 1:10,000 or 1:40,000) diluted in PBS-TX. Sections were rinsed 3 times in PBS-TX and incubated at room temperature for 2 hr in biotinylated secondary antiserum (1:200, Vectastain ABC Rabbit Kit, Burlingame, CA). This was followed by three rinses in PBS-TX and a 1 hr incubation at room temperature in an avidin-biotin horseradish peroxidase complex (1:100, Vectastain ABC Rabbit Kit, Burlingame, CA). Sections were then rinsed twice in PBS-TX, once in 0.05 M tris

buffered saline (TBS), and finally incubated in 1% 3,3'-diaminobenzidine containing 0.0025% H₂O₂ in TBS for 15 min at room temperature. Sections were then rinsed once in TBS, five times in PBS, and placed in vials containing dH₂O until they were mounted onto gel-coated slides. Mounted sections were dehydrated in increasing concentrations of alcohol, cleared in Hemo-De (Fisher, Pittsburgh, PA), and coverslipped.

Immunostaining Controls:

Specificity of GnRH+ staining was determined using three controls. The first two controls eliminated either the primary or secondary antiserum. No staining occurred under either of these two conditions. In the third control, the primary antiserum (1:10,000) was preadsorbed with 1µg/ml of synthetic GnRH (Sigma, St. Louis, MO) at 4°C for 24 hr. While preadsorption eliminated GnRH+ staining in the MS, DBB/OVLT, and cPOA, staining remained lateral to the DBB/OVLT in both juvenile and adult males. This staining was not found near the MS or cPOA GnRH cell populations. There were several differences between the cells remaining after preadsorption (termed ambiguous cells) and GnRH+ cells. First, nearly all of the ambiguous cells resided lateral and somewhat ventral to GnRH+ cell populations in the

DBB/OVLT. These cells were generally found around the olfactory tubercle. In addition, these cells displayed poor staining quality in comparison to the GnRH+ cells. While GnRH+ cell body staining was punctate, staining in the ambiguous cells was hazy and light, making the cells difficult to focus. The ambiguous cells also had remarkably large nuclei and were often multipolar (Figure 2B), whereas the GnRH+ cells had smaller nuclei and were unipolar or bipolar (Figure 2C). Finally, the ambiguous cells did not stain with the HU4H GnRH antiserum (mouse anti-GnRH obtained from Dr. Henryk Urbanski, Oregon Health Sciences Center, used at 1:2000 with the Vectastain ABC mouse kit) nor did they express GnRH mRNA (Parfitt, Thompson, Richardson, Romeo, and Sisk, 1999), further indicating that they were not GnRH producing cells. Any cells with the characteristics of the ambiguous cells were not counted in the microscopic analysis.

Microscopic Analysis

One experimenter blind to the condition of the animals was responsible for all of the microscopic analyses. Tissue was microscopically examined under brightfield illumination. Cells were

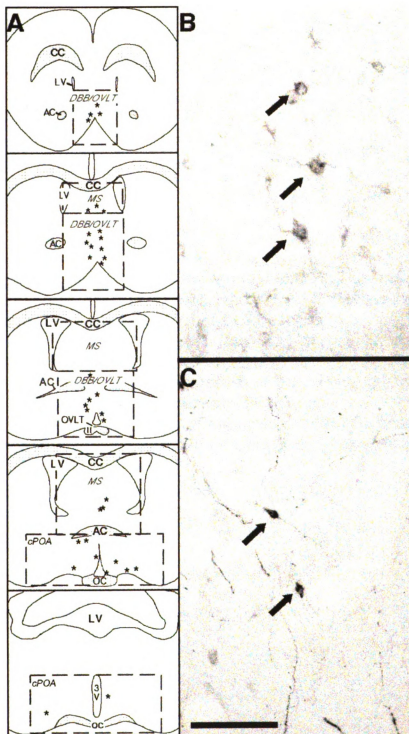


Figure 2. Camera lucida line drawings depicting the three regions analyzed: DBB/OVLT, MS, and cPOA (A, dashed boxes). Asterisks represent the location of GnRH+ cells in a representative animal. *Abbreviations* : CC, corpus callosum; LV, lateral ventricle; AC, anterior commissure; II, optic nerve; 3V, 3rd ventricle; OVLT, organum vasculosum of the lamina terminalis; OC, optic chiasm. Photomicrographs depicting immunocytochemical staining of ambiguous cells (B, arrows) and GnRH cells (C, arrows) using LR-1 (1:10,000). Bar, 100 μ m.

considered GnRH+ if they contained brown reaction product in the cytoplasm, were unipolar or bipolar in shape, and displayed no characteristics of the ambiguous cells. The average number of sections analyzed per animal did not differ between ages (15.7 ± 1.17 , juveniles; 15.88 ± 3.00 , adults, $p \leq 0.05$). Because there was variation in the number of sections analyzed within groups (due to problems with tissue processing), GnRH+ cell number was expressed in GnRH+ cells/section. A regional analysis was performed on the number of GnRH+ cells/section in three operationally defined areas: MS, DBB/OVLT, and cPOA, which together contained more than 90% of the total GnRH+ cells. Although the landmark-based boxes used to delineate and standardize analysis of each area (Figure 2A) extended beyond the Nissl-based boundaries of the areas, they were termed as such because the majority of GnRH+ cells within these boxes resided within these anatomical structures. One experimenter blind to the condition of the animals was responsible for all of the microscopic analyses.

Statistics

Group differences in plasma testosterone concentration and testis and seminal vesicle weights were analyzed by two-tailed *t* tests.

Anatomical data were analyzed using a mixed design two factor analysis of variance [age (independent factor) X antiserum dilution (repeated measure)]. Significant interactions and main effects were probed using Tukey HSD and Fisher's PLSD tests, respectively. Differences were considered significant if $p \leq 0.05$. All data are presented as mean \pm SEM. Due to poor tissue quality, one adult was eliminated from the microscopic and statistical analyses.

Results

Peripheral Measures

Adult males had significantly heavier paired testis (2.732 g \pm 0.137 vs 0.684 g \pm 0.053, $p \leq 0.05$), seminal vesicle weights (0.209 g \pm 0.020 vs 0.028 g \pm 0.002, $p \leq 0.05$), and higher circulating levels of testosterone (2.215 ng/ml \pm 0.361 vs 0.376 ng/ml \pm 0.156, $p \leq 0.05$) compared to juveniles.

Distribution of GnRH+ Cells

GnRH+ cells were distributed throughout the forebrain. Cells were found in regions as anterior as the medial parolfactorial area and posterior as the arcuate nucleus. Cells were also found in the vertical and horizontal bands of the diagonal band of Broca, medial and lateral

septum, organum vasculosum of the lamina terminalis, preoptic area, and ventral medial hypothalamus. The largest number of cells was found within the vertical band of the diagonal band of Broca, the second largest in the MS, and the third largest within the cPOA.

Analysis of GnRH+ Cells

Within the DBB/OVLT, juveniles had more GnRH+ cells/section compared with adults (Figure 3A, $p \leq 0.05$). There was no effect of antiserum dilution and no interaction in the DBB/OVLT. Within the MS, there was an interaction between age and antiserum dilution (Figure 3B, $p \leq 0.05$). Specifically, juveniles had more GnRH+ cells/section than adults only under the 1:40,000 antiserum dilution condition. No effects of age or antiserum dilution on GnRH+ cells/section were found in the cPOA (Figure 3C).

Discussion

The present study demonstrates a region-specific decrease in GnRH+ cell number associated with pubertal maturation in the male Syrian hamster. Adults have fewer GnRH+ cells in the DBB/OVLT and MS than juveniles, but the number of GnRH+ cells within the cPOA does not differ between adults and juveniles. The most likely

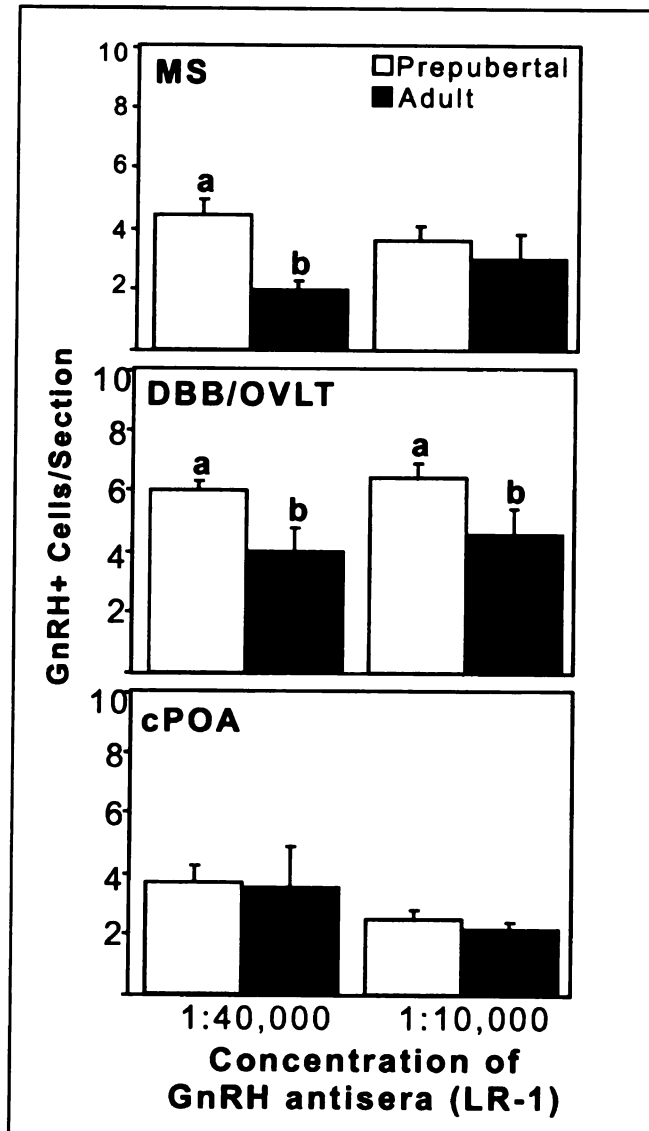


Figure 3. Mean (\pm SEM) number of GnRH+ cells/section in the MS (A), DBB/OVLT (B), and cPOA (C) of juvenile and adult males in which brain tissue was stained with a low (1:40,000) or high (1:10,000) dilution of LR-1 antiserum. Letters in panel A indicate a significant main effect of age, with juvenile males ("a") having significantly more GnRH+ cells/section in the DBB/OVLT than adult males ("b") independent of antiserum dilution ($p \leq 0.05$). Letters in panel B indicate that juvenile males ("a") had significantly more GnRH+ cells/section than adult males ("b") only with the 1:40,000 dilution of LR-1 ($p \leq 0.05$).

explanation of these data is that fewer GnRH neurons within the DBB/OVLT and MS are detectable in adults because increased secretory activity of these neurons during puberty results in lower somal levels of GnRH. Cells within the DBB/OVLT and MS of adult hamsters could be undetectable because they no longer exist or no longer produce GnRH in adulthood. However, the pubertal difference in cell number was attenuated in the MS when the 1:10,000 dilution of primary antiserum was used. Thus, it is probable that the cells within the MS were not detected with the 1:40,000 dilution because somal levels of GnRH were low in these cells. Furthermore, the number of GnRH mRNA expressing cells within the DBB/OVLT is similar in juvenile and adults animals (Parfitt *et al.*, 1999). Thus, the decrease in GnRH+ cells within the MS and DBB/OVLT in adults is in all likelihood not due to cell death or a change in phenotype, but rather to a reduction in GnRH somal stores resulting from increased GnRH release in adulthood.

Cells in the cPOA did not show a pubertal reduction in number. It is possible that cPOA cells contain higher amounts of GnRH than the other populations and therefore remain detectable following GnRH release. Thus, a pubertal decrease in cell number would not be found

in this region even though it may also play a role in increased GnRH release in adulthood. However, *in situ* hybridization indicates that GnRH cellular mRNA is not significantly higher in cPOA cells than in the MS and DBB/OVLT cells (Parfitt *et al.*, 1999). Thus, these data only provide evidence for the MS and DBB/OVLT GnRH neurons being involved in the pubertal increase in GnRH secretion.

In contrast to the present findings, Urbanski *et al.* (Urbanski, Doan, and Pierce, 1991) did not find a pubertal decrease in GnRH+ cell number in male Syrian hamsters. Variations in experimental method could account for the difference between studies. For example, they used a different antiserum (HU4H) than that used in the current study (LR-1) recognizes only the mature decapeptide form of GnRH, whereas LR-1 recognizes both the mature and the preprohormone forms. In addition, the immunocytochemical conditions used in Urbanski *et al.* (Urbanski, Doan, Pierce, Fahrenbach, and Collins, 1992) may have been sensitive enough to detect low somal stores of GnRH.

In female hamsters, many GnRH neurons in the caudal POA express Fos-immunoreactivity (Fos-ir), a marker of neuronal activity (Morgan and Curran, 1991), across the entire 4-day estrous cycle. On the other hand, cells within the DBB and MS/rostral POA express Fos-ir

only on day 4, just following the preovulatory LH surge (Berriman *et al.*, 1992). In another report, an increase in Fos-ir was observed in the OVLT GnRH cells just following the LH surge in female hamsters (Doan and Urbanski, 1994). Taken together, the two studies suggest that rostral GnRH cells are recruited for the preovulatory LH surge in females. These data from female hamsters and the present data from males suggest that rostral populations of GnRH neurons in the hamster are more likely to be involved in steroid-dependent dynamic changes in GnRH secretion than are caudal populations. The reduction in responsiveness to testosterone negative feedback, which occurs during pubertal maturation in male hamsters (Sisk *et al.*, 1983a), may result in increased release primarily from GnRH neurons residing in the MS and DBB/OVLT.

In summary, we have demonstrated a brain region-specific decrease in the number of GnRH+ neurons in the male Syrian hamster as a result of pubertal maturation. These data suggest that populations of GnRH cells in the MS and DBB/OVLT play an integral role in the pubertal increase in GnRH release. Furthermore, these data support the idea of inherent differences in regional populations of GnRH neurons, raising interesting questions about when and how

conditions dictate a change in GnRH release. Thus, GnRH neurons in particular anatomical locations may be responsive to regulation by certain stimuli, such as gonadal steroids, while other populations may not.

CHAPTER 3:

DOES TESTOSTERONE REGULATE GnRH mRNA?

Introduction

The last chapter provides evidence for heterogeneity among cells within the GnRH system. In general, the more rostral populations of cells showed a reduction in immunoreactive cell number with puberty, indicating that they are involved in the pubertal increase in gonadotropin release. *In situ* hybridization data from our lab also demonstrated an pubertal increase in GnRH mRNA in all GnRH subpopulations, but it was more pronounced in the DBB/OVLT. These data together suggest an important role of the more rostral GnRH cells in puberty.

The threshold for steroid negative feedback regulation of the HPG axis varies with reproductive status. Responsiveness to negative feedback is particularly high prior to puberty in many species. For example, in hamsters, when testosterone is experimentally clamped at physiological levels in juvenile males, gonadotropin secretion is completely suppressed. However, as the males enter puberty, plasma gonadotropin levels rise despite the constantly maintained levels of

testosterone (Sisk *et al.*, 1983a). Thus, a change in the negative feedback set point is involved in the pubertal rise in gonadotropin secretion in hamsters.

The cellular mechanisms underlying negative feedback inhibition of GnRH neuronal activity are not well understood, nor is it known if they change during development. One reason for this lack of understanding is related to the diffuse distribution of GnRH neurons throughout the forebrain, a feature that makes it difficult to study the system as a whole. Since GnRH neuronal phenotype and afferents vary with brain region (Hoffman, Lee, Attardi, Yann, and Fitzsimmons, 1990; Wu, Segal, Miller, Gibson, and Silverman, 1992; Mitchell, Bouret, Prevot, Jennes, and Beauvillain, 1999; Prevot, Bouret, Croix, Takumi, Jennes, Mitchell, and Beauvillain, 2000), the cellular level at which steroids regulate GnRH neurons may also vary with brain region.

Regulation of GnRH mRNA is one cellular level at which steroids exert feedback effects on the HPG axis. The effects of steroids on GnRH mRNA are brain region-dependent (Selmanoff, Shu, Petersen, Barraclough, and Zoeller, 1991; Porkka-Heiskanen, Urban, Turek, and Levine, 1994; Petersen, McCrone, Keller, and Shores, 1995; Spratt and Herbison, 1997). Thus, the goals of the current experiment were two-

fold: 1) to conduct a brain regional analysis of testosterone regulation of GnRH mRNA, and 2) to determine whether a change in the specific cell groups in which GnRH mRNA is decreased by testosterone is a correlate of the pubertal decrease in steroid negative feedback.

In some of the sections analyzed in the experiment presented in chapter 2, an interesting phenotype of GnRH cells was found (Figure 4). These cells were quite rostral, were more clustered together, and were embedded within a plexus of GnRH fibers. At that time, they were considered to be the most rostral aspects of the DBB/OVLT and MS. However, several atlases define the region in which these cells reside as the tenia tecta. Thus, from this point on, those cells were separated out from the other GnRH cells and analyzed as a distinct population of GnRH neurons. These subdivisions are shown in figure 5. Little is known about tenia tecta GnRH neurons, but they appear to be activated by sensory stimuli to produce the preovulatory luteinizing hormone (LH) surge in the musk shrew, a reflex ovulator (Dellovade and Rissman, 1994;Dellovade, Hunter, and Rissman, 1995a;Dellovade, Ottinger, and Rissman, 1995b).

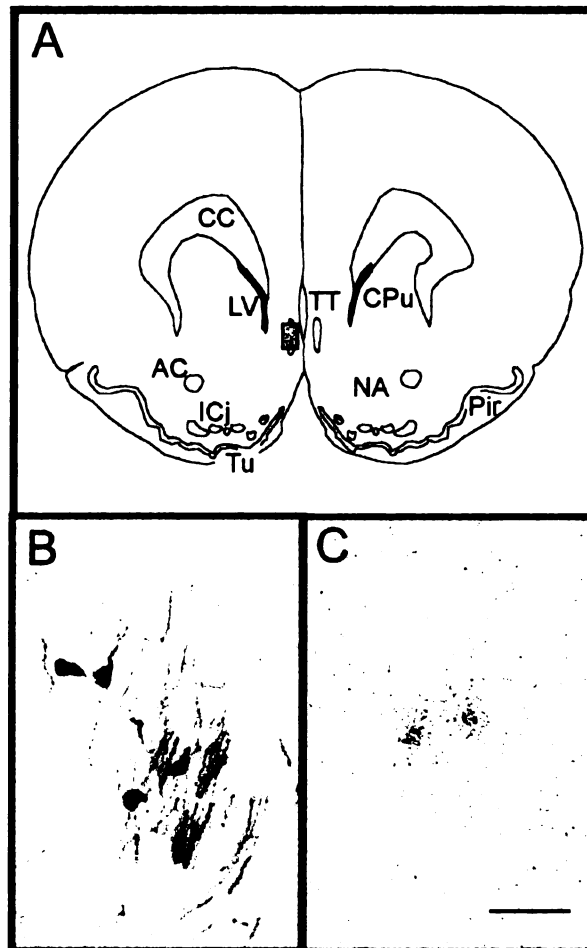


Figure 4. A: Drawing of an anatomical section (adapted from Morin and Wood, 2001) delineating the location of GnRH cells in the tenia tecta. B: GnRH-immunoreactive cells and fibers in the tenia tecta (see Chapter 2 for details on GnRH immunocytochemistry methods). C: GnRH-mRNA labeled cells in the tenia tecta. Differences in section thickness (40 μm for immunocytochemistry vs. 10 μm for ISSH) likely account for the different number of cells in the two photomicrographs. Bar, 20 μm .

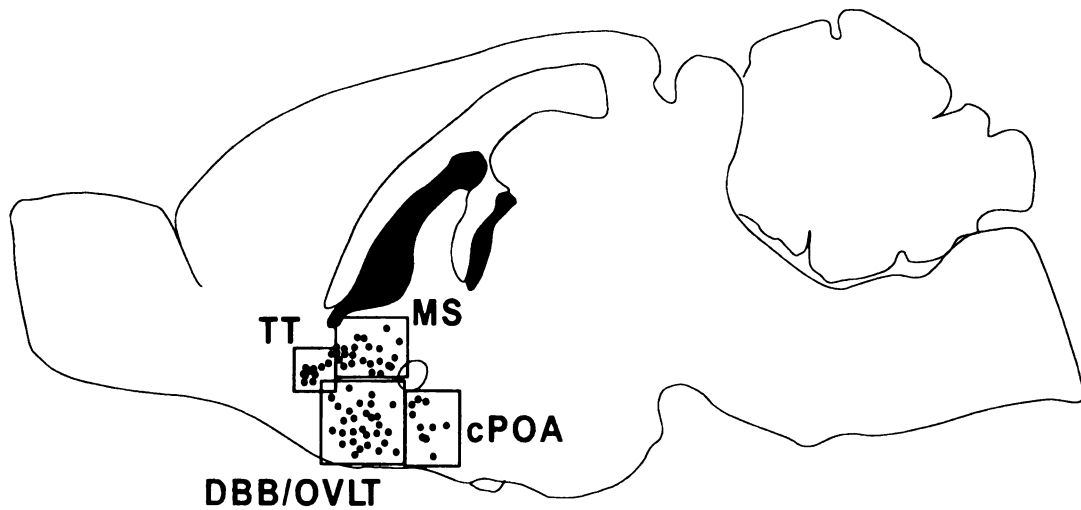


Figure 5. Drawing of a sagittal view of the male Syrian hamster brain summarizing four GnRH subpopulations: tenia tecta (TT), medial septum (MS) diagonal band of Broca/organum vasculosum of the lamina terminalis (DBB/OVLT), and caudal preoptic area (cPOA). Red boxes delineate the boundaries of each subpopulation.

In situ hybridization histochemistry was performed to measure GnRH mRNA in the tenia tecta and MS, DBB/OVLT, and cPOA in testosterone-treated gonadectomized juvenile and adult male Syrian hamsters. We provide evidence for the first time that GnRH mRNA in neurons in the tenia tecta is reduced by testosterone in both juvenile and adult males. While GnRH mRNA is only modestly regulated by testosterone overall in the brain, this regulation is most pronounced in tenia tecta neurons.

Methods

Animals, Experimental Design, and Tissue Collection

One day after arrival from Charles River (Kingston, NY), twelve prepubertal (23 days old) and twelve adult (60 days old) male Syrian hamsters (*Mesocricetus auratus*) were anesthetized with methoxyflurane (Metofane, Mallinckrodt Veterinary Inc., Mundelein, IL, USA), castrated, and implanted subcutaneously with either a placebo (blank) or a 2.5 mg timed-release testosterone pellet (n=6 per treatment group, Innovative Research, Sarasota, FL). Following treatment, all animals were singly housed in clear polycarbonate cages (37.5 X 33 X 17 cm) with wood chips (Aspen Chip Laboratory Bedding,

Warrensburg, NY). Throughout the experiment room temperature was maintained at $21 \pm 2^{\circ}\text{C}$ and the light-dark schedule was 14 hr light/10 hr dark (lights on at 0600 hr EST). Animals had *ad libitum* access to rodent chow (Teklad Rodent Diet No. 8640, Harlan, Madison, WI) and water throughout the study. Animals were treated in accordance with the NIH Guide for the Care and Use of Laboratory Animals and protocols were approved by the Michigan State University All-University Committee for Animal Use and Care.

Seven days following gonadectomy and steroid treatment (at 30 or 67 days old), animals were anesthetized with Metofane and decapitated. Trunk blood was collected for measurement of plasma concentrations of testosterone and LH. Brains were rapidly removed and snap frozen in an isopentane/dry ice bath. Frozen brains were stored at -80°C until sectioning on the cryostat. Every other coronal section (10 μm) was collected and thaw-mounted onto poly-L-lysine coated slides to produce a total of four sets. Slides were stored with desiccant at -80°C until *in situ* hybridization histochemistry was performed.

GnRH mRNA In Situ Hybridization Histochemistry

One set of sections from each brain was processed for *in situ*

hybridization using a ³⁵S-cRNA probe generated from Syrian hamster GnRH cDNA (generously donated by Dr. Heiko Jansen, Washington State Univ.). The antisense probe was transcribed in a reaction mixture containing 1 µg of linearized DNA (BamH I linearized plasmid), 5x transcription buffer (Epicentre Technologies, Madison, WI, USA), 80 µCi [³⁵S]UTP, 120 µCi [³⁵S]CTP, 150 µM ATP, 150 µM GTP, 12.5 mM dithiothreitol, 20 U RNase inhibitor, and 6 U T7 RNA polymerase (Epicentre Technologies). Following an incubation at 37°C for 2 h, unincorporated nucleotides were separated by Sephadex G50-50 chromatography and the antisense probe diluted in 50% hybridization buffer (Amresco, Solon, OH, USA) to obtain ~1.0 x 10⁶ CPM/70 µl of buffer. Slides were removed from the -80°C freezer and placed immediately in 4% paraformaldehyde for 1 h. They were then washed several times in 2x NaCl/Na citrate (SSC) before a 10 min incubation in 0.1 M triethanolamine (TEA) containing 0.25% acetic anhydride. Slides were washed in dH₂O and dehydrated through a series of alcohols.

Diluted probe (70 µl) was applied onto each slide and a glass coverslip was gently placed over the sections to prevent evaporation of the probe during hybridization. Slides were placed in plastic boxes

lined with filter paper saturated with 50% formamide. The boxes were covered with plastic lids, wrapped with plastic wrap, and incubated at 55°C for 16 h. Following hybridization, the coverslips were removed by washes in 2x SSC and the slides were then incubated in RNase A buffer (200 µg/ml) for 1 h at 37°C. This incubation was followed by several washes in decreasing concentrations of SSC (2x, 1x, 0.5x, and 0.1x) and an incubation in 0.1x SSC for 1 h at 70°C. Afterwards, slides were washed in 0.1x SSC and dH₂O rinses, dehydrated in graded alcohols, and air-dried. Once completely dry, slides were exposed to XAR film (Eastman Kodak, Rochester, NY, USA) for 14 days. After removal from film, they were emulsion-dipped (NTB2 emulsion from Eastman Kodak diluted 1:1 in distilled water), stored in light-tight boxes at 4°C for 3 days, and developed using standard procedures (Parfitt *et al.*, 1999) for microscopic analysis of silver grains. Sections were then lightly counterstained with thionin to visualize cell bodies, dehydrated in alcohols, cleared, and coverslipped. Incubation of tissue sections with a sense probe does not result in labeling of cells (Parfitt *et al.*, 1999).

Redefining GnRH Subpopulations and Microscopic Analysis

Four populations of GnRH neurons were analyzed: tenia tecta,

DBB/OVLT, MS, and cPOA. These brain regions are operationally defined in Figure 6. All analyses were carried out by one investigator blind to the treatment conditions using a Leitz Laborlux S microscope equipped with a CCD video camera (Sony, XC-77). Labeled cells were located under darkfield microscopy at 100x or 200x magnification and then were analyzed individually at a magnification of 400x in brightfield microscopy. Images were captured through a blue no. 47 filter used to subtract Nissl staining (Tiffen, Hauppauge, NY, USA), and analyzed using NIH Scion Image 1.57 on a Power Macintosh 7100 computer. Each cell profile was first traced and Nissl area was measured. After the cell profile was traced and Nissl area measured, a threshold was set so that only silver grains were visualized, and the area (μm^2) covered by silver grains was measured. Although silver grains over intensely labeled cells were not confined to the Nissl boundary, we quantified only silver grain labeling over Nissl stain because it provided an objective definition of the cell. Thus, this measurement is a conservative estimate of the amount of silver grain labeling associated with the cell. The cell tracing was then moved to a nearby region without specific hybridization to determine

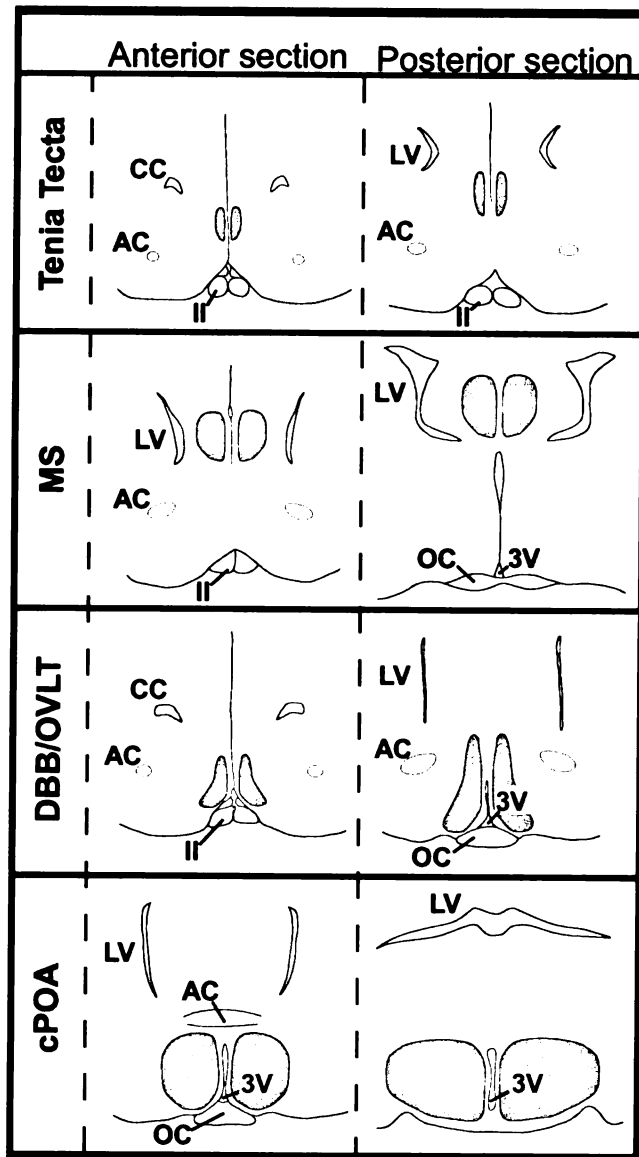


Figure 6. Camera lucida drawings of the most anterior and posterior sections of the four brain regions analyzed: tenia tecta, medial septum (MS), diagonal band of Broca/organum vasculosum of the lamina terminalis (DBB/OVLT), and caudal preoptic area (cPOA). The area within which the GnRH cells reside is indicated by shading. *Abbreviations:* II, optic nerve; 3V, 3rd ventricle; AC, anterior commissure; CC, corpus callosum; LV, lateral ventricle; OC, optic chiasm.

background silver grain area. A GnRH-mRNA expressing cell was defined as a cell in which the area covered by silver grains was $\geq 5x$ that of background. Background grain area was subtracted from the Nissl cell grain area to obtain GnRH mRNA grain area for individual cells. The silver grain area of all cells within each brain region was averaged for each animal. Finally, mean silver grain area for each region was averaged across animals within each treatment group to obtain mean silver grain area for the tenia tecta, MS, DBB/OVLT, and cPOA.

Hormone Radioimmunoassays

Plasma testosterone levels were measured in duplicate samples using the Coat-A-Count Total Testosterone Kit (Diagnostic Products, Los Angeles, CA). This radioimmunoassay (RIA) has been validated in our laboratory for the measurement of plasma testosterone concentrations in Syrian hamsters (Parfitt *et al.*, 1999). The lower limit of detectability was 0.1 ng/ml and the intra-assay coefficient of variation (CV) was 8.8%.

Plasma LH levels were determined by a double antibody RIA using reference preparation RP-3 and reagents in the rat LH kit obtained from the National Institute of Diabetes and Digestive and

Kidney Diseases and Dr. A.F. Parlow. To validate this assay for the Syrian hamster, samples from intact and castrated male plasma pools were assayed at five different dilutions. These results were compared to a standard curve generated with the LH reference preparation ranging from 0.8 ng to 30 ng/ml. LH values obtained from the diluted pools were parallel to the standard curve and maintained linearity throughout its range. All samples were run in duplicate in a single assay. Values are reported as nanogram equivalents of NIDDK-rLH-RP-3. The lower limit of detectability was 0.93 ng/ml and the intra-assay coefficient of variance (CV) was 13.6%.

Statistical Analysis

Two-way analysis of variance (ANOVA) was used to analyze the effects of age and steroid treatment on plasma testosterone concentrations, plasma LH concentrations, number of labeled cells, and mean grain area (μm^2 occupied by silver grains). Significant main effects were probed using Fisher's PLSD tests. The number of labeled cells and mean grain area were analyzed separately for GnRH neurons within the tenia tecta, DBB/OVLT, MS, and cPOA. Although each treatment group consisted of 6 animals, actual sample sizes for the brain regional analysis of GnRH mRNA varied because of poor tissue

quality resulting from occasional difficulties during sectioning or *in situ* hybridization. When sections from a particular brain region were not analyzable, data from that region for that animal were eliminated from the analysis.

Because ANOVA revealed no significant age effects, data from adults and juveniles were combined for the frequency distribution and regression analyses. Kolmogorov-Smirnov two-sample tests were used to determine whether frequency distributions of cells categorized by intensity of silver grain labeling were different for testosterone-treated and control animals within each brain region. For this analysis, a p-value ≤ 0.001 was required for statistical significance. Finally, using data from individual animals in all age and treatment groups, simple regression analyses were used to determine the correlation between plasma LH levels and mean silver grain area in each brain region. Except as noted above, p-values ≤ 0.05 were considered statistically significant.

Results

Plasma Hormone Levels

Plasma testosterone levels were undetectable (<0.1 ng/ml) in

juvenile and adult castrates treated with blank pellets (Figure 7, top). At both ages, treatment with 2.5 mg testosterone resulted in plasma hormone levels that were within adult physiological range (Sisk *et al.*, 1983a; Meek, Romeo, Novak, and Sisk, 1997; Parfitt *et al.*, 1999).

Thus, there was a significant increase in plasma testosterone in castrates treated with 2.5 mg testosterone ($p \leq 0.05$, Figure 7, top).

Plasma testosterone levels in testosterone-treated juveniles and adults were not significantly different.

A significant effect of treatment on LH plasma concentrations was found, with testosterone-treated castrates having lower plasma LH levels than blank-treated castrates ($p \leq 0.05$, Figure 7, bottom). There was no interaction between age and testosterone on LH, indicating that the 2.5 mg dose of testosterone reduced LH levels to a similar degree in juvenile and adult castrates.

Number of Labeled Cells

Neither age nor hormone treatment significantly affected the number of labeled cells in any of the four brain regions analyzed separately, or when regions were considered together (Table 1).

Silver Grain Analysis

Figure 8 shows labeled cells in representative adult castrates

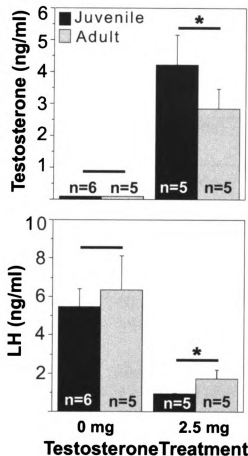


Figure 7. Plasma testosterone (top panel) and LH (bottom panel) levels in juvenile and adult males following castration and treatment with 0 or 2.5 mg testosterone. Asterisk and bars indicate a main effect of testosterone treatment on plasma testosterone and LH ($p \leq 0.05$) and no interaction within age. Thus, hamsters treated with 2.5 mg testosterone had significantly higher plasma testosterone than hamsters treated with 0 mg testosterone (top panel). Hamsters treated with 2.5 mg testosterone had significantly lower plasma LH than hamsters treated with 0 mg testosterone (bottom panel).

Table 1. Mean (\pm SEM) number of GnRH mRNA expressing cells.

Treatment Group	Brain Region (# of labeled cells)				
	Tenia Tecta	DBB/OVLT	MS	cPOA	Total
Juvenile (0 mg testosterone)	13.80 \pm 3.37	35.33 \pm 7.47	35.17 \pm 7.55	10.40 \pm 0.6	98.50 \pm 9.67
Adult (0 mg testosterone)	11.60 \pm 2.79	47.40 \pm 3.72	40.20 \pm 4.47	10.80 \pm 3.5	110.00 \pm 11.07
Juvenile (2.5 mg testosterone)	9.40 \pm 1.89	31.40 \pm 8.62	26.00 \pm 3.03	8.25 \pm 1.97	77.25 \pm 12.20
Adult (2.5 mg testosterone)	15.25 \pm 6.05	41.25 \pm 5.63	31.50 \pm 4.94	7.60 \pm 1.6	95.75 \pm 15.45

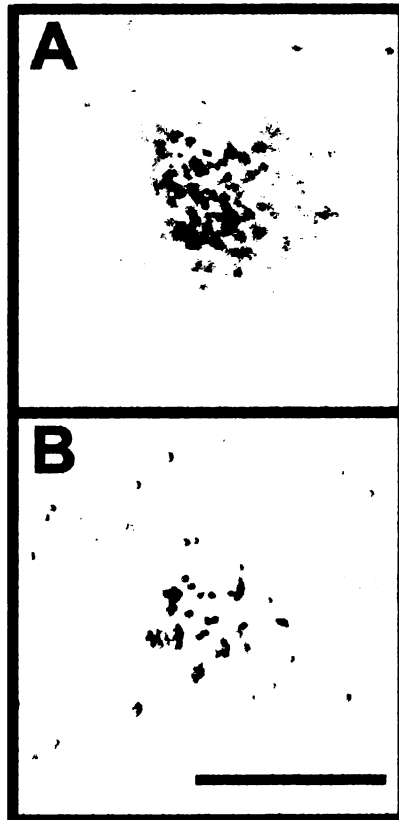


Figure 8. Photomicrographs of labeled cells in the tenia tecta from castrated adults treated with 0 mg testosterone (A) or 2.5 mg testosterone (B). Only silver grains over the Nissl stain were measured (dark grains in plane of focus), providing a conservative estimate of the total silver grain staining associated with each cell. Bar, 20 μ m.

treated with either 0 (A) or 2.5 mg of testosterone (B). Approximately 100 GnRH neurons were analyzed in each animal (all labeled cells identified in the 1-in-8 series of sections). Mean silver grain area values for each animal were averaged within a treatment group for the statistical analyses. There was no effect of age or testosterone treatment on mean silver grain area when all brain regions were analyzed together (juvenile 0 mg testosterone, $6.96 \pm 0.79 \mu\text{m}^2$; adult 0 mg testosterone, $6.73 \pm 0.56 \mu\text{m}^2$; juvenile 2.5 mg testosterone, $5.81 \pm 0.76 \mu\text{m}^2$; adult 2.5 mg testosterone, $5.06 \pm 0.64 \mu\text{m}^2$). When brain regions were analyzed separately, there was a significant reduction in mean silver grain area with testosterone treatment only in the tenia tecta ($P \leq 0.05$, Figure 9, top panel). This effect was independent of pubertal status. Smaller and non-significant trends toward decreased silver grain area in testosterone-treated castrates were observed in the DBB/OVLT, MS, and cPOA (Figure 9, bottom three panels).

Because there was neither an effect of age nor an interaction between age and treatment on area covered by silver grains, labeled cells from juveniles and adults were pooled to create a frequency distribution based on mean silver grain area. In the tenia tecta and

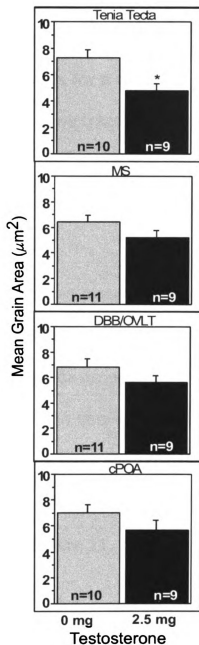


Figure 9. Mean grain area (μm^2) in the tenia tecta, DBB/OVLT, MS, and cPOA in castrates (collapsed across age) treated with 0 or 2.5 mg of testosterone. Asterisk indicates a significant effect of treatment only in the tenia tecta ($p \leq 0.05$). Testosterone treatment significantly reduced GnRH mRNA mean grain area within this group of GnRH neurons.

MS, the frequency distributions for vehicle- and testosterone-treated groups were significantly different, indicating an increase in the number of lightly labeled cells (or a decrease in the number of heavily labeled cells) with testosterone treatment (Figure 10, $P \leq 0.001$). The frequency distributions of cells within the DBB/OVLT and cPOA did not differ for testosterone and blank-treated animals.

Regression Analyses

The relationship between plasma LH and GnRH mRNA in each brain region was examined by simple regression analyses of data from individuals in all treatment/age groups. There was a modest, but significant, positive correlation between plasma LH levels and mean silver grain area in the tenia tecta ($P \leq 0.05$, Figure 11, top panel). In contrast, LH levels and mean grain area were not correlated in DBB/OVLT, MS, or cPOA (Figure 11, bottom three panels).

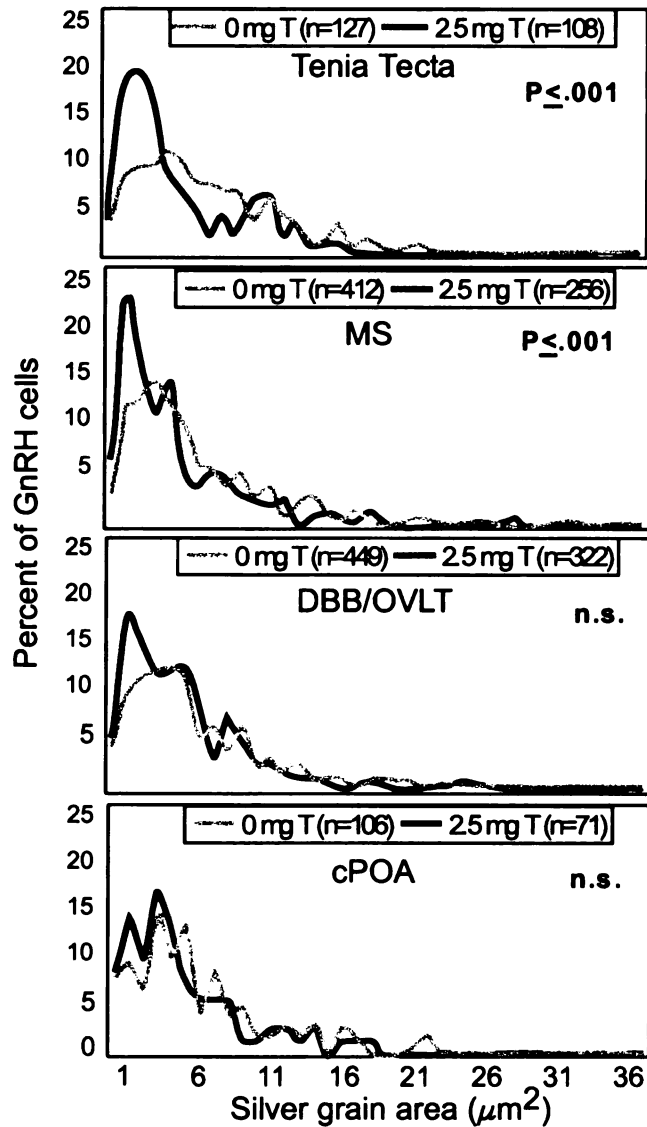


Figure 10. Frequency distribution of the percentage of GnRH neurons within the tenia tecta, DBB/OVLT, MS, and cPOA in each category of GnRH mRNA grain area (μm^2). Mean grain area for each analyzed cell was rounded to the nearest whole number and the cells were categorized into bins ranging from 1 μm^2 -36 μm^2 . The total number of cells for each treatment group determined *n*. Data from both juveniles and adults were included in the treatment groups. Frequency distributions for castrates and testosterone-treated males were significantly different ($P \leq .001$) only in the tenia tecta and MS.

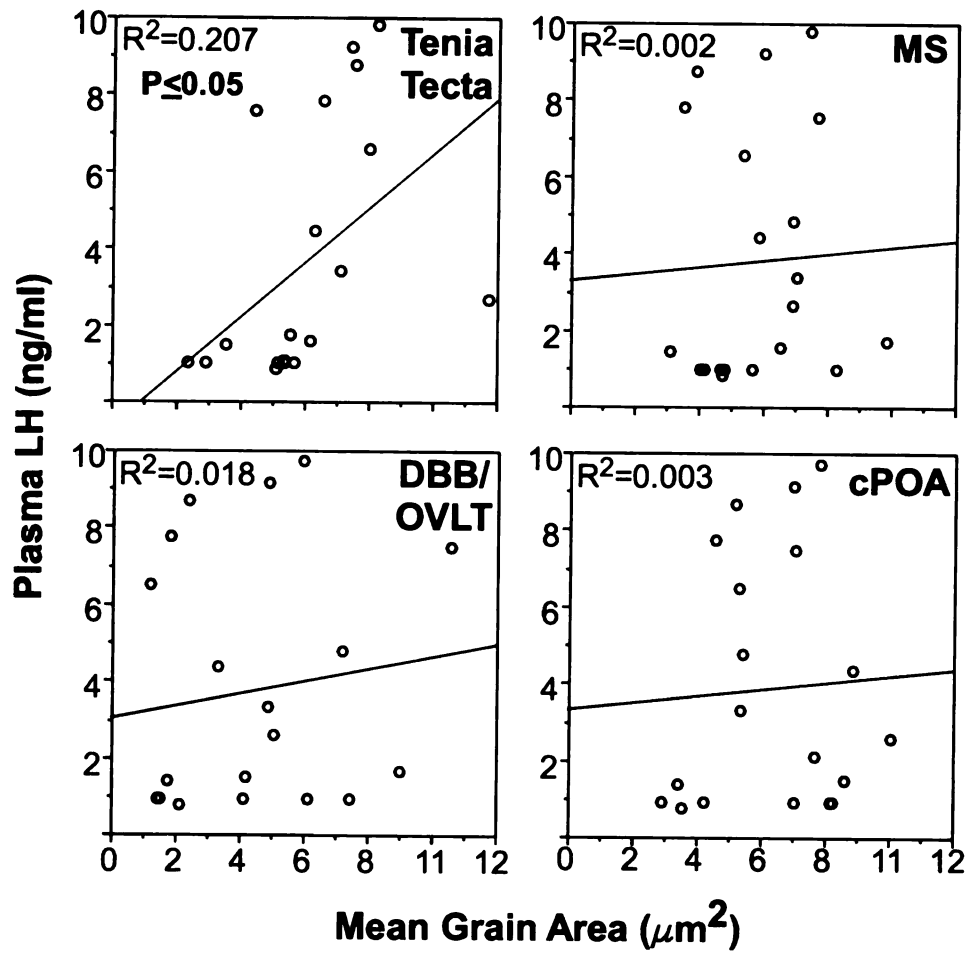


Figure 11. Simple regression analyses of GnRH mRNA mean grain area (μm^2) and plasma LH for the tenia tecta, DBB/OVLT, MS, and cPOA. All age and treatment groups are represented in these analyses and each dot represents data from an individual animal. There was a significant correlation ($P \leq .05$) between plasma LH and GnRH mRNA mean grain area only within the tenia tecta.

Discussion

This study demonstrates that testosterone treatment results in brain region-dependent reductions in GnRH mRNA, as determined by analysis of *in situ* hybridization silver grain labeling. Reduced GnRH mRNA in the presence of testosterone was reflected by 1) a significant decrease in the area of neurons covered by silver grains in the tenia tecta, and 2) a significant shift toward a greater percentage of lightly labeled cells in both tenia tecta and medial septum. In the DBB/OVLT and cPOA, these indices of GnRH mRNA were unaffected by testosterone. Thus, regulation of GnRH mRNA by testosterone is most pronounced in tenia tecta neurons, intermediate in medial septum, and absent in DBB/OVLT and cPOA. We conclude that steroid negative feedback regulation of the GnRH neuronal system includes modest reductions in GnRH mRNA, particularly in rostral brain regions, but also involves other cellular mechanisms.

These data are in agreement with earlier reports that steroid negative feedback regulation of GnRH neurons is associated with a decrease in GnRH mRNA (Wray, Zoeller, and Gainer, 1989; Selmanoff *et al.*, 1991; Spratt *et al.*, 1997). However, it is unlikely that steroid negative feedback is exclusively exerted at the level of GnRH mRNA

expression. First, the magnitude of the reduction in GnRH mRNA induced by steroid treatment in current and previous (Spratt *et al.*, 1997) studies is relatively modest compared with the magnitude of the reduction in LH secretion. Second, other studies report that castration results in either no change in GnRH mRNA (Wiemann, Clifton, and Steiner, 1990; Malik, Silverman, and Morrell, 1991; Ronchi *et al.*, 1992b) or in an increase in GnRH mRNA (Park, Park, Cho, and Kim, 1988). Factors that potentially contribute to these different findings include mRNA detection methods, time between castration and hormone treatment, tissue collection methods, and brain regions analyzed. Collectively, the literature suggests that steroid negative feedback regulation of GnRH neurons is complex, occurs at multiple cellular levels in a brain region-dependent fashion, and is dynamic after experimental manipulation.

In the current study, the GnRH cells most affected by testosterone negative feedback were the tenia tecta GnRH cells. The population of GnRH neurons in the tenia tecta has not been as thoroughly studied as those in other forebrain and hypothalamic areas. In female musk shrews, tenia tecta GnRH cells have been strongly linked to the sensory-induced preovulatory gonadotropin surge evoked

by interactions with a male, and the number of GnRH-immunoreactive cells in tenia tecta correlates with plasma estradiol levels (Dellovade *et al.*, 1994;Dellovade *et al.*, 1995a;Dellovade *et al.*, 1995b). The present study is the first to link tenia tecta neurons to steroid regulation of gonadotropin secretion in males, as GnRH mRNA was most robustly affected by testosterone in these cells, and also was positively correlated with plasma LH levels.

The number of GnRH neurons in the tenia tecta of the hamster is relatively small, only slightly larger than size of the population of GnRH neurons in the cPOA and representing approximately 10-15% of the total population of GnRH cells. However, a small number of cells does not preclude an important role for them in the regulation of gonadotropin secretion. For example, studies in which GnRH neurons were implanted into the hypothalamus of the hypogonadal (*hpg*) mutant mouse (Gibson, Krieger, Charlton, Zimmerman, Silverman, and Perlow, 1984) demonstrate that only a few GnRH neurons are sufficient to reinstate gonadotropin secretion and reproductive fertility (Gibson *et al.*, 1984). In addition, a general principle of the organization of the GnRH neuronal system is specialization with respect to afferent input and co-localization of neuropeptides and

neurotransmitter receptors. For example, only 5-20% of GnRH neurons appear to express NMDA receptors (Abbud and Smith, 1995; Gore, Wu, Rosenberg, and Roberts, 1996), and only about 30% of GnRH neurons receive vasoactive intestinal polypeptide afferents (van der Beek, van Oudheusden, Buijs, van der Donk, Van den Hurk, and Wiegant, 1994). Thus, tenia tecta GnRH neurons may represent a population of median eminence projecting cells in which steroid negative feedback regulation occurs at the level of GnRH mRNA expression or stability. It will be important in future studies to characterize other phenotypic traits of this group of cells in order to understand their role in the HPG axis or other central roles. For example, are GnRH to GnRH contacts more prevalent within this population of cells, as is suggested by the position of GnRH cell bodies within a dense plexus of GnRH fibers in the tenia tecta? Experiment 5 addresses this question.

We found no evidence that testosterone regulates GnRH mRNA in different populations of cells before and after puberty. We could not determine from this experiment whether the threshold for inhibition of GnRH mRNA increases in parallel with the increase in threshold for inhibition of LH following pubertal maturation. The dose of

testosterone used in the present experiment resulted in nearly undetectable levels of LH in both juveniles and adults. Thus, while high testosterone levels clearly reduce GnRH mRNA in both prepubertal and adult males, it was not possible to learn whether pubertal status interacts with testosterone in the regulation of GnRH mRNA. Experiment 3 will determine whether doses of testosterone that differentially lower LH levels in juveniles and adults also differentially results in brain region-dependent reductions of GnRH mRNA at these two ages.

Conclusion

Among the four populations of GnRH neurons, testosterone treatment regulated GnRH mRNA most robustly in the tenia tecta, which was also the only population of GnRH neurons to show a significant correlation between GnRH mRNA and LH levels. The more refined parcellation of GnRH neurons in the current study revealed functional differences among GnRH cells that might have been overlooked if tenia tecta cells had been grouped with MS and DBB/OVLT neurons as before (Chapter 2 and Parfitt *et al.*, 1999). Additional information on neighboring cell types, neural input, and intracellular phenotype of GnRH neurons is necessary to further

elucidate how steroid negative feedback regulation of GnRH neurons varies among cells in different brain regions. The experiment in Chapter 6 provides information about the neuronal input to the various GnRH subpopulations.

CHAPTER 4:
THE INFLUENCE OF TESTOSTERONE ON GnRH mRNA
BEFORE AND AFTER PUBERTY

Introduction

The previous experiment demonstrated that testosterone reduces GnRH mRNA, as measured by *in situ* hybridization, within the tectal and MS subpopulations in both juveniles and adults. Although these data indicate that testosterone impacts similar populations of GnRH neurons before and after puberty, it does not address the issue of whether there is a decrease in sensitivity of the GnRH system to steroid negative feedback upon GnRH mRNA in adulthood. This was the focus of Chapter 4.

A pivotal event in the onset of puberty is activation of the GnRH neuronal system (Watanabe and Terasawa, 1989; Plant, 1994; Ojeda *et al.*, 1994; Foster, 1994; Sisk, Richardson, Chappell, and Levine, 2001). The mechanisms by which GnRH neurons are activated at puberty are not fully understood, and may involve both an increased excitatory tone and decreased inhibitory tone. In males, testosterone (or its intracellular metabolites) inhibits GnRH secretion via hormonal

negative feedback, and feedback varies with development and reproductive status (Sisk *et al.*, 1983a; Sisk and Turek, 1983b; Sisk, 1987; Berglund and Sisk, 1990; Lehman, Goodman, Karsch, Jackson, Berriman, and Jansen, 1997). In many mammalian species, including humans, puberty is accompanied by a decrease in sensitivity (or increased threshold) of the HPG axis to steroid negative feedback (Gupta, Rager, Zarzycki, and Eichner, 1975; Sisk *et al.*, 1983a; Sisk, 1987; Foster, Hassing, Mendes, Hale, Padmanabhan, Hopwood, Beitins, Marshall, and Kelch, 1989). For example, when prepubertal hamsters or lambs are treated with a low dose of testosterone, gonadotropin secretion is initially attenuated to undetectable levels (Sisk *et al.*, 1983a; Foster *et al.*, 1985). However, when these animals reach puberty, gonadotropin levels rise despite the clamped levels of testosterone. Thus, the ability of gonadal steroids to inhibit gonadotropin release decreases with pubertal maturation.

Steroid negative feedback is exerted at both the hypothalamic and pituitary levels (Levine, Bauer-Dantoin, Besecke, Conaghan, Legan, Meredith, Strobl, Urban, Vogelsong, and Wolfe, 1991). Centrally, testosterone appears to inhibit GnRH secretion, and

in many experimental paradigms, also reduces GnRH mRNA. It is not clear whether the pubertal change in set point for negative feedback involves central mechanisms, and if so, whether these mechanisms include a decrease in the magnitude of steroid dependent reduction of GnRH mRNA.

Our lab has studied pubertal maturation of the GnRH system in male Syrian hamsters, a species in which pubertal and seasonal changes in neuroendocrine and behavioral responses to steroid hormones are well-documented (Sisk *et al.*, 1983a; Meek *et al.*, 1997; Romeo, Cook-Wiens, Richardson, and Sisk, 2001). In an early study, a single dose of testosterone was shown to be more effective in inhibiting LH secretion in prepubertal males than in adults (Sisk *et al.*, 1983a). More recent work demonstrated that GnRH mRNA increased with puberty in male hamsters (Parfitt *et al.*, 1999) and is decreased by testosterone in a brain-region dependent manner (Chapter 3). The goal of the current study was to determine whether a pubertal change in testosterone inhibition of LH secretion is paralleled by a similar change in testosterone inhibition of GnRH mRNA, and LH and GnRH mRNA dose response curves to testosterone were compared in pre- and post-pubertal male hamsters to address this.

Methods

Animals

Twenty-four prepubertal (21 days of age) and 24 adult (60 days of age) male Syrian hamsters (Charles River, Kingston, NY) were used in the current study. The experiment was run in two identical cohorts that were run within two weeks of each other. Animals were housed in clear polycarbonate cages (37.5 X 33 X 17 cm) in triads from the same treatment group. All animals had *ad libitum* access to food (Teklad Rodent Diet No. 8640, Harlan, Madison, WI) and water throughout the study. The vivaria were on a 14 hr light/10 hr dark light-dark schedule (lights on at 0700 hr EST) and the temperature was maintained at 21 ± 2 °C. All animals were treated in accordance with the NIH Guide for the Care and Use of Laboratory Animals, and the protocols were approved by the Michigan State University All-University Committee for Animal Use and Care.

Surgery and Tissue Collection

On the day of arrival, animals were castrated under methoxyflurane anesthesia and immediately implanted with 3-week time release pellets (Innovative Research of America, Sarasota, FL)

containing either 0, 0.5, 1.5, or 2.5 mg of testosterone (n=6/dose and age). Seven days after treatment, animals were weighed, rapidly decapitated, and trunk blood samples and seminal vesicles were collected.

Brain Tissue Dissections

Brains were immediately removed after decapitation and rapidly dissected into three tissue blocks, which were frozen on dry ice and stored at -80° C until RNA extraction. The tenia tecta and medial septum subpopulations could not be easily dissected from one another. Therefore, the three tissue blocks contained GnRH neurons in the tenia tecta/medial septum combined (TT/MS), diagonal band of Broca/organum vasculosum of the lamina terminalis (DBB/OVLT) and caudal preoptic area (cPOA). Figure 12 depicts the brain dissection procedure. Dissections were performed by placing the brain with the ventral surface up and coronal cuts were made at the olfactory fissure (1st cut), the optic chiasm (2nd cut), and just anterior to the median eminence (3rd cut). The first of two dissected blocks (block A) was then placed on its caudal face and two vertical cuts were made just lateral to the left and right arms of the anterior commissure. A horizontal cut was made just dorsal to the anterior commissure.

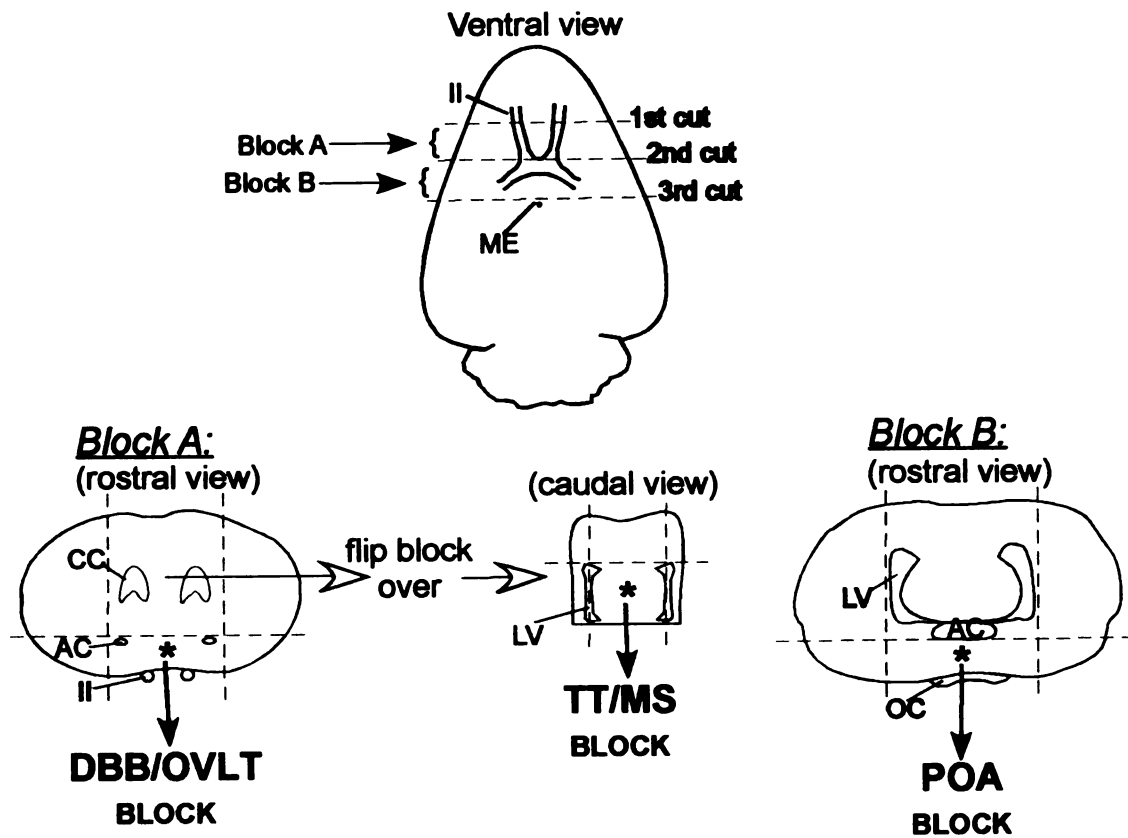


Figure 12. Camera lucida drawings of the tissue dissection procedure. Asterisks mark the three tissue blocks collected for the RNase protection assay: tenia tecta and medial septum (TT/MS), DBB/OVLT, and cPOA. *Abbreviations:* II, optic nerve; 3V, 3rd ventricle; AC, anterior commissure; CC, corpus callosum; LV, lateral ventricle; OC, optic chiasm; ME, median eminence.

The block below this horizontal cut and residing within the vertical cuts contained the DBB/OVLT. The block above the horizontal cut and within the vertical cuts was removed, flipped over so that the caudal face was visible, and further dissected with vertical cuts just medial to and a horizontal cut just dorsal to the lateral ventricle to generate the TT/MS block. Block B was placed with the rostral face up and two vertical cuts were made outside the left and right sides of the lateral ventricle. Then, a horizontal cut was made just ventral to the anterior commissure and the tissue block below this horizontal cut and within the vertical cuts was the POA dissection.

RNA Extraction and RNase Protection Assay

In collaboration with Dr. Andrea Gore at the Mount Sinai School of Medicine (New York, NY), GnRH mRNA levels were measured in tissue blocks using the following protocol. Frozen dissected tissues were homogenized in cold Trizol (Gibco, Rockville, MD), and RNA was extracted with chloroform and isopropanol, followed by an ethanol wash of the RNA-containing pellet. The pellet was resuspended in 30 μ l diethyl pyrocarbonate-treated (DEPC) water, and a 1 μ l aliquot was used for determination of total mRNA by spectrophotometry. Samples were aliquoted so that each contained 30 μ g of total mRNA and then

were concentrated in a Speedvac, and resuspended in 20 μ l of hybridization buffer (0.1 M EDTA, pH 8, 4 M guanidine thiocyanate; final pH 7.5) for RNase protection assay.

To detect GnRH mRNA, probe (antisense) and reference (sense) RNAs were transcribed *in vitro*, using a clone containing 191 bp of the hamster GnRH cDNA, inserted into the *EcoRI* site of the pCRII vector (obtained from Dr. Heiko Jansen, Washington State University, Pullman, WA). Standard *in vitro* transcription methods were used to label the GnRH mRNA probe with 32 P-UTP to high specificity activity (\sim 1,300,000 cpm/ng) (Jakubowski, Blum, and Roberts, 1991; Gore and Roberts, 1994). Cyclophilin mRNA levels were determined within the same samples to control for gel-loading variation, using a 111-bp clone, spanning from the *Pst*I and *Xmn*I restriction sites, and subcloned into a Bluescript KS(+) vector (Jakubowski *et al.*, 1991), and labeled with 32 P-UTP to low specificity activity (\sim 60,000 cpm/ng). Both probes were brought to a final volume of 5 μ l and added to samples and standards (20 μ l each) for a final volume of 25 μ l. For standard curves, probes were mixed with increasing known amounts of GnRH and cyclophilin reference RNAs. After hybridization for 18 h at 30° C, the rest of the assay was conducted as described in

(Jakubowski and Roberts, 1992;Gore *et al.*, 1994). Samples were electrophoresed on 6% polyacrylamide gels, the gels were dried, and exposed to x-ray film for 18-36 hr in order to produce an audiogram, then exposed to a phosphor-imaging screen (Molecular Dynamics, Sunnyvale, CA) for 18 hr for quantification. The amount of radioactivity was compared to the amount of reference RNA in the standards (Figure 13A), and regression analysis performed to produce a standard curve (Figure 13B). The resulting regression formula was then used to determine the absolute amount of RNA in each sample.

Hormone Radioimmunoassays

Plasma testosterone concentrations were measured in duplicate in two different assays using the Coat-A-Count Total Testosterone Kit (Diagnostic Products, Los Angeles, CA) and sample volumes of 50 μ l. The lower limit of detectability for both assays was 0.1 ng/ml and the intraassay coefficients of variation (CV) were 12.9% and 9.2%. The interassay CV was 11%.

Plasma LH concentrations were measured in duplicate (sample volume, 50 μ l) in a single assay using reagents in the rat LH kit obtained from the National Institute of Diabetes, Digestive, and Kidney Diseases (NIDDK) and Dr. A.F. Parlow. Values are reported as

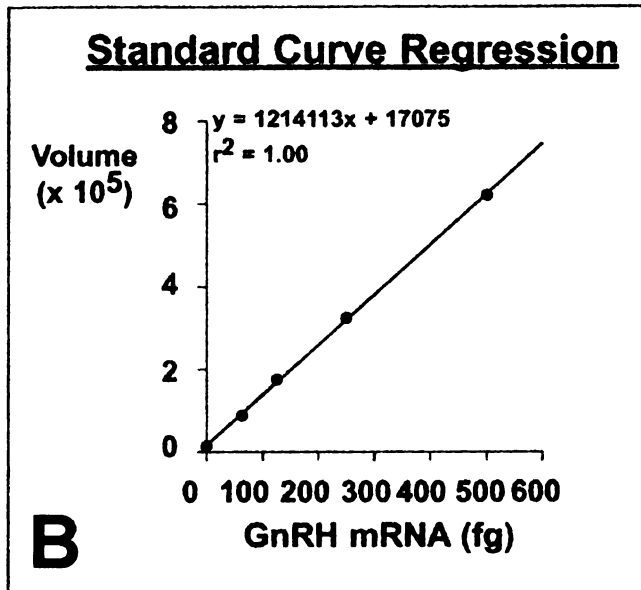
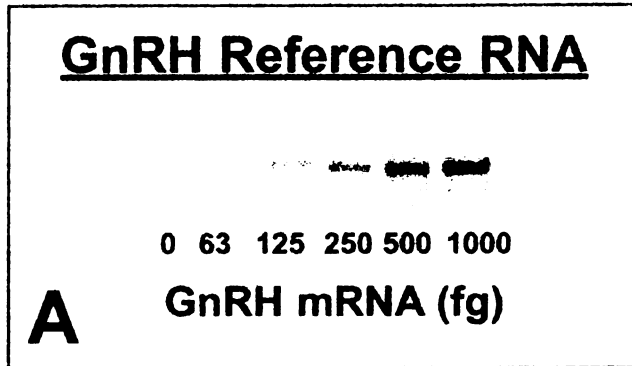


Figure 13. GnRH mRNA RNase protection assay reference standards (A) and standard curve (B).

nanogram equivalents of NIDDK-rLH-RP-3. The lower limit of detectability was 0.66 ng/ml and the intraassay CV was 8.6%.

Statistical Analysis

Body and seminal vesicle weights and hormone concentrations were analyzed using two-way ANOVAs (age X testosterone treatment). GnRH mRNA data were analyzed using a three-way mixed design ANOVA [brain region (within subject) x testosterone treatment (between subject) x age (between subject)]. Significant interactions and main effects were further probed with Tukey HSD tests and Fisher's PLSD tests, respectively. A Chi-square analysis was used to determine whether proportion of animals responding to testosterone treatment with plasma LH concentrations falling below detectability differed with age. Differences were considered significant when $p \leq 0.05$. All data are reported as mean \pm SEM.

Results

Plasma Testosterone and Physiological Measures

There was a significant main effect of testosterone treatment on plasma testosterone levels ($p \leq 0.05$). Testosterone treatment resulted in dose-dependent increases in plasma testosterone in both juveniles

and adults (Figure 14). There was neither an effect of age nor an interaction, such that within each dose of testosterone juveniles and adults had equivalent plasma testosterone levels.

Mean body weight of adults was significantly heavier than that of juveniles ($p \leq 0.05$), but body weight was not affected by testosterone at either age (Table 2). Testosterone treatment significantly increased seminal vesicle weight in both juveniles and adults in dose dependent manner (Table 2, $p \leq 0.05$). At all doses of testosterone, adults had significantly heavier seminal vesicle weights than juveniles.

Plasma LH

There were significant main effects of testosterone treatment and age on plasma LH (Figure 15, $p \leq 0.05$). Even though there was not a significant interaction between testosterone treatment and age, plasma LH remained relatively high in adults, even with increasing doses of testosterone. While the 1.5 mg testosterone pellet decreased LH by only 14% in adults (compared to 0 mg treated adults), this same dose decreased LH by 89% in juveniles (compared to 0 mg treated juveniles). Indeed, Chi-Square analysis revealed that there was a significantly higher percentage of juveniles (73%) with

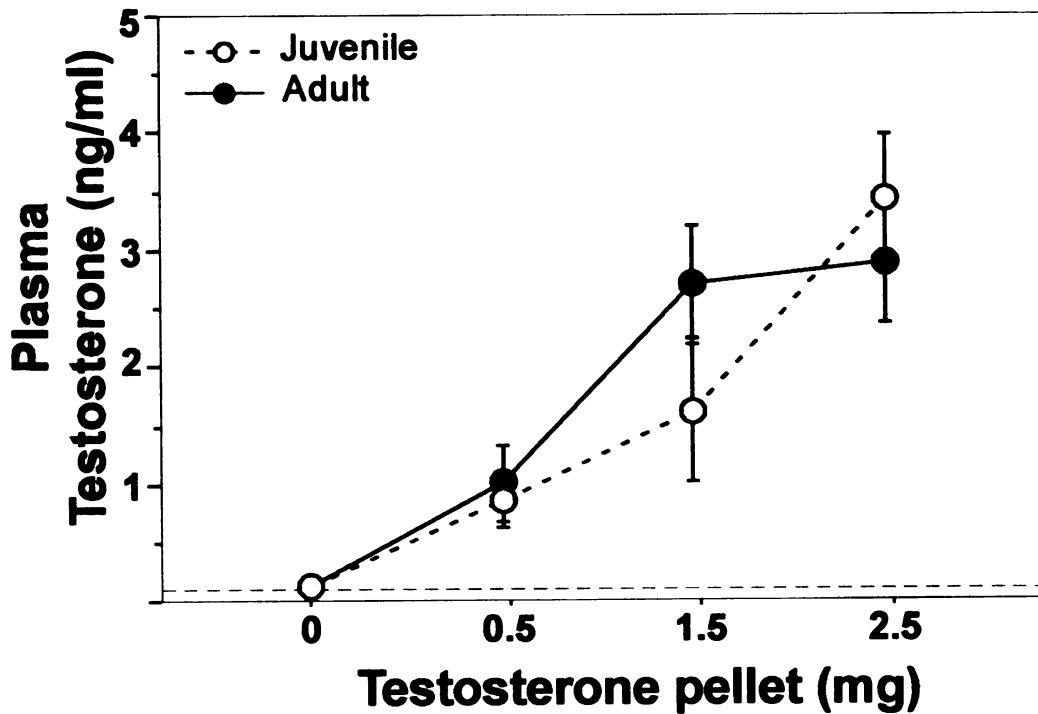


Figure 14. Plasma testosterone levels following testosterone treatment. Treatment significantly increased plasma testosterone in a dose dependent manner ($p \leq 0.05$). Juveniles and adults did not differ in plasma testosterone levels with any dose.

Table 2. Mean body weight \pm SEM and mean seminal vesicle weight \pm SEM of juveniles and adults treated with different doses of testosterone. Within each physiological measure, identical letters indicate no differences between groups, whereas different letters indicate significant differences between groups.

Age	Dose of Testosterone	Body Weight (g)	Seminal Vesicle Weight (mg)
Juvenile	0 mg	71 \pm 3^a	0.021 \pm 0.001^a
	0.5 mg	71 \pm 3^a	0.055 \pm 0.009^b
	1.5 mg	74 \pm 1^a	0.091 \pm 0.008^c
	2.5 mg	72 \pm 1^a	0.096 \pm 0.006^c
Adult	0 mg	124 \pm 1^b	0.108 \pm 0.010^d
	0.5 mg	125 \pm 2^b	0.231 \pm 0.012^e
	1.5 mg	128 \pm 4^b	0.225 \pm 0.026^e
	2.5 mg	121 \pm 2^b	0.263 \pm 0.027^e

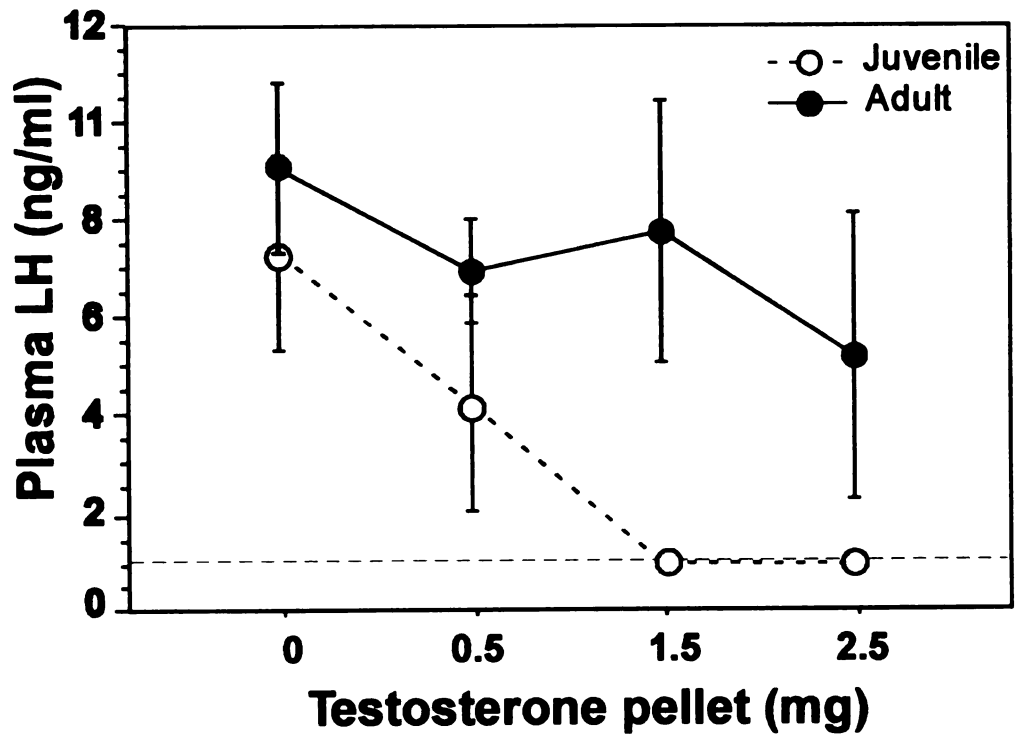


Figure 15. Plasma LH levels following treatment with different doses of testosterone. Plasma LH was significantly reduced by testosterone treatment in a dose dependent manner ($p \leq 0.05$). Adults had significantly higher plasma LH than juveniles ($p \leq 0.05$).

undetectable levels of plasma LH than adults (29%) following testosterone treatment (0.5 mg, 1.5, and 2.5 doses combined, $\chi^2 = 5.811$, $df = 1$, $p \leq 0.05$).

GnRH mRNA

Representative GnRH mRNA hybridization signals in TT/MS, DBB/OVLT, and cPOA from individual animals are shown in Figure 16. Quantified group means are shown in Figure 17. Three-way ANOVA (region X age X testosterone dose) revealed both region x age and region x dose interactions on mean GnRH mRNA levels ($p \leq 0.05$). Since the effects of both testosterone and age were dependent on brain region, these interactions were further analyzed by performing separate two-way ANOVAs (age X dose) for each brain region. Significant main effects of age and testosterone on GnRH mRNA were observed only within the TT/MS dissection (Figure 17, top panel, $p \leq 0.05$). GnRH mRNA was significantly higher in adults and was significantly lowered by testosterone. Although there was not a significant interaction between age and treatment, testosterone reduced TT/MS GnRH mRNA in a dose-dependent manner in adults and did not appear to systematically affect GnRH mRNA in juveniles (Figure 17, top panel). There was no effect of age or treatment on

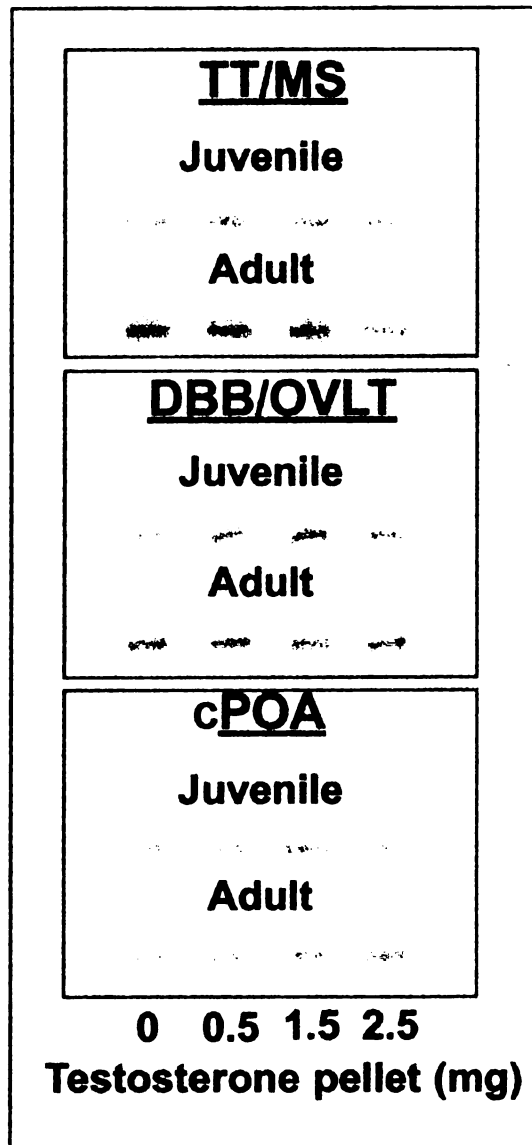


Figure 16. Representative examples of GnRH mRNA levels in the TT/MS, DBB/OVLT, and cPOA of gonadectomized juvenile and adult males exposed to 0, 0.5, 1.5, or 2.5 mg testosterone pellets.

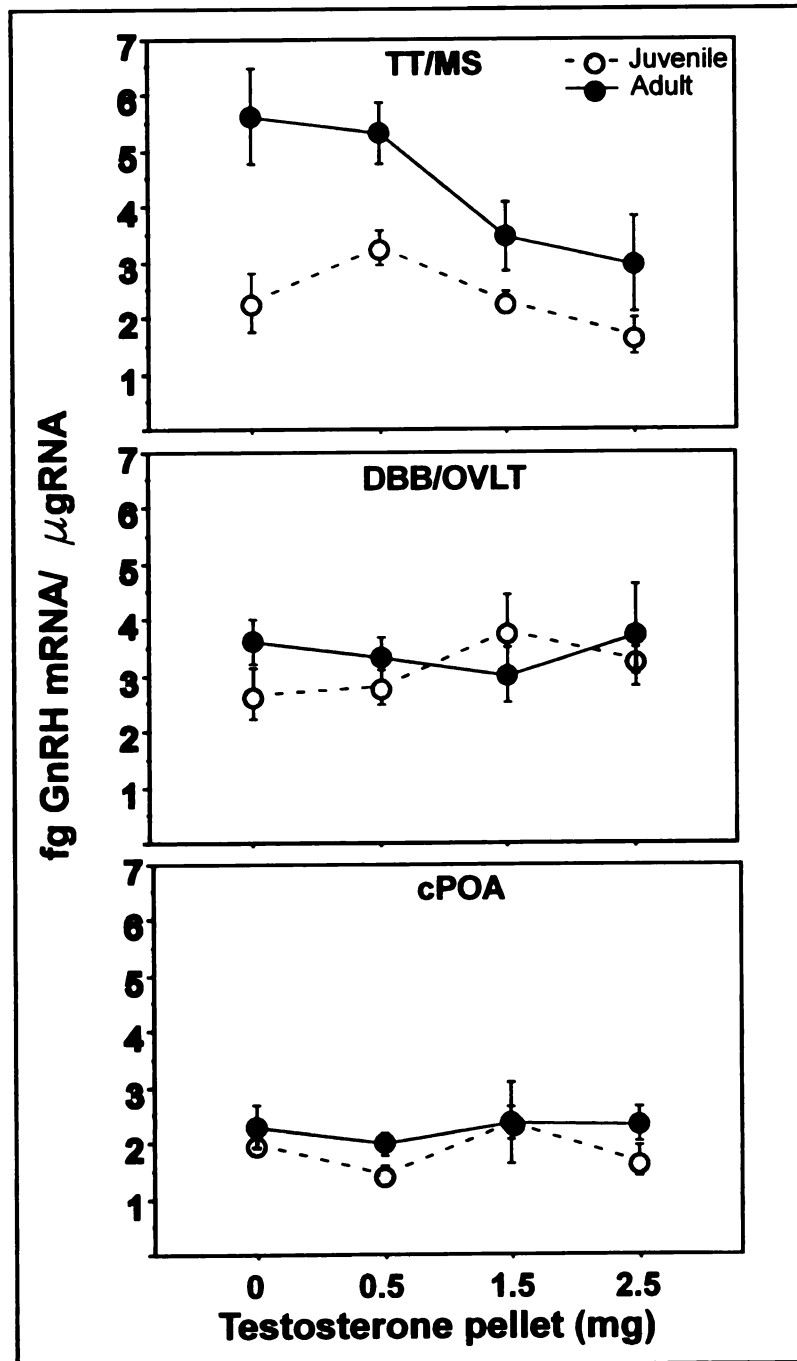


Figure 17. Mean GnRH mRNA levels in the TT/MS, DBB/OVLT, and cPOA following treatment with testosterone. Age and treatment effects were significant only in the TT/MS ($p \leq 0.05$). Within the TT/MS adults had higher mean levels of GnRH mRNA and testosterone treatment reduced mean levels of GnRH mRNA in a dose dependent manner.

GnRH mRNA levels in the DBB/OVLT or cPOA (Figure 17, bottom two panels).

Discussion

The current study demonstrates that both testosterone and pubertal status significantly affected both LH secretion and GnRH mRNA in rostral brain regions. Interestingly, however, testosterone inhibition of LH was more pronounced in juveniles, whereas testosterone inhibition of GnRH mRNA was more pronounced in adults. Thus the pubertal decrease in negative feedback regulation of gonadotropin secretion does not appear to involve a decrease in testosterone inhibition of GnRH mRNA.

Although ANOVA did not reveal a statistically significant interaction between age and treatment on LH, this was likely due to the variance in terminal LH samples inherent in the pulsatile nature of LH secretion. Notwithstanding, it is clear from the LH dose response curves to testosterone treatment that juveniles were more sensitive to negative feedback upon LH than adults, since the two highest doses reduced LH to undetectable levels in juveniles, yet had little impact on LH in adults. In fact, Chi Square analysis showed that a higher

proportion of juveniles, than adults, respond to testosterone with undetectable levels of LH. This corresponds well with earlier data (Sisk *et al.*, 1983a), in which the same amount of testosterone treatment inhibited plasma LH release to a greater degree before puberty than after. Thus, increased gonadotropin release in adulthood may be attributable to decreased sensitivity of the HPG axis to steroid negative feedback sensitivity. Whether this change in sensitivity is occurring at the level of the pituitary (a change in responsiveness of gonadotropes to GnRH) or brain (increased GnRH release that is not reflected by increased GnRH mRNA), or both, is not known.

GnRH mRNA in the TT/MS was significantly affected by pubertal status and testosterone treatment. Several interesting points arise from these results. First, in the absence of testosterone, adults have 2.5 times higher GnRH mRNA in the TT/MS than juveniles. Second, testosterone reduces GnRH mRNA in the TT/MS in a dose-dependent manner, and this reduction appears to be more robust in adults than in juveniles. Together these two findings indicate that in adults, and to a lesser extent in juveniles, there is tonic inhibition of GnRH mRNA by testosterone. Furthermore, since removal of steroid negative feedback and subsequent testosterone replacement results in no change in

GnRH mRNA in the DBB/OVLT or cPOA in juveniles or adults, it can also be assumed that there is not tonic inhibition of GnRH mRNA by gonadal hormones in these brain regions at either age. Finally, the fact that adults are not less sensitive to testosterone negative feedback regulation of GnRH mRNA in the TT/MS than juveniles argues against a decreased ability of testosterone to suppress GnRH mRNA as an explanation for the pubertal rise in gonadotropin release.

Since GnRH neuronal phenotype and afferents vary with brain region (Hoffman *et al.*, 1990; Wu *et al.*, 1992; Mitchell *et al.*, 1999; Prevot *et al.*, 2000), it is not surprising that puberty and testosterone have a differential impact on GnRH mRNA across the regional subpopulations of GnRH neurons. Brain region-dependent changes in GnRH mRNA in response to puberty and testosterone negative feedback are consistent with data published from this and other laboratories (Chapter 3; Spratt *et al.*, 1997; Tang *et al.*, 1997). In the current study these two variables affected GnRH mRNA exclusively in the dissection that included the tenia tecta and MS GnRH neurons. This finding corresponds well with previous results from the *in situ* hybridization experiment (Chapter 3), in which GnRH mRNA was most robustly reduced by testosterone in the tenia tecta, and to a

lesser extent in MS. Furthermore, testosterone did not affect *in situ* hybridization signal of GnRH mRNA in the DBB/OVLT or cPOA. Since GnRH neurons in all brain regions project to the median eminence, we assume that they all release GnRH to regulate gonadotropin secretion. Yet, two different methods of quantifying GnRH mRNA lead to the conclusion that GnRH mRNA is most highly regulated in rostral populations of GnRH neurons and that overall, fluctuations in GnRH mRNA do not predict fluctuations in LH secretion. Thus, there may be heterogeneity among GnRH neurons in the relationship between mRNA, protein, and release.

In summary, these data demonstrate a pubertal increase in plasma LH and in GnRH mRNA levels in the tenia tecta and medial septum. The pubertal increase in LH secretion appears to depend on a decrease in sensitivity to steroid negative feedback. Puberty results in decreased sensitivity to testosterone inhibition of plasma LH, but this is not accompanied by a decreased sensitivity to testosterone inhibition of GnRH mRNA. Thus, although testosterone attenuated GnRH mRNA in the TT/MS, the ability of testosterone to do so was not enhanced in juveniles. While these two components of the HPG axis clearly undergo changes in response to puberty and testosterone, they do not

appear to be directly related to one another. Instead, the developmental shift in the set point of negative feedback regulation of gonadotropin secretion may permit increased activity of the GnRH system at puberty, an event that is occurring simultaneously, but possibly through unrelated, steroid-independent mechanisms.

CHAPTER 5: PHEROMONES AND THE GnRH SYSTEM

Introduction

In many species, including humans (Jacob, Hayreh, and McClintock, 2001), various social cues pertinent to reproduction are conveyed to the brain through the vomeronasal and olfactory systems. In rodents, urine or vaginal secretions from the female contain chemosensory stimuli that have a powerful influence over the reproductive neuroendocrine system and behavior in the male (Meredith, 1998). Presenting a receptive female to the male induces gonadal steroid release and initiates mating behavior from the male. GnRH is thought to play a critical role in these responses (Meredith, 1998). Interruption of chemosensory processing (e.g., vomeronasectomy) blocks both the rise in androgens and the behavioral response to females (Wysocki *et al.*, 1991; Meredith *et al.*, 1992; Pfeiffer and Johnston, 1994), and central microinjection of GnRH reinstates behavior in these animals (Meredith *et al.*, 1992; Fernandez-Fewell *et al.*, 1995).

The neuroendocrine response to female pheromones has been

investigated in rodent species. In male Syrian hamsters, exposure to female pheromones causes a rise in plasma testosterone 30-60 min later (Macrides *et al.*, 1974;Wirsig-Wiechmann, 1993;Pfeiffer *et al.*, 1994;Romeo *et al.*, 1998). This is assumed to occur because of an elevation in plasma LH secondary to increased release of GnRH. However, while an elevation in LH following exposure to female urine has been documented in mice (Coquelin *et al.*, 1984) and rats (Graham *et al.*, 1980), evidence for such a response in hamsters is lacking. Unpublished studies from our lab have consistently demonstrated statistically non-significant trends toward elevated plasma LH following exposure of males to vaginal secretions from females. The most probable reason for an ambiguous LH response is that the pulsatile nature of LH results in inherent individual variability, which potentially precludes detection of group differences in mean LH in terminal blood samples. In addition, the timing and amplitude of the LH response may vary across animals. One way to resolve this issue is to obtain frequent blood samples from individual animals following exposure to pheromones, which allows for comparison of pheromone-induced changes in plasma LH within an animal.

Evidence for GnRH's role in behavior comes from research in

which *icv* administration of GnRH reversed the impairment of male sexual behavior brought about by vomeronasalectomy (Wysocki *et al.*, 1991; Meredith *et al.*, 1992; Pfeiffer *et al.*, 1994; Fernandez-Fewell *et al.*, 1995). GnRH has also been used to condition a place preference in males (de Beun *et al.*, 1991), suggesting that it may have rewarding properties and be involved in motivation aspects of behavior. These studies argue for GnRH's involvement in chemosensory processing and behavior, but do not provide answers to how the sensory information is relayed to and regulates the GnRH system. Attempts to utilize *c-fos* expression as a marker of neuronal activity in GnRH neurons in males have not been successful, and therefore have not provided answers to questions (Meredith, 1998).

The goals of the current study were two-fold: 1) to document and characterize the LH response of male hamsters to female pheromones and 2) to investigate whether pheromone exposure results in brain region-dependent increases in GnRH mRNA. In order to address these questions, two separate experiments were carried out using adult male Syrian hamsters. First, animals were fitted with jugular catheters in order to obtain serial blood samples prior to and following exposure to cotton swabs containing female pheromones or

control cotton swabs. Second, animals were presented with female pheromones, and at 0, 60, or 120 min after exposure brains were collected for *in situ* hybridization analysis of GnRH mRNA within the tectum tectum, MS, DBB/OVLT, and cPOA.

Methods

Experiment 1: Time course of LH response to female pheromones in adult males.

Animals

Fourteen sexually naive adult male Syrian hamsters (Charles River, Kingston, NY) were used in this study. Animals were singly-housed in clear polycarbonate cages (30.5 X 20.5 X 30.5 cm). All animals had *ad libitum* access to food (Teklad Rodent Diet No. 8640, Harlan, Madison, WI) and water throughout the study. The vivaria were on a 14 hr light/10 hr dark light-dark schedule (lights on at 0600 hr EST) and the temperature was maintained at 21 ± 2 °C. All animals were treated in accordance with the NIH Guide for the Care and Use of Laboratory Animals, and the protocols were approved by the Michigan State University All-University Committee for Animal Use and Care.

Jugular Catheterizations

Cateterization and blood sampling protocols were modifications of the procedures used in (Gillespie, van der Beek, Mintz, Mickley, Jasnow, Huhman, and Albers, 1999) for repeated blood sampling. Under sodium pentobarbital anesthesia (80 mg/kg, *ip*), animals were fitted with catheters into the right jugular vein. Catheters were made from 7 cm lengths of silastic tubing (Dow Corning, Midland, MI, $od=0.037$ in $id=0.020$ in), and a silastic cuff was secured with a small amount of super glue 2.5-2.8 cm from the proximal (animal) end of the catheter, which was bevel-cut for easier insertion into the jugular vein. A piece of L-shaped metal tubing (22 guage) was attached to the opposite end of the tubing. The catheter was inserted into a small incision within the jugular vein and held in place by suture ties on either side of the cuff. The entire catheter was subcutaneous, except the metal portion, which exited from animal's back, at the nape of the neck (secured in place by wound clips and super glue). This metal connector allowed for the animal to be easily hooked up to a long piece of polyethylene tubing ($od=0.038$ in $id=0.023$ in, Becton Dickinson and Company, Sparks, MD) on the day of blood sampling, so that he would not have to be tethered after surgery and could freely move

around his home cage throughout the experiment. In between surgery and blood sampling, the distal 2-3 cm portion of the catheter was filled with a viscous heparinized solution containing Polyvinyl Pyrrolidone (PVP, mol wt 40,000 Sigma, St. Louis, MO), and the metal connector was capped with a short piece of PE tubing closed off at one end. PVP helped keep the catheter patent so that the animals could be allowed a few days recovery after surgery before blood sampling.

Blood Sampling and Experimental Design

On the day of blood sampling, the animal was briefly restrained, the polyethylene cap was removed, and a long piece of polythene tubing filled with heparinized sterile saline was attached to the metal connector. This tubing was connected to 22 gauge blunted needle on a 3 cc syringe, which was used to draw up the PVP followed by a small amount of blood. The volume drawn out was replaced with heparinized saline (0.3-0.5 cc).

Blood sampling began 15-45 min later (~2-3 hr before lights out, 1300). The animal remained in his home cage throughout the sampling procedure. Four baseline samples were taken (5 min apart, 0.2 cc blood/sample) and a cotton swab (containing either vaginal secretions from estrous female hamsters or left dry) was presented

during the 5th baseline sample. Blood sampling continued at the same rate (0.2 cc, every 5 min) until 30 min after swab exposure. Three more samples were taken at 15 min intervals so that the last sample was withdrawn 75 min after the swab was first presented to the animal, and 95 min after baseline blood sampling began. Throughout the sampling period, the animal was given back his own red blood cells (diluted with heparinized saline), which were obtained following centrifugation and removal of plasma from earlier samples. Pilot work demonstrated that blood replacement did not alter plasma LH levels.

Following the sampling period, the animal was briefly restrained, the tubing was removed, a small amount of PVP was injected into the catheter, and the PE cap was replaced. When possible, animals were used twice for blood sampling (allowing at least 4 days between sampling). In an attempt to randomize experience, animals were exposed to either pheromone swabs for both sampling periods, control swabs for both sampling periods, a pheromone swab for the 1st and a control swab for the 2nd sampling period, or a control swab for the 1st and a pheromone swab for the 2nd sampling period. Of the 14 animals, 8 had patent catheters and could be used for blood sampling. One of these 8 was eliminated from the study because blood samples weren't

obtainable throughout the entire sampling period and another was eliminated because he died a day after the sampling, indicating that he might have been sick during the sampling period. Of the remaining 6 animals, 3 were sampled twice and 3 sampled from once for a total of 9 sampling periods (5 pheromone swab exposure and 4 blank swab exposure, Table 3) that could be used to generate time response curves.

Plasma LH Radioimmunoassays

Plasma LH levels were determined in single samples for in two assays using the methods described in Chapter 3. The intra-assay CVs were 8.7% and 13.1% and the inter-assay CV was 11.5%. The minimum detectable levels of LH were 0.38 ng/ml and 0.39 ng/ml.

Data Analyses

The data from each sampling period were plotted as percent change from baseline. Baseline was determined for each sampling period by averaging the 3rd, 4th, and 5th baseline samples (or 2 of these, when 3 were not available). The percent change from baseline was then calculated for each sample after this point, for each individual profile. Since data were not independent (e.g., two sampling periods generated from the same animal), non-parametric statistics were used for the analyses. Separate Kruskal-Wallis tests were used to

Table 3. Sampling periods and swab exposure treatments of animals used to generate time response curves.

Animal	1st Sampling	2nd sampling
95	blank	---
104	blank	---
105	blank	blank
594	pheromone	pheromone
595	pheromone	pheromone
976	pheromone	—

investigate plasma LH changes across time following exposure to pheromone and following exposure to control swabs. A Mann-Whitney U test was used to compare plasma LH levels following exposure to pheromone versus control swabs, collapsed across time. Differences were considered statistically significant when $p \leq 0.05$.

Experiment 2: Pheromonal regulation of GnRH mRNA in adult males.

Animals

Fifteen sexually naive adult male Syrian hamsters were obtained from Charles River (Charles River, Kingston, NY). Animals were singly-housed in clear polycarbonate cages (37.5 X 33 X 17 cm. All animals had *ad libitum* access to food (Teklad Rodent Diet No. 8640, Harlan, Madison, WI) and water throughout the study. The vivaria were on a 14 hr light/10 hr dark light-dark schedule (lights on at 2300 hr EST) and the temperature was maintained at 21 ± 2 °C. All animals were treated in accordance with the NIH Guide for the Care and Use of Laboratory Animals, and the protocols were approved by the Michigan State University All-University Committee for Animal Use and Care.

Experimental Design

Between 0900 and 1200 cotton swabs containing vaginal

secretions from estrous females were dropped into animals' cages. Animals were killed by decapitation at 0 (no swab dropped), 60, and 120 minutes after exposure to the pheromone containing swab (n=5/time point). The actual clock time of exposure was counter-balanced across animals from the different groups in order to control for the effects of circadian time on plasma LH and testosterone. Terminal blood samples were obtained for measurement of LH and testosterone by radioimmunoassay, and brains were collected, snap-frozen on dry ice, and stored at -80°C until sectioning on the cryostat. Every other coronal section (10 µm) was collected and thaw-mounted onto poly-L-lysine coated slides to produce a total of four sets. Slides were stored with desiccant at -80°C until *in situ* hybridization histochemistry was performed.

GnRH mRNA In Situ Hybridization Histochemistry

One set of sections from each brain was processed for *in situ* hybridization using the protocol described in Chapter 3.

Microscopic Analysis

All analyses were carried out by one investigator blind to the treatment conditions using a protocol similar to that described in Chapter 3. However, in addition to obtaining the area of silver grains

covering the Nissl-defined cell body covered by silver grains ("cell grain area"), the area of the entire cluster of silver grains associated with a particular cell (which sometimes extended beyond the Nissl-defined cell body; "spread grain area") was also measured in the current study. Both analyses were performed in order to determine if the pattern of results was similar when more (cell grain area) or less (spread grain area) conservative estimates of labeling were used. Thus, three variables were measured in each animal in the current study: number of labeled cells, cell grain area, and spread grain area within the tenia tecta, MS, DBB/OVLT, and cPOA.

Plasma Hormone Radioimmunoassays

Plasma LH levels were measured in duplicate in a single assay, using the methods described in Chapter 3. The intra-assay CV was 12.4%. The lowest detectable level of LH was 0.73 ng/ml.

Plasma testosterone levels were measured in duplicate samples using the methods described in Chapter 3. The intra-assay CV was 16.4% and minimum detectable was 0.1 ng/ml.

Data Analyses

Mean number of labeled cells, mean cell grain area, and mean spread grain area for the tenia tecta, MS, DBB/OVLT, and cPOA were

compared across the different time points using separate one-way ANOVAs for each brain region. Data were also analyzed by combining data across brain regions. Plasma LH and testosterone levels were compared between the different groups using one-way ANOVAs. Significant main effects were probed using Fisher's PLSD tests. Differences were considered significant when $p \leq 0.05$.

Results

Experiment 1: Time course of LH response to female pheromones in adult males.

Examples of individual LH profiles following exposure to pheromone versus control swabs are shown in Figure 18. There was a rise in plasma LH that began around 10 min after exposure to pheromone (Figure 18 A). This rise was seen in all animals to which pheromones were presented, although individual responses differed slightly with respect to the magnitude and timing of elevations in LH across sampling periods. Plasma LH levels remained elevated until 25-30 minutes after the pheromone-containing swab was first introduced. Plasma LH levels did not rise when animals were exposed

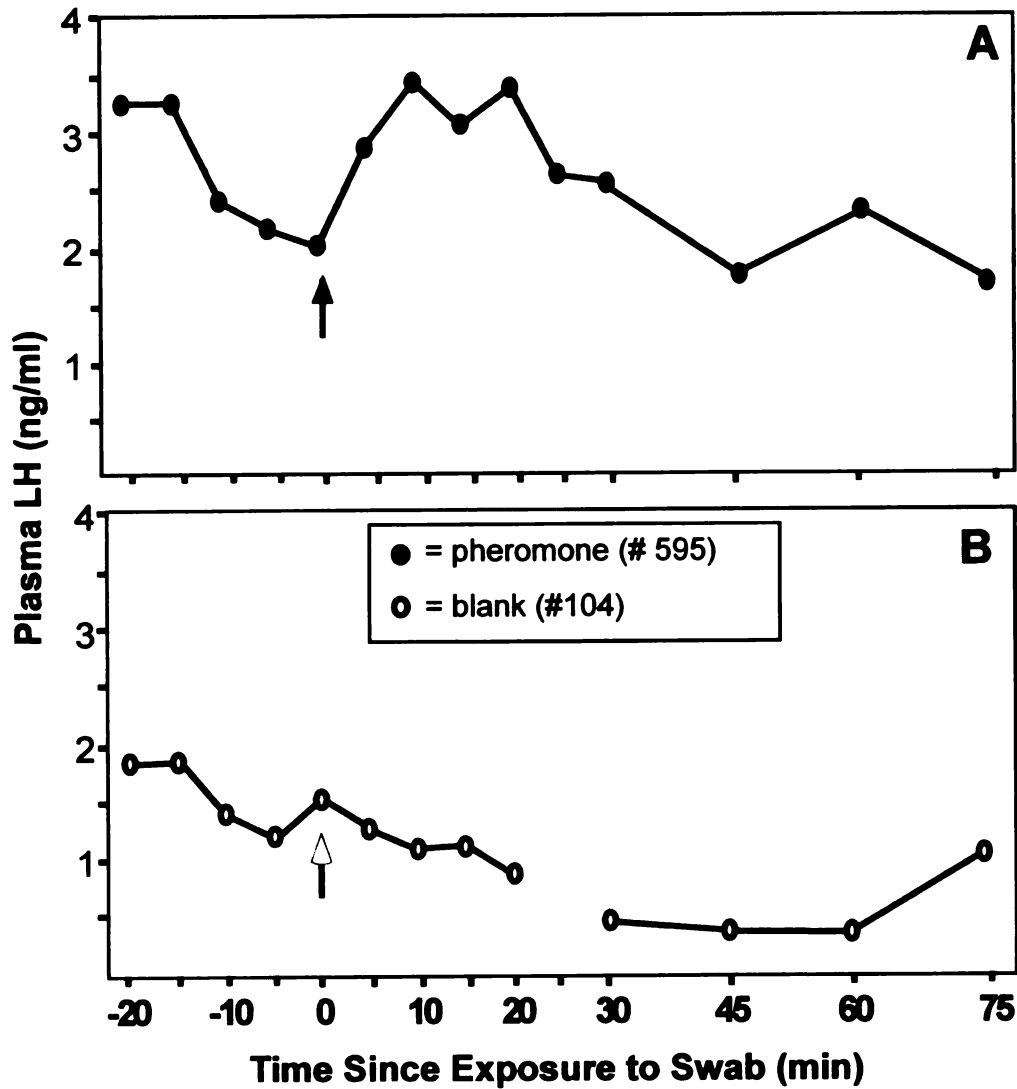


Figure 18. Representative example plasma LH profiles following exposure to a cotton swab containing pheromone (A) or a control swab (B). The arrows indicate delivery of the swab (pheromone=black arrow, blank=clear arrow).

to control swabs (Figure 18 B). Figure 19 shows sampling periods, which are grouped according to swab exposure and expressed as % change from baseline. Nonparametric analyses revealed a significant change in plasma LH from baseline across time in response to pheromone exposure ($p \leq 0.05$). Exposure to control swabs did not result in significant changes across time. Overall, there was a greater change from baseline LH levels with pheromone exposure, as compared to control swab exposure ($p \leq 0.05$).

Experiment 2: Pheromonal regulation of GnRH mRNA in adult males

Plasma Hormone Levels

There was not a significant effect of time after pheromone exposure on plasma LH levels (Figure 20). However, there was a significant effect of time after pheromone exposure on plasma testosterone (Figure 21, $p \leq 0.05$). Plasma testosterone was significantly higher at 60 min as compared to 0 min and 120 min after exposure to pheromone.

Number of Labeled Cells

Pheromone exposure did not significantly affect the number of labeled cells in any of the four brain regions, either when analyzed separately or when regions were considered together (Table 4).

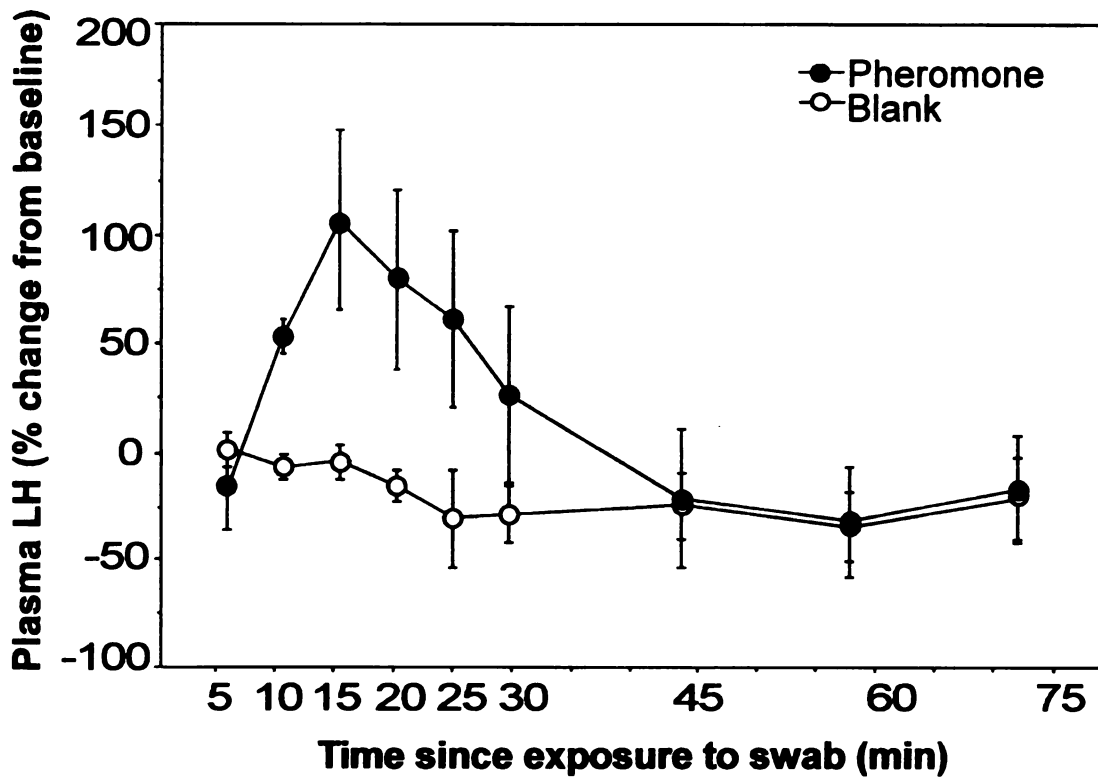


Figure 19. Time response curves of mean (\pm SEM) plasma LH (% change from baseline) following exposure to pheromone or blank swabs. There was a significant increase in plasma LH only after exposure to pheromone ($p \leq 0.05$).

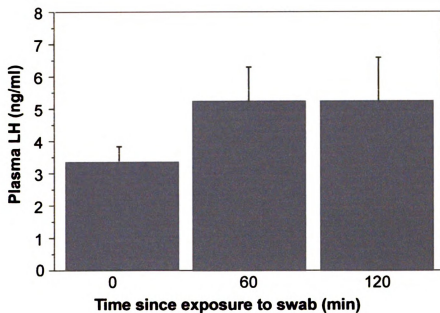


Figure 20. Mean (\pm SEM) plasma LH levels (ng/ml) 0, 60, and 120 min following exposure to swabs containing pheromone. There was not a significant effect of pheromone on LH across time ($p>0.05$).

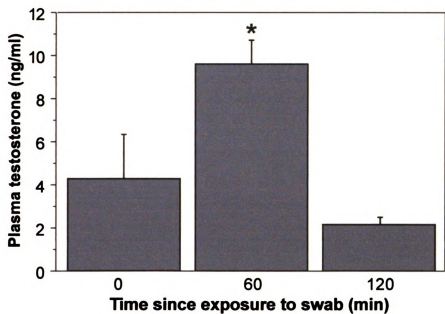


Figure 21. Mean (\pm SEM) plasma testosterone levels (ng/ml) 0, 60, and 120 min following exposure to swabs containing pheromone. Testosterone was significantly elevated 60 min after exposure ($p \leq 0.05$).

Table 4. Mean (\pm SEM) number of GnRH mRNA expressing cells 0, 60, and 120 minutes after exposure to a swab containing pheromone.

Time since exposure to swab (min)	Brain Region (# of labeled cells)				
	Tenia Tecta	MS	DBB/OVLT	cPOA	Total
0	18.67 \pm 3.84	31.80 \pm 4.57	42.00 \pm 11.00	9.00 \pm 2.30	98.67 \pm 22.21
60	9.00 \pm 2.27	38.80 \pm 4.01	46.00 \pm 8.67	9.60 \pm 5.77	102.00 \pm 14.22
120	13.60 \pm 2.52	29.20 \pm 2.08	38.60 \pm 5.80	6.00 \pm 5.52	87.40 \pm 7.47

However, there was a trend (although non-significant, $P=0.13$) of a reduction in the number of labeled cells within the tenia tecta.

Silver Grain Analysis

There was no effect of time following exposure to pheromone on mean cell grain area (0 min= $12.27 \pm 0.87 \mu\text{m}^2$, 60 min= $12.45 \pm 0.91 \mu\text{m}^2$, 120 min= $12.58 \pm 1.35 \mu\text{m}^2$) or mean spread grain area (0 min= $39.32 \pm 0.72 \mu\text{m}^2$, 60 min= $40.99 \pm 5.85 \mu\text{m}^2$, 120 min= $41.00 \pm 5.36 \mu\text{m}^2$) when the four subpopulations were considered together. Figure 22 shows mean cell grain and spread grain areas separately for the tenia tecta, MS, DBB/OVLT, and cPOA. There were no significant effects in any of the four GnRH subpopulations of pheromone exposure on mean cell grain area (left graphs) or mean cell spread area (right graphs).

Discussion

These data demonstrate that chemosensory information from the female impacts the hypothalamic-pituitary-gonadal axis at both the level of plasma LH and testosterone in sexually naive adult male Syrian hamsters. Pheromone exposure results in a rise in plasma LH that peaks at about 15 minutes and a subsequent rise in testosterone by 60

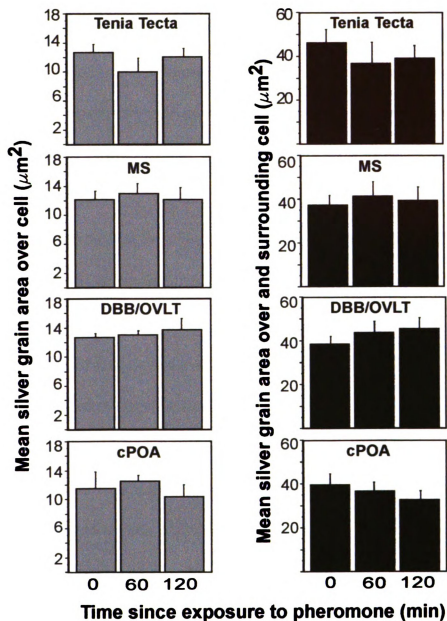


Figure 22. Mean area of silver grains (μm^2) as measured within the boundary of the cell body (left graphs) and within and surrounding the cell body (right graphs) in the tenia tecta, MS, DBB/OVLT, and cPOA of pheromone exposed males. Pheromones did not affect GnRH mRNA, as measured by either index, at any time point following exposure ($p > 0.05$).

minutes after exposure. Activation of the HPG-axis by female pheromones, however, did not result in changes in GnRH mRNA at either 60 or 120 minutes after exposure. Thus, although pheromones likely induce GnRH secretion to result in elevated LH, activation of GnRH neurosecretion is not accompanied by increases in GnRH mRNA at the time points studied.

To our knowledge, this is the first description of an LH response to female pheromones in male Syrian hamsters. Since LH begins to rise within 10 min after presentation of the pheromone stimulus, we infer that activation of the GnRH system is an immediate neural response to the stimulus (Levine and Ramirez, 1982). This timing fits well with a proposed central role of GnRH in male reproductive behavior, which is initiated within 30 seconds of being introduced to a receptive female (Meek *et al.*, 1997; Romeo *et al.*, 2001).

The pheromone-induced rise in testosterone by 60 min corresponds well with previous data from this lab (Romeo *et al.*, 1998). Based on previous studies, testosterone levels are elevated before 60 minutes (Macrides *et al.*, 1974; Pfeiffer and Johnston, 1992; Wirsig-Wiechmann, 1993; Pfeiffer *et al.*, 1994). However, even if testosterone levels are increased earlier, it is not likely that this rise in gonadal

steroids is necessary for reproductive behavior with the female at that time. Since male hamsters often engage in the whole suite of behaviors, including ejaculation, within minutes of being placed with a receptive female, the rise in testosterone 30-60 min after exposure to chemosensory information from the female probably does not play an acute role in behavior, but instead, might have long-term functions (e.g., altering neural or behavioral responses to females in future encounters).

Pheromones did not result in changes in GnRH mRNA, as measured by labeled cell number, mean grain cell area, or mean grain spread area either 60 or 120 min after exposure. It could be argued that changes in GnRH mRNA could be occurring earlier than 60 min, since plasma LH levels are high 15 min following exposure to pheromones. However, in a recent report, GnRH mRNA was not altered in male mice exposed to bedding containing female urine 45 min following exposure, even though plasma LH levels were significantly higher than control-treated animals 45-90 min after exposure (Gore, Wersinger, and Rissman, 2000). Thus, although pheromones clearly affect GnRH release, as indexed by plasma LH, this response does not result in altered levels of GnRH mRNA in these cells.

One important finding from these data is that assessing GnRH mRNA by measuring silver grains within and surrounding the Nissl-defined cell body (spread grain area) provides similar trends as measuring silver grains exclusively within the Nissl-defined body (cell grain area). Thus, the more conservative estimate of silver grain labeling (assessing only those cells that reside over the Nissl-defined cell) does not account for the lack of changes in GnRH mRNA following exposure to pheromones.

Another interesting finding is that there was a trend towards a reduction in cell number and GnRH mean grain area in the tenia tecta at 60 minutes, indicating that GnRH mRNA may be slightly lowered in this cell group following pheromone exposure. On the other hand, perhaps this is not related to pheromone-induced release of GnRH from these cells, but rather to the high levels of testosterone at 60 min. Testosterone reduces GnRH mRNA specifically in the tenia tecta (Chapter 3). Perhaps the rise in testosterone 60 min following pheromone might be high enough to initiate negative feedback reduction of GnRH mRNA levels in these cells.

In summary, the first experiment of this chapter demonstrated that chemosensory information from females induced a rise in plasma

LH from baseline 10-30 minutes after exposure that was followed by a return to baseline levels 15 minutes later. The second experiment demonstrated that pheromones also induced an increase in plasma testosterone by 60 minutes following exposure. Although this hormone response is likely reflecting increased GnRH release shortly after exposure to pheromones, GnRH activation is not reflected in changes in GnRH mRNA. Thus, either the GnRH response is not large enough to stimulate synthesis and measurable changes in mRNA, or the timing of such changes occurs earlier or later than 1-2 hours after exposure to pheromones.

CHAPTER 6:
ANATOMICAL RELATIONSHIPS AMONG GNRH NEURONS
AND MEDIAL AMYGDALA EFFERENTS

Introduction

As stated in the last chapter, an important external signaler of the reproductive neuroendocrine system in male Syrian hamsters is chemosensory information from the female. Female pheromones induce neuroendocrine (rise in LH and testosterone) and behavioral responses from the male, and the GnRH system is thought to be involved in both (Meredith, 1998). How chemosensory information from the periphery reaches GnRH neurons is largely unknown. Much research has focused on how chemosensory information reaches cell groups comprising the behavioral circuit in male Syrian hamsters. This experiment takes advantage of what has been established about the neural circuitry underlying chemosensory processing and sexual behavior in the male Syrian hamster to address questions about how chemosensory information may reach the GnRH system.

When adult males are exposed to vaginal secretions from females, the immediate early gene protein product Fos, a marker of

neuronal activation (Morgan *et al.*, 1991), is expressed in virtually all components of the forebrain circuit underlying male sexual behavior (Fiber, Adames, and Swann, 1993;Fiber and Swann, 1996;Kollack-Walker and Newman, 1997;Swann and Fiber, 1997;Romeo *et al.*, 1998). Stimulated brain regions include the anterior (MeA) and posterior (MeP) portions of the medial amygdala, posteriomedial subdivision of the bed nucleus of the stria terminalis (BNSTpm), and medial preoptic nucleus (MPN).

The current study focused on the efferent projections of the medial amygdala. It has already been established that the anterior portion of the medial amygdala sends moderate projections to the vertical (Gomez *et al.*, 1992;Coolen *et al.*, 1998) and horizontal (Gomez *et al.*, 1992) limbs of the diagonal band of Broca, lighter projections to the medial septum (Gomez *et al.*, 1992), and dense projections to the medial POA (Kevetter and Winans, 1981;Maragos, Newman, Lehman, and Powers, 1989;Gomez *et al.*, 1992;Coolen *et al.*, 1998). All of these areas contain GnRH cell bodies, and chemosensory information could be delivered to the GnRH system via any of these routes.

This experiment was designed to address whether GnRH cells are

innervated by efferents from the medial amygdala. Given the diffuse distribution of GnRH cell bodies, retrograde tract tracing cannot be effectively used to answer questions about neural input to the GnRH system. Instead, anterograde tract tracing was used to determine whether efferents from the amygdala project directly to GnRH cell bodies, and if so, whether projections were to cells within specific GnRH subpopulations. Biotinylated dextran amine (BDA) was used as a neuronal tract tracer in combination with GnRH ICC to determine whether projections from medial amygdala make apparent contacts onto GnRH cell bodies. GnRH subpopulations were analyzed separately to determine whether the proportion of GnRH neurons receiving medial amygdala appositions varied with brain region.

Since immunocytochemical procedures in the current study were designed to optimize GnRH immunoreactivity, and each GnRH cell was individually analyzed at high magnification for close appositions from BDA-immunoreactive fibers anyway, close appositions from GnRH-immunoreactive fibers were also assessed in these brain sections. The close proximity of GnRH neurons in the tenia tecta to GnRH immunoreactive fibers (discussed in Chapters 2 and 3) suggests a greater amount of GnRH-GnRH communication within this

subpopulation. Thus, the proportion of GnRH neurons receiving close appositions from GnRH processes was determined and comparisons were made across the four GnRH subpopulations.

Methods

Animals

Sexually naive adult male Syrian hamsters (Charles River, Kingston, NY) were used in this study. Animals were group-housed until stereotaxic surgery and were singly housed afterwards. Cages were made of clear polycarbonate (37.5 X 33 X 17 cm) and contained wood chips (Aspen Chip Laboratory Bedding, Warrensburg, NY). All animals had *ad libitum* access to food (Teklad Rodent Diet No. 8640, Harlan, Madison, WI) and water throughout the study. The vivaria were on a 14 hr light/10 hr dark light-dark schedule (lights on at 0600 hr EST) and the temperature was maintained at 21 ± 2 °C. Animals were treated in accordance with the NIH Guide for the Care and Use of Laboratory Animals, and the protocols were approved by the Michigan State University All-University Committee for Animal Use and Care.

Iontophoretic Injections

On the day of surgery, animals were anesthetized with sodium pentobarbital (80 mg/kg). The head was shaved and positioned in a stereotaxic apparatus (David Kopf Instruments, Tujunga, CA) and 0.03 cc of local anesthetic, lidocaine HCL 2% and epinephrine (1:10,000 Injection USP, Abbot Laboratories, North Chicago, USA) was injected under the skin just before surgery. Biotinylated dextran amine (BDA, 10%, MW 10,000 Sigma, St. Louis, MO) was delivered through a glass micropipette, which was pulled from Kwikfil microtubules (World Precision, Sarasota, FL) so that the tip had an inner diameter of 10-20 μm . The micropipette was slowly lowered into the brain to the medial amygdala (0.5 mm anterior and 2.8 mm lateral to bregma, and 6.5 mm ventral to dura) alternating sides randomly among animals. BDA was iontophoretically injected using a current source (Midguard, Stoelting, Wood Dale, IL) that delivered +5 μA positive (cathodal) alternating current (at 7 sec on/7 sec off intervals). After the injection, the current was turned off and micropipette left in place for 10 min. A 0.1 μA of negative (anodal) current was applied as the micropipette was slowly withdrawn from the head to prevent diffusion of BDA out of the micropipette.

Post-Injection Survival Time

Although tract tracers generally have a predominant direction of transport, either retrograde or anterograde, transport can go in both directions (Lanciego, Luquin, Guillen, and Gimenez-Amaya, 1998). Analysis after different post-injection survival times can help determine the degree to which a tracer will result in retrograde versus anterograde labeling (Angelucci, Clasca, and Sur, 1996; Lanciego *et al.*, 1998). Therefore, a pilot study was performed in which animals were killed at 2, 4, 7, and 14 days following BDA injection in order to determine the survival time for that resulted in the least amount of retrograde staining, while allowing enough time anterograde transport from the amygdala to the most rostral region of interest in this study, the tenia tecta. A survival time of 7 days was selected for several reasons. First, if animals were killed 2 days after the injection, BDA was diffusely spread across the neuropil, rather than within a defined group of cell bodies, making the center of the injection difficult to assess (Figure 23, top two panels). This was somewhat improved by 4 days, but the boundaries of the injection sites were the most distinct following 7- and 14-day survival times. Second, retrogradely-filled cells were found in areas outside the injection site following 4,

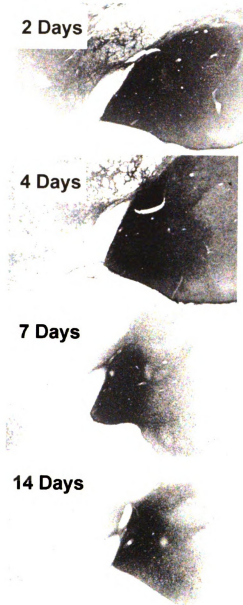


Figure 23. Photomicrographs showing medial amygdala BDA injection sites in representative animals killed 2, 4, 7, and 14 days after surgery. Survival times of 2 and 4 days resulted in diffuse spread of BDA. The injection sites were more distinct 7 and 14 days after surgery.

7, and 14 day survival times. Thus, there was no advantage of selecting a 4-day survival time given that the injection site was clearer at 7 and 14 days. Since 7 days resulted in sufficient anterograde transport (from the amygdala to rostral forebrain areas), this survival time was chosen for the experiment.

Perfusion and Histology

Animals were overdosed with sodium pentobarbital and perfused intracardially with 100 ml Buffered Saline Rinse, followed by 150 ml 4% paraformaldehyde. Brains were removed from the skull and post-fixed in 4% paraformaldehyde. Pilot work revealed that post-fixing brains for 12 hr, as compared to 1 and 4 hr, improved immunocytochemical staining of GnRH cell bodies and fibers, especially in the tenia tecta and MS. Following post-fixation, brains were submerged into 30% sucrose for 24 hours. Four sets (40 μ m) of coronal sections were cut using a cryostat and stored in phosphate buffer/sodium azide at 4°C if immunocytochemistry was run within a few weeks or in cryoprotectant at -20°C for longer storage periods. Storage of sections did not affect immunocytochemical staining of BDA or GnRH. One set of tissue was processed and analyzed from each animal.

A double labeling immunocytochemical procedure was employed to visualize BDA and GnRH in the same sections. A protocol was generated using modifications of published methods described to visualize BDA (Coolen *et al.*, 1998) and GnRH (Chapter 2). Sections were washed several times in 0.1 M PBS/2% Triton X-100 (PBS-TX) and incubated in 3% H_2O_2 /methanol for 30 minutes at room temperature to block endogenous peroxidase activity. They were then rinsed with 0.1 M PBS-TX and incubated in with normal goat serum (1:67, Vectastain Elite Kit, Vector) for 30 minutes at room temperature. Immediately following this step, sections were submerged in vials containing LR-1 anti-GnRH primary antiserum (1:10,000 in PBS-TX, R. Benoit, Montreal General Hospital) and incubated for 24 hours at -4° C.

Following incubation in anti-GnRH primary antiserum, sections were processed through a series of steps to visualize BDA staining. Sections were removed from vials containing the antisera and rinsed several times in 0.1 M PBS, followed by an incubation in ABC-HRP, 1:800, Vectastain ABC Elite Kit, Vector) for 1 hour. Tissue was then rinsed several times in 0.1 M PBS and the HRP was visualized with NiCl-enhanced 3,3'-diaminobenzidine chromagen to produce a blue-black product over BDA labeled neurons and axons. Most

photomicrographs in this chapter are displayed in color so that GnRH (black) and GnRH (brown) staining can be differentiated from one another.

After completion of this reaction, sections were taken through the rest of the steps for visualization of GnRH. First, tissue was rinsed several times in 0.1 M PBS and incubated at room temperature in 1% H₂O₂/PBS for 10 minutes to block unreacted HRP from the BDA visualization steps. Sections were then rinsed several times in 0.1 M PBS-TX and incubated for 120 minutes at room temperature in secondary biotinylated goat-anti rabbit antiserum (1:200, Vectastain ABC Elite Kit, Vector). This was followed by several rinses in 0.1 M PBS-TX and a 60 min incubation at room temperature in ABC-HRP (1:100 Vectastain ABC Elite Kit, Vector). Tissue was rinsed two times in 0.1 M PBS-TX, once in 0.05 M Tris Buffered Saline, and HRP was visualized with 3,3'-diaminobenzidine chromagen to produce a brown product over GnRH labeled neurons and axons. Sections were mounted onto glass slides, dehydrated in increasing concentrations of alcohol, cleared in Hemo-De (Fisher, Pittsburgh, PA), and coverslipped for microscopic analysis.

Microscopic Analysis

Eleven animals were selected for analysis of BDA and GnRH appositions onto GnRH neurons. Nine of the animals had injection sites that were within or encompassed the medial amygdala. Two had injections that were on the medial side of the optic tract within the substantia innominata (SI) and served as controls. Sections from these brains were examined under brightfield illumination. GnRH cells were analyzed in the tenia tecta, MS, DBB/OVLT, and cPOA. Cells were first located and counted at 200x magnification. Each cell was then analyzed individually at a magnification of 1000x using a 100x oil objective and viewing through 10x eyepiece.

Since synaptic contacts onto GnRH neurons could not be established using light microscopy, close appositions onto GnRH neurons were assessed in the current study. The criteria for identifying a GnRH neuron with close appositions from a GnRH process ("GnRH-GnRH cell") were as follows. GnRH appositions most often appeared as large brown dots (similar in size to the boutons along GnRH axons), and less often as finer processes, onto a GnRH cell body, or dendritic or axonal process. The GnRH fiber had to be distinguishable from the cell body (i.e., not just a region of punctate GnRH-immunoreactive staining

within that particular cell), but had to appear to be contacting the GnRH neuron at 1000x magnification. Often, processes would appear to be in close apposition to a GnRH cell under lower magnification (e.g., 500x), but at 1000x magnification it became evident that the process was either above or below the cell. Thus, a 3-dimensional view of the entire cell was obtained by adjusting the focus through the depth of the cell, which allowed for the elimination of false positives (when the processes appeared to be closely apposed to the cell, but actually was just above or below it). The place in which the apposition and GnRH neuron "contacted" had to come into focus together in the same focal plane in order to be considered a close apposition. Each GnRH cell with one or more close appositions from GnRH-immunoreactive processes was counted as a single GnRH-GnRH cell.

Requirements for identifying close appositions of BDA onto GnRH neurons were essentially the same as for GnRH appositions (e.g., the place where the BDA apposition touched the GnRH cell had to be visible in the same focal plane at 1000x), except the requirements were somewhat stricter. Black dots and small lines that resided exclusively within the boundaries of GnRH cells were not counted. The reason for a more conservative criteria for BDA appositions is that GnRH-

immunoreactive staining is sometimes characterized by very dark brown staining around the perimeter of the cell body and axons, which is hard to distinguish from black immunoreactive staining. In order to avoid mistaking this staining for BDA appositions, a BDA-immunoreactive processes had to be visible approaching the GnRH cell and also be visible in the same focal plane as the GnRH cell (at the place of "contact") in order to be considered a BDA close apposition. Each GnRH cell with one or more close appositions from a BDA-immunoreactive process was counted as a single BDA-GnRH cell.

For each animal, the number of GnRH neurons in the tenia tecta, MS, DBB/OVLT, and cPOA was first counted on each side of the brain (ipsi- and contralateral to the injection). The number of GnRH-GnRH and BDA-GnRH cells was then assessed for the different subpopulations on each side of the brain. These values were then used to determine GnRH-GnRH and BDA-GnRH ratios. The GnRH-GnRH ratio was calculated by dividing the number of GnRH-GnRH cells by the total number of GnRH neurons (within a subpopulation on the ipsi or contralateral side of the brain). The BDA-GnRH ratio was calculated by dividing the number of BDA-GnRH cells by the total number of GnRH neurons (within a subpopulation on the ipsi or contralateral side of the

brain). For statistical comparisons, mean GnRH-GnRH ratios and BDA-GnRH ratios were determined for animals within a group (SI versus medial amygdala injected animals). Since injection site did not alter GnRH-GnRH ratios, mean GnRH-GnRH ratios from all animals were combined for statistical analyses. Comparisons between mean GnRH-GnRH ratios on the ipsi- versus contralateral side of the brain and across GnRH subpopulations were made using a repeated measures 2 (side of brain) x 4 (brain region) ANOVA. A repeated measures 2 (side of brain) x 4 (brain region) ANOVA was used to compare mean BDA-GnRH ratios on the ipsi- versus contralateral side of the brain and across GnRH subpopulations in animals with medial amygdala injections. Few BDA-GnRH cells were found in animals with SI injections and these animals were not included in the mean BDA-GnRH ratio statistical comparisons. Significant main effects were probed using Fisher's PLSD tests. Differences were considered significant when $p \leq 0.05$.

Results

An average of 133.78 ± 6.84 immunoreactive GnRH cells were analyzed for each animal. The mean number of cells varied across areas: tenia tecta, 26.90 ± 2.80 ; MS, 48.09 ± 3.00 ; DBB/OVLT, 37.27 ± 3.43 ; and cPOA, 21.55 ± 2.95 .

BDA Appositions

There was some variation in the size and location of injection sites, but in all cases of injections into the amygdala, a considerable portion of the injection included the medial amygdala. Examples of two medial amygdala injection sites (one small and one large) and one SI injection site are shown in Figure 24. In all medial amygdala injected animals, fiber tracts were seen connecting the medial amygdala, BNST, and MPN, as previously described (Gomez *et al.*, 1992; Coolen *et al.*, 1998). Interestingly, GnRH and BDA labeled fibers were found traveling in separate groups, but beside one another, in the stria terminalis (Figure 25). GnRH fibers were also found within the stria terminalis in the two substantia innominata injected brains, but the BDA fiber tract patterns seen in animals with medial amygdala injections (Gomez *et al.*, 1992; Coolen *et al.*, 1998) were not evident in the SI injected animals. A few GnRH processes

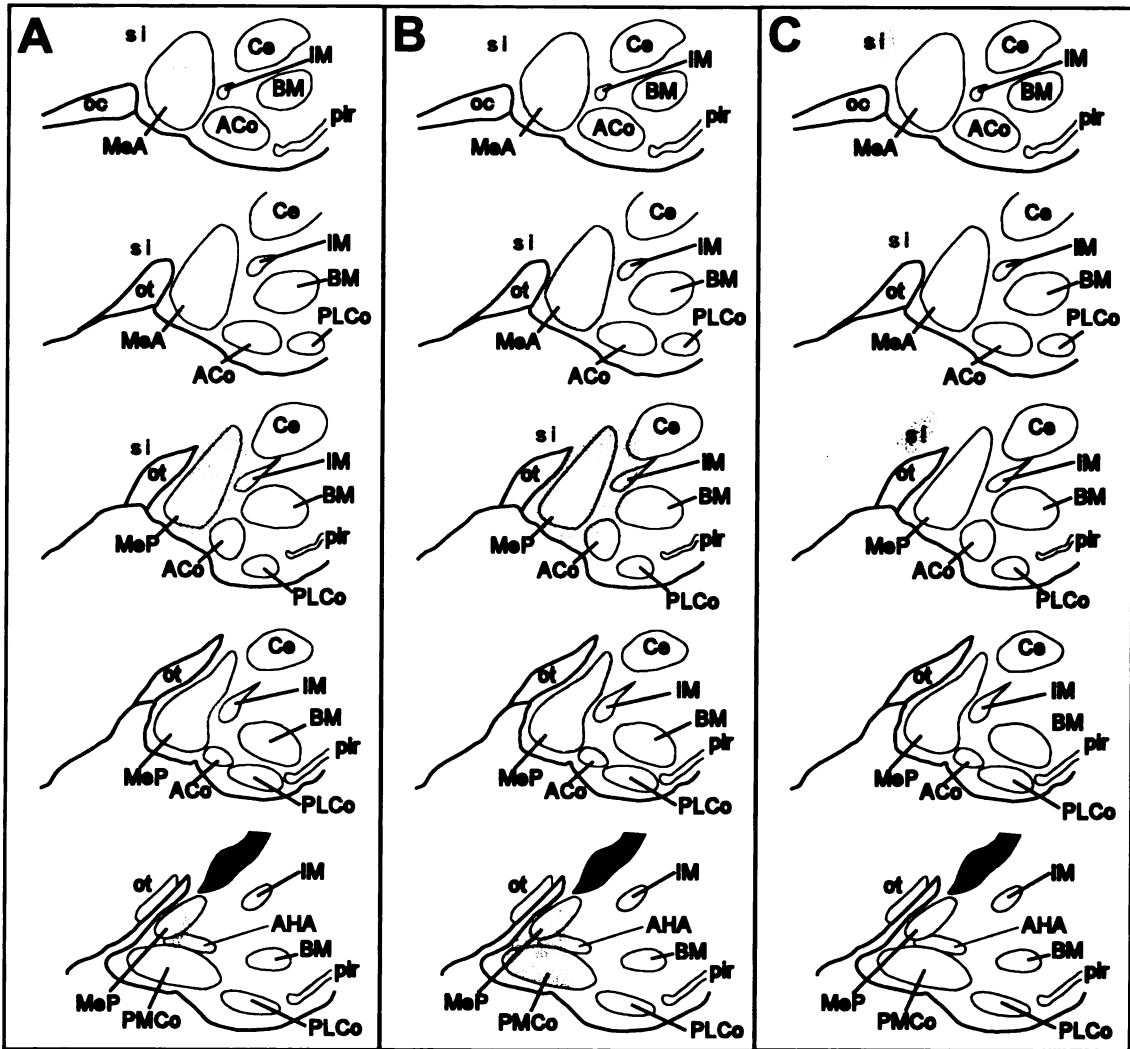


Figure 24. Schematic representations of animals with BDA injections into the medial amygdala (A, #806; B, #809) and substantia innominata (C, #810). Animal #806, #809, and #810 had BDA-GnRH ratios of 1.0, 0.9, and 0, respectively, in the cPOA ipsilateral to the injection. *Abbreviations:* ACo, anterior cortical nucleus of the amygdala; AHA, amygdalohippocampal area; BM, basolateral nucleus of the amygdala; Ce, central nucleus of the amygdala; IM, intercalated mass cell; MeA, anterior medial amygdala; MeP, posterior medial amygdala group; oc, optic chiasm; ot, optic tract; PMCo, posteromedial cortical nucleus of the amygdala; PLCo, posterolateral cortical nucleus of the amygdala; si; substantia innominata.

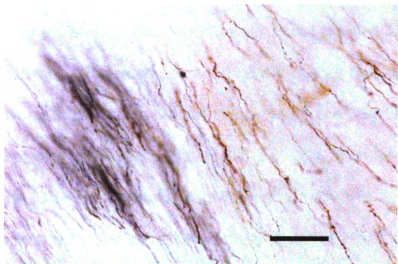


Figure 25. GnRH and BDA fibers in the stria terminalis from an animal with a medial amygdala BDA injection. Bar, 20 μ m.

were also found within the amygdala, and in one case, a GnRH axon was double-labeled with BDA (presumably due to retrograde transport, Figure 26).

In animals with injections into the medial amygdala, BDA-labeled fibers closely apposed GnRH neurons in all four brain regions. Close appositions of BDA onto GnRH neurons were found on the cell body (Figure 27, top), and on the dendritic or axonal (Figure 28) processes of GnRH neurons. There was a significantly higher proportion of BDA-GnRH neurons in the same side of the brain as the BDA injection, independent of brain region (Figure 29, $p \leq 0.05$). Few appositions were found on the side contralateral to the injection (Figure 29). On the side ipsilateral to the medial amygdala injection, cPOA had a higher proportion of BDA-GnRH cells, as compared to the tenia tecta, MS, and DBB/OVLT (Figure 29, $p \leq 0.05$). BDA-GnRH cells were seldom found on either side of the brain or in any of the GnRH subpopulations in the two animals with substantia innominata injections (data not shown).

GnRH Appositions

GnRH appositions onto GnRH neurons were evident in all brain regions. Figure 27 (bottom) shows a GnRH neuron with two close

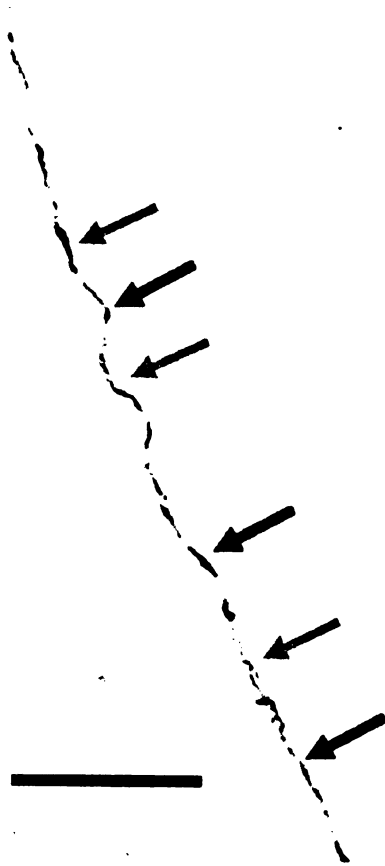


Figure 26. GnRH (gray arrows) and BDA (black arrows) double labeled fiber from an animal with a medial amygdala injection. Bar, 20 μ m.

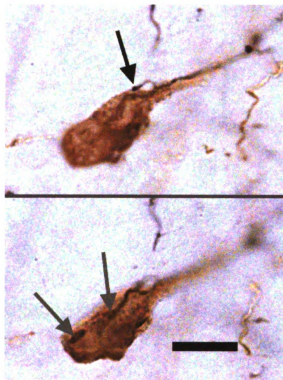


Figure 27. Photomicrographs of a GnRH cell in the cPOA viewed in different focal planes from an animal with a medial amygdala BDA injection. The black arrow indicates a BDA close apposition and gray arrows indicate GnRH close appositions onto the same cell. Bar, 10 μm .

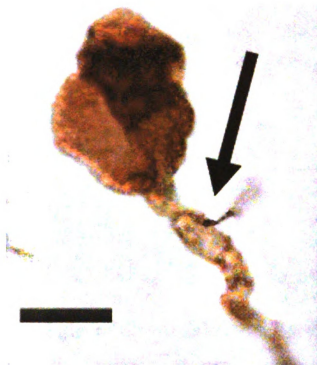


Figure 28. Photomicrograph of a GnRH neuron in the tenia tecta with a BDA apposition onto the axon from an animal with a medial amygdala BDA injection. Also note that a second GnRH cell body is in close apposition to this GnRH neuron. Bar, 10 μ m.

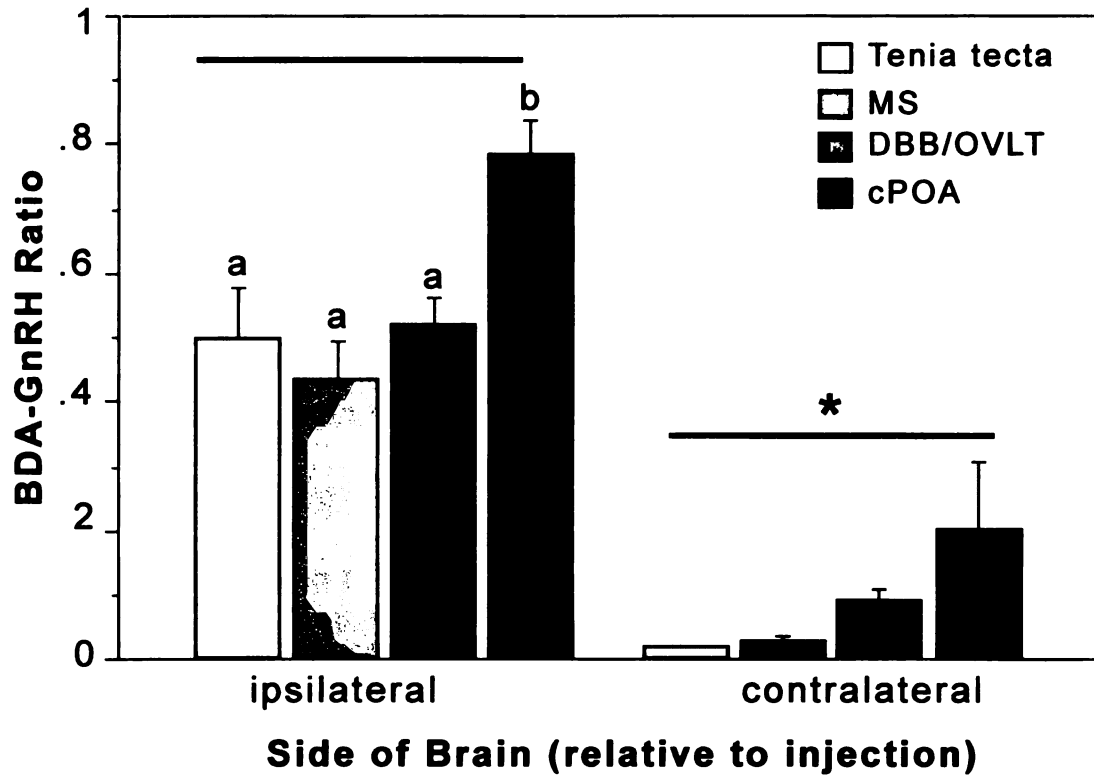


Figure 29. Ratio of the number of GnRH cells with BDA appositions to the total number of GnRH cells within the tenia tecta, MS, DBB/OVLT, and cPOA on the side of the brain ipsi- or contralateral to the BDA injection into the medial amygdala. Independent of brain region there was a significantly higher proportion of BDA appositions onto GnRH neurons on the side ipsilateral to the injection (asterisk, $p \leq 0.05$). On the ipsilateral side, cPOA had a higher BDA-GnRH ratio compared to the tenia tecta, MS, and DBB/OVLT (b is different from a, ($p \leq 0.05$)).

appositions onto the cell body from GnRH processes. In most cases, GnRH neurons in the tenia tecta and MS had multiple GnRH appositions (Figure 30), however the number of appositions per cell were not quantified. Analysis of mean proportion of GnRH cells receiving one or more close GnRH appositions is summarized in Figure 31. There was no difference between the ipsi- or contralateral side of the brain in the GnRH-GnRH ratio ($p > 0.05$). Therefore, ipsi- and contralateral GnRH-GnRH ratios in the tenia tecta, MS, DBB/OVLT, and cPOA were averaged and these data are shown in Figure 31. There was a higher proportion of GnRH-GnRH cells in the tenia tecta and MS as compared to the DBB/OVLT and cPOA ($p \leq 0.05$). There were no significant differences between GnRH-GnRH ratios in the tenia tecta and MS ($p > 0.05$), or between GnRH-GnRH ratios in the DBB/OVLT and cPOA ($p > 0.05$). An interesting phenomenon was noted in these sections. In all brains analyzed, a small number of GnRH cell bodies was found adjacent to one another (Figures 28 and 32). In some cases, as many as four GnRH cell bodies were found closely apposed. This phenomenon was seen in all GnRH subpopulations, but to a lesser extent in the cPOA, in which closely apposed GnRH cell bodies were found in only a few animals.

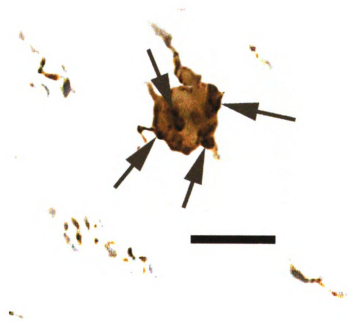


Figure 30. Four GnRH close appositions (gray arrows) onto a single GnRH neuron in the tenia tecta. Bar, 10 μm .

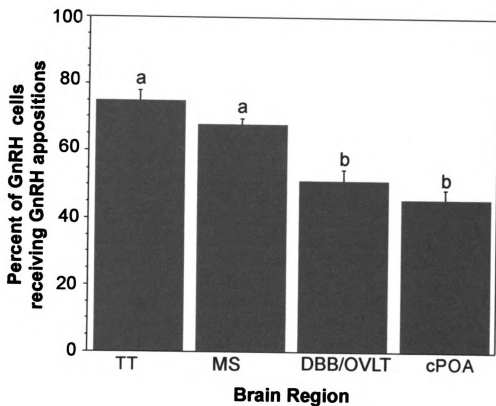


Figure 31. Mean GnRH-GnRH ratios (both ipsi - and contralateral sides combined) in the tenia tecta, MS, DBB/OVLT, and cPOA. The proportion of GnRH cells with one or more GnRH appositions was significantly greater in the tenia tecta and MS as compared to the DBB/OVLT and cPOA (a is different from b, $p \leq 0.05$).



Figure 32. Three closely apposed GnRH cell bodies (gray arrows) within the tenia tecta. Bar, 10 μ m.

Discussion

The current study implicates the medial amygdala as a possible relay station for chemosensory information to GnRH neurons.

Anterogradely labeled projections from the medial amygdala were found in close proximity to GnRH neurons in all subpopulations, with the largest proportion of close appositions to GnRH neurons in the cPOA. This is the first evidence of direct efferent projections from the amygdala to GnRH cells, providing an a potential pathway by which pheromonal stimuli from the female can reach the neuroendocrine system.

Although these data demonstrate an anatomical relationship between the medial amygdala and GnRH neurons, it remains to be determined whether there is a synaptic relationship between medial amygdala and GnRH neurons. Electron microscopy is one approach that could help establish evidence of a synaptic relationship between amygdala projections and GnRH neurons. Electron microscopic studies have reported a relatively small number of synaptic inputs onto GnRH cell bodies (Witkin and Silverman, 1985; Lehman *et al.*, 1988). However, due to the scattered distribution of GnRH neurons and technical difficulties in fixing tissue for visualization of GnRH

immunoreactivity at both the light and electron microscopic levels (Witkin, 1999), only a small number of neurons (e.g., 2 cells/brain, Lehman *et al.*, 1988) have been analyzed to generate these data. Studies using confocal microscopy coupled with synaptophysin labeling to investigate synaptic input to GnRH cells, which allows for the analysis of more GnRH neurons per brain, have reported higher estimates of synaptic input to GnRH cells (Rajendren and Gibson, 2001; Dudas and Merchenthaler, 2001; Rajendren and Li, 2001). Future investigations using confocal microscopy to estimate synaptic input from the medial amygdala to GnRH neurons would provide further anatomical support for communication between this region of the brain and the GnRH system.

The fact that BDA close appositions were most prevalently found on cPOA GnRH neurons compared with other GnRH subpopulations raises the possibility that these cells are particularly more responsive to chemosensory stimuli. With such a small amount of information known about how pheromones influence GnRH cells, it is of particular interest that electrical stimulation to the vomeronasal organ (Meredith and Fewell, 2001) elicits expression of Fos, used as an index of neuronal activation, in GnRH neurons only in the cPOA. The importance of the

medial amygdala in chemosensory processing (Fiber *et al.*, 1993;Fiber *et al.*, 1996;Kollack-Walker *et al.*, 1997;Swann *et al.*, 1997;Romeo *et al.*, 1998) and the fact that these cells project to GnRH neurons predominantly in the cPOA, the GnRH subpopulation activated by vomeronasal organ stimulation (Meredith *et al.*, 2001), supports the hypothesis that pheromones influence the neuroendocrine system through this pathway.

The medial amygdala is comprised of cells of various phenotypes, including cells that make substance P (Swann and Newman, 1992) and steroid receptors (Wood, Brabec, Swann, and Newman, 1992;Coolen *et al.*, 1998). In addition to chemosensory information, projections to the GnRH system may be relaying other information. Perhaps the amygdalar projections to some of the GnRH cells are coming from androgen or estrogen receptor expressing cells. Since steroid action upon GnRH cells is most likely indirect (Herbison, Robinson, and Skinner, 1993;Herbison, Horvath, Naftolin, and Leranth, 1995), these cells might serve as indirect means by which steroid could negatively feedback upon GnRH mRNA. Information from smaller, more defined injections, combined with steroid-receptor immunocytochemistry could help clarify this issue.

In addition to projections from cells in the medial amygdala to GnRH neurons, close appositions from GnRH fibers were also found on GnRH neurons. The proportion of GnRH-GnRH cells was greatest in the tenia tecta and MS. Within the tenia tecta and MS GnRH cells frequently had many appositions from GnRH fibers. GnRH cell bodies also found closely apposed to one another in these same populations. These findings correspond well with the fact that these cells appear different from other populations (especially the DBB/OVLT and cPOA cells), in that they appear close together and ensconced in a bed of fibers (Chapter 2). This experiment does not establish the origin of the GnRH fibers apposing GnRH neurons or whether these appositions contain synapses, but the findings strongly suggest some form of communication within the GnRH system. An interesting possibility is that there could be gap junctions between GnRH fibers and cell bodies and between cell bodies that are closely apposed to one another. Gap junctions have been identified in the GnRH immortalized cell line, GT-1 cells, and shown to important for synchronized pulsatile activity of these cells (Witkin, 1999; Terasawa, 2001; Funabashi, Suyama, Uemura, Hirose, Hirahara, and Kimura, 2001; Vazquez-Martinez, Shorte, Boockfor, and Frawley, 2001). In addition, GnRH cell bodies have been

shown to form an intercellular bridge (Witkin, 1999). Perhaps both synaptic and non-synaptic mechanisms underly communication within the GnRH system, and this allows cells to be coordinated together and send meaningful signals to the pituitary gland.

In summary, these data provide evidence of direct projections from the medial amygdala to GnRH neurons. Cells within the cPOA had a large proportion of BDA appositions. The data indicate possible pathway by which chemosensory information can reach the GnRH system to influence release and that GnRH–GnRH communication varies depending on the brain region. Future work with more refined injections and immunocytochemical identification of the various medial amygdala cellular pheontypes could reveal whether the same population of medial amygdala neurons are projecting to GnRH neurons in the tenia tecta, MS, DBB/OVLT, and cPOA.

CHAPTER 7: GENERAL DISCUSSION

The overall goal of this dissertation research was to gain a better understanding of how a unique and important set of peptidergic neurons are organized within the brain to respond to various internal and external stimuli. GnRH cells govern the entire reproductive system through their regulation of the hypothalamic pituitary gonadal (HPG) axis. While their contribution to biological function is greatly appreciated, it is largely unknown how these cells operate to respond to and integrate variables that determine reproductive function. The wide-spread distribution of such a small number of neurons has impeded a full understanding this system.

Experiments in this dissertation demonstrated that the anatomical location of GnRH cells relates to how these cells are regulated by internal and external stimuli, and following pubertal maturation. These findings are summarized along with other work in our lab (Parfitt *et al.*, 1999) in Table 5 and Fig 33. Data presented throughout the dissertation provide evidence for heterogeneity within the GnRH system in male Syrian hamsters in response to different

Table 5. Summarized data from the experiments described in this dissertation and in Parfitt, Thompson, Richardson, Romeo, and Sisk, 1999, 1999, asterisks). Arrows indicate the direction of change in GnRH protein or mRNA (\leftrightarrow represents no change). Checks indicate appositions from the medial amygdala or GnRH fibers onto GnRH neurons. A higher number of checks reflects a higher proportion of appositions.

	Detectable cell number				GnRH mRNA				Appositions onto GnRH neurons			
	puberty	puberty	puberty	n/a	puberty	puberty	puberty	puberty	testosterone	pheromone	medial amygdala	GnRH
TT				n/a	\uparrow	\downarrow	\leftrightarrow	\leftrightarrow	\downarrow	\leftrightarrow	\checkmark	$\checkmark\checkmark$
MS	\downarrow				\uparrow^*	\downarrow	\leftrightarrow	\leftrightarrow	\downarrow	\leftrightarrow	\checkmark	$\checkmark\checkmark$
DBB/OVLT	\downarrow				\uparrow^*	\leftrightarrow	\leftrightarrow	\leftrightarrow	\leftrightarrow	\leftrightarrow	\checkmark	\checkmark
cPOA	\leftrightarrow				\uparrow^*	\leftrightarrow	\leftrightarrow	\leftrightarrow	\leftrightarrow	\leftrightarrow	$\checkmark\checkmark$	\checkmark

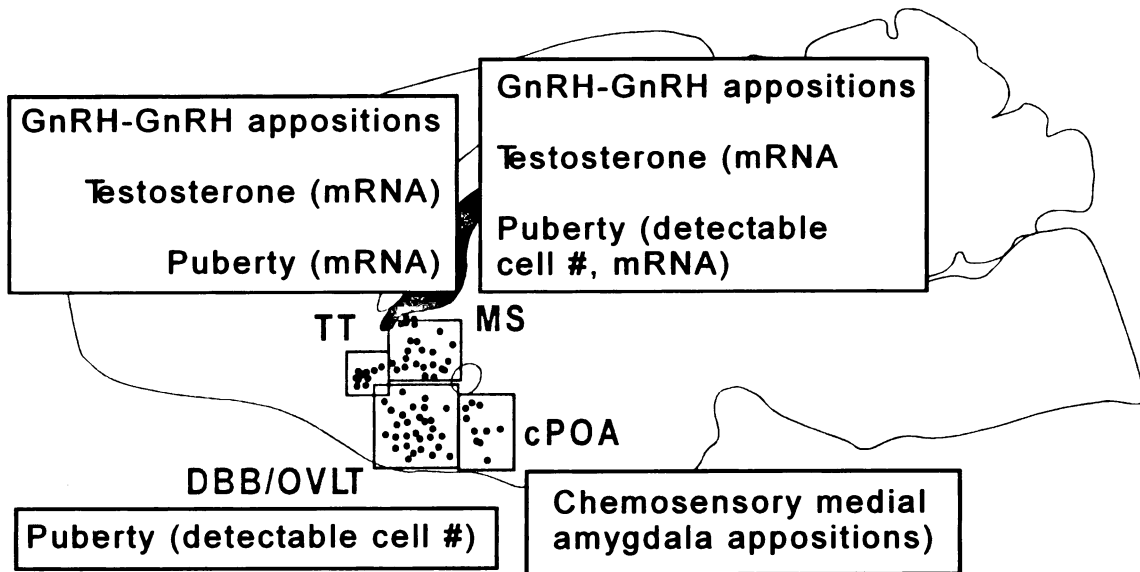


Figure 33. Drawing of a sagittal view of the Syrian hamster (adapted from Morin *et al.*, 2001) brain summarizing differences in pubertal, testosterone, or chemosensory regulation of GnRH protein (detectable cell #), GnRH mRNA in, or neuronal projections (appositions) to the various GnRH subpopulations.

factors, a finding that corresponds well with other reports (Shivers *et al.*, 1983; King *et al.*, 1987; Berriman *et al.*, 1992; Ronchi *et al.*, 1992a; Rubin *et al.*, 1994; I'Anson *et al.*, 1997; Tang *et al.*, 1997).

There is variation among the four forebrain GnRH populations, tenia tecta, MS, DBB/OVLT, and cPOA, under different developmental states (before and after puberty), and in response to an strong internal stimulus (testosterone). Furthermore, there is anatomical evidence for subpopulation differences in potential communication within the GnRH system and between other non-GnRH neurons within the medial amygdala and the GnRH system. Thus, function and regulation of GnRH neurons may be related to the location within the brain because neuronal input to GnRH cells varies with location.

Rostral populations of GnRH neurons appear to play an important role in puberty. There is a reduction in detectable cell number in the DBB/OVLT and MS, which is thought to reflect increased GnRH release from these cells. Furthermore, there is a pubertal increase in GnRH mRNA in the tenia tecta and MS, which may also be related to GnRH release. Because the tenia tecta GnRH subpopulation was not analyzed as a separate population from the MS and DBB/OVLT in first study, it is not clear whether pubertal changes in detectable cell number also

occurs in tenia tecta neurons, or if some of these cells contributed to the changes shown in the MS and DBB/OVLT. Consequently, comparisons between pubertal changes in GnRH protein and mRNA are limited because analyses of GnRH subpopulations were different in these two studies. Nevertheless, assuming there is some overlap between GnRH cell groups that show pubertal changes in GnRH protein (presumed to be reflecting increased release) and mRNA, an important question to ask is whether the pubertal rise in GnRH mRNA precedes the increased release of the peptide at puberty.

The relationship between GnRH synthesis and release is not well understood. Explant cultures of neonatal hypothalamic slices have been used to investigate regulation of GnRH mRNA (Maurer and Wray, 1997). Under these *in vitro* conditions, GnRH neurons have the most rapid mRNA turnover rate ($t_{1/2}$, 5-13 min) reported for neuropeptides. The decay of mRNA corresponds well, temporally, with the descending portion of GnRH secretory episodes measured *in vivo* (Levine and Ramirez, 1980; Levine *et al.*, 1982; Dluzen and Ramirez, 1987), which argues for a tight coupling between GnRH synthesis and release. If these *in vitro* GnRH mRNA findings generalize to GnRH neurons *in vivo*, increased synthesis of GnRH might precede increased levels of secreted

hormone at puberty. However, it is also possible that the primary event associated with puberty is activation of GnRH release, which leads secondarily to an increase in GnRH synthesis as the demand for releasable hormone goes up. Thus, if there is a causal relationship between increases in GnRH mRNA and GnRH release at puberty, the causal direction is presently not known.

The role steroids play in increased activity of the GnRH at puberty depends on the species. While the pubertal increase in GnRH release in primates occurs in the absence of steroid negative feedback (Terasawa *et al.*, 2001), the pubertal increase in GnRH mRNA in ferrets seems to involve changes in steroid negative feedback of the GnRH system (Tang *et al.*, 1997). Data presented in this dissertation provide evidence in against a relationship between sensitivity to steroids and pubertal changes in GnRH mRNA in male Syrian hamsters. Pubertal maturation resulted in higher levels of GnRH mRNA in the tenia tecta and MS (Chapter 4). In the absence of steroids adults had over two-fold higher levels of GnRH mRNA and adults were *more*, not *less*, sensitive to testosterone negative feedback upon GnRH mRNA. Thus, while the pubertal increase in GnRH mRNA might be due to increased excitatory (Petersen, McCrone, Keller, and Gardner, 1991; Gore *et al.*, 1994) or

decreased inhibitory (Sim, Skynner, Pape, and Herbison, 2000) tone upon cells within the tenia tecta and MS, steroids are clearly not driving this process. This is different from the pubertal increase in gonadotropin release, which involves a change in steroid negative feedback (Chapter 4; Sisk *et al.*, 1983a). When steroid negative feedback is removed, plasma LH is equivalent in adults and juveniles (Chapter 4). However, in the presence of the same dose of testosterone, plasma LH is suppressed in juveniles, but not adults (Chapter 4; Sisk *et al.*, 1983a). Therefore, steroids are involved in the rise in gonadotropins at puberty. While GnRH mRNA and plasma LH undergo changes in response to puberty and testosterone, these two components of the HPG axis do not appear to be related to one another. Instead, the developmental shift in the set point of negative feedback regulation of gonadotropin secretion may permit increased activity of the GnRH system at puberty, an event that is occurring simultaneously, but possibly through unrelated, steroid-independent mechanisms.

A dissociation between GnRH mRNA and plasma LH was also demonstrated in Chapter 5. GnRH mRNA does not appear to be regulated by chemosensory stimuli. Exposure to female pheromones elicited an increase in plasma LH, but this was not accompanied by in

changes in GnRH mRNA. Thus, while pheromones ostensibly stimulate GnRH release (as indexed by plasma LH release), this release is either not great enough to result in measurable changes in GnRH mRNA using *in situ* hybridization histochemistry, or message levels are changing earlier than 60 min after exposure. However, a recent report on mice demonstrated that GnRH mRNA does not change in response to pheromones even when measured 45 min after exposure using the highly sensitive technique, RNase protection assay to measure GnRH mRNA, arguing against pheromone-induced changes in GnRH mRNA.

Given that regulation of GnRH depends on where cells reside in the forebrain, it is important to ask how GnRH subpopulations differ from one another. GnRH neuronal phenotype and afferents vary with brain region, a phenomenon that has also been demonstrated other species (Hoffman *et al.*, 1990;Wu *et al.*, 1992;Mitchell *et al.*, 1999;Prevot *et al.*, 2000). Anatomical investigations in this dissertation suggest that neuronal input from GnRH and non-GnRH neurons also varies with brain region. The cPOA GnRH subpopulation had the highest proportion of GnRH cells with close appositions of processes coming from cells in the medial amygdala, an area important for chemosensory processing (Fiber *et al.*, 1993;Fiber *et al.*,

1996;Kollack-Walker *et al.*, 1997;Swann *et al.*, 1997;Romeo *et al.*, 1998). GnRH neurons in the cPOA also express the immediate early gene protein product Fos in response to electrical stimulation of the vomeronasal organ (Meredith *et al.*, 2001). Taken together, these studies suggest that medial amygdala projections to GnRH neurons in the cPOA is one possible pathway by which chemosensory information can reach the neuroendocrine system. Since cells within many subdivisions of the medial amygdala are rich with steroid receptors (Wood *et al.*, 1992;Coolen *et al.*, 1998), it is also conceivable that steroid negative feedback regulation of GnRH might occur through action upon cells within the medial amygdala that project to GnRH neurons.

In addition to input from other neuronal phenotypes, GnRH cells also receive information from GnRH cells. Communication within the system is one mechanism by which neuronal activity can be synchronized, an event necessary for relaying a meaningful peptidergic signal to the pituitary gland (Witkin, 1999). GnRH-GnRH communication may be occurring by synaptic and non-synaptic contact between GnRH cells and fibers (Witkin, 1999). Gap junctions have been identified in the GnRH immortalized cell line, GT-1 cells, and

shown to important for synchronized pulsatile activity of these cells (Witkin, 1999;Terasawa, 2001;Funabashi *et al.*, 2001;Vazquez-Martinez *et al.*, 2001). In addition, GnRH cell bodies have been shown to form an intercellular bridge (Witkin, 1999), another mechanism by which neuronal activity could be synchronized. Since the greatest proportion of GnRH neurons with close appositions from GnRH processes was found in the tenia tecta and MS, and several GnRH cell bodies were found to be closely apposed to one another in these same cell groups, it is conceivable that synaptic or non-synaptic communication within tenia tecta and MS GnRH cells allows for synchronous activity of GnRH release and this drives the pubertal rise in gonadotropin release.

In summary, the work presented in this dissertation and elsewhere (Shivers *et al.*, 1983;King *et al.*, 1987;Berriman *et al.*, 1992;Tang *et al.*, 1992;Ronchi *et al.*, 1992a;Rubin *et al.*, 1994;I'Anson *et al.*, 1997;Tang *et al.*, 1997) conveys an overall theme about the GnRH neuronal system. GnRH cells should not simply be considered together as a single homogeneous entity, but instead as a complex neuronal system comprised of separate cell groups whose responsiveness to various stimuli depends on where they reside within

the brain. Function and regulation could differ because of variation in neuronal input to and receptor expression within different populations of GnRH neurons. In addition, the types of connections between GnRH neurons of a subpopulation (i.e., synaptic connection, gap junction, or bridge-like intercellular connections) likely affects how that cell group responds to internal or external stimuli. Future investigations of these potential differences in GnRH subpopulations would enhance our understanding of how cells that are scattered so far apart could communicate within and across a subpopulation to synchronize activity and regulated reproductive status.

REFERENCES

1. Abbud, R. and Smith, M. S. (1995). Do GnRH neurons express the gene for the NMDA receptor? *Brain Res.* **690**, 117-120.
2. Angelucci, A., Clasca, F., and Sur, M. (1996). Anterograde axonal tracing with the subunit B of cholera toxin: a highly sensitive immunohistochemical protocol for revealing fine axonal morphology in adult and neonatal brains. *J. Neurosci. Methods* **65**, 101-112.
3. Berglund, L. A. and Sisk, C. L. (1990). Pituitary responsiveness to luteinizing hormone-releasing hormone in prepubertal and postpubertal male ferrets. *Biol. Reprod.* **43**, 335-339.
4. Bernard, D. J., Abuav-Nussbaum, R., Horton, T. H., and Turek, F. W. (1999). Photoperiodic effects on gonadotropin-releasing hormone (GnRH) content and the GnRH-immunoreactive neuronal system of male Siberian hamsters. *Biology of Reproduction* **60**, 272-276.
5. Berriman, S. J., Wade, G. N., and Blaustein, J. D. (1992). Expression of Fos-like proteins in gonadotropin-releasing hormone neurons of Syrian hamsters: effects of estrous cycles and metabolic fuels. *Endocrinology* **131**, 2222-2228.
6. Coolen, L. and Wood, R. (1998). Bidirectional connections of the

medial amygdaloid nucleus in the Syrian hamster brain: simultaneous anterograde and retrograde tract tracing. *Journal of Comparative Neurology* **399**, 189-209.

7. Coquelin, A., Clancy, A. N., Macrides, F., Noble, E. P., and Gorski, R. A. (1984). Pheromonally induced release of luteinizing hormone in male mice: involvement of the vomeronasal system. *J. Neurosci.* **4**, 2230-2236.

8. Daikoku-Ishido, H., Okamura, Y., Yanaihara, N., and Daikoku, S. (1990). Development of the hypothalamic luteinizing hormone-releasing hormone-containing neuron system in the rat: *In vivo* and transplantation studies. *Developmental Biology* **140**, 374-387.

9. Dellovade, T. L., Hunter, E., and Rissman, E. F. (1995a). Interactions with males promote rapid changes in gonadotropin-releasing hormone immunoreactive cells. *Neuroendocrinology* **62**, 385-395.

10. Dellovade, T. L., Ottinger, M. A., and Rissman, E. F. (1995b). Mating alters gonadotropin-releasing hormone cell number and content. *Endocrinology* **136**, 1648-1657.

11. Dellovade, T. L. and Rissman, E. F. (1994). Gonadotropin-releasing hormone-immunoreactive cell numbers change in response to

social interactions. *Endocrinology* **134**, 2189-2197.

12. Dluzen, D. E. and Ramirez, V. D. (1987). In vivo activity of the LHRH pulse generator as determined with push- pull perfusion of the anterior pituitary gland of unrestrained intact and castrate male rats. *Neuroendocrinology* **45**, 328-332.

13. Doan, A. and Urbanski, H. F. (1994). Diurnal expression of Fos in luteinizing hormone-releasing hormone neurons of Syrian hamsters. *Biol. Reprod.* **50**, 301-308.

14. Dudas, B. and Merchenthaler, I. (2001). Catecholaminergic axons innervate LH-releasing hormone immunoreactive neurons of the human diencephalon. *J. Clin. Endocrinol. Metab* **86**, 5620-5626.

15. Fernandez-Fewell, G. D. and Meredith, M. (1995). Facilitation of mating behavior in male hamsters by LHRH and AcLHRH5- 10: interaction with the vomeronasal system. *Physiol Behav.* **57**, 213-221.

16. Fiber, J. M., Adames, P., and Swann, J. M. (1993). Pheromones induce c-fos in limbic areas regulating male hamster mating behavior. *NeuroReport* **4**, 871-874.

17. Fiber, J. M. and Swann, J. M. (1996). Testosterone differentially influences sex-specific pheromone- stimulated Fos expression in limbic regions of Syrian hamsters. *Horm. Behav.* **30**, 455-473.

18. Foster, C. M., Hassing, J. M., Mendes, T. M., Hale, P. M., Padmanabhan, V., Hopwood, N. J., Beitins, I. Z., Marshall, J. C., and Kelch, R. P. (1989). Testosterone infusion reduces nocturnal luteinizing hormone pulse frequency in pubertal boys. *J. Clin. Endocrinol. Metab* **69**, 1213-1220.
19. Foster, D. L. (1994). Puberty in the sheep. In E. Knobil and J. D. Neill (Eds.), *The Physiology of Reproduction*, Vol. 2, pp. 411-451. Raven Press, New York.
20. Foster, D. L. and Olster, D. H. (1985). Effect of restricted nutrition on puberty in the lamb: patterns of tonic LH secretion and competency of the LH surge system. *Endocrinology* **116**, 375-381.
21. Freeman, M. E. (1994). The neuroendocrine control of the ovarian cycle of the rat. In E. Knobil and J. D. Neill (Eds.), *The Physiology of Reproduction*, Vol. 2, pp. 613-658. Raven Press, New York.
22. Funabashi, T., Suyama, K., Uemura, T., Hirose, M., Hirahara, F., and Kimura, F. (2001). Immortalized gonadotropin-releasing hormone neurons (GT1-7 cells) exhibit synchronous bursts of action potentials. *Neuroendocrinology* **73**, 157-165.
23. Gibson, M. J., Krieger, D. T., Charlton, H. M., Zimmerman, E. A., Silverman, A. J., and Perlow, M. J. (1984). Mating and pregnancy can

occur in genetically hypogonadal mice with preoptic area brain grafts. *Science* **225**, 949-951.

24. Gillespie, C. F., van der Beek, E. M., Mintz, E. M., Mickley, N. C., Jasnow, A. M., Huhman, K. L., and Albers, H. E. (1999). GABAergic regulation of light-induced c-Fos immunoreactivity within the suprachiasmatic nucleus. *J. Comp Neurol.* **411**, 683-692.

25. Gomez, D. M. and Newman, S. W. (1992). Differential projections of the anterior and posterior regions of the medial amygdaloid nucleus in the Syrian hamster. *J. Comp Neurol.* **317**, 195-218.

26. Gore, A. C. and Roberts, J. L. (1994). Regulation of gonadotropin-releasing hormone gene expression by the excitatory amino acids kainic acid and N-methyl-D,L-aspartate in the male rat. *Endocrinology* **134**, 2026-2031.

27. Gore, A. C., Wersinger, S. R., and Rissman, E. F. (2000). Effects of female pheromones on gonadotropin-releasing hormone gene expression and luteinizing hormone release in male wild-type and oestrogen receptor-alpha knockout mice. *J. Neuroendocrinol.* **12**, 1200-1204.

28. Gore, A. C., Wu, T. J., Rosenberg, J. J., and Roberts, J. L. (1996). Gonadotropin-releasing hormone and NMDA receptor gene expression

and colocalization change during puberty in female rats. *J. Neurosci.* **16**, 5281-5289.

29. Graham, J. M. and Desjardins, C. (1980). Classical conditioning: induction of luteinizing hormone and testosterone secretion in anticipation of sexual activity. *Science* **210**, 1039-1041.

30. Gupta, D., Rager, K., Zarzycki, J., and Eichner, M. (1975). Levels of luteinizing hormone, follicle-stimulating hormone, testosterone and dihydrotestosterone in the circulation of sexually maturing intact male rats and after orchidectomy and experimental bilateral cryptorchidism. *J. Endocrinol.* **66**, 183-193.

31. Herbison, A. E., Horvath, T. L., Naftolin, F., and Leranth, C. (1995). Distribution of estrogen receptor-immunoreactive cells in monkey hypothalamus: relationship to neurones containing luteinizing hormone-releasing hormone and tyrosine hydroxylase. *Neuroendocrinology* **61**, 1-10.

32. Herbison, A. E., Robinson, J. E., and Skinner, D. C. (1993). Distribution of estrogen receptor-immunoreactive cells in the preoptic area of the ewe: co-localization with glutamic acid decarboxylase but not luteinizing hormone-releasing hormone. *Neuroendocrinology* **57**, 751-759.

33. Hoffman, G. E., Lee, W. S., Attardi, B., Yann, V., and Fitzsimmons, M. D. (1990). Luteinizing hormone-releasing hormone neurons express c-fos antigen after steroid activation. *Endocrinology* **126**, 1736-1741.
34. I'Anson, H., Terry, S. K., Lehman, M. N., and Foster, D. L. (1997). Regional differences in the distribution of gonadotropin-releasing hormone cells between rapidly growing and growth-restricted prepubertal female sheep. *Endocrinology* **138**, 230-236.
35. Jacob, S., Hayreh, D. J., and McClintock, M. K. (2001). Context-dependent effects of steroid chemosignals on human physiology and mood. *Physiol Behav.* **74**, 15-27.
36. Jakubowski, M., Blum, M., and Roberts, J. L. (1991). Postnatal development of gonadotropin-releasing hormone and cyclophilin gene expression in the female and male rat brain. *Endocrinology* **128**, 2702-2708.
37. Jakubowski, M. and Roberts, J. L. (1992). Multiplex Solution Hybridization-Ribonuclease Protection Assay for Quantitation of Different Ribonucleic Acid Transcripts from Snap-Frozen Neuroendocrine Tissues of Individual Animals. *Journal of Neuroendocrinology* **4**, 79-89.
38. Jennes, L. and Stumpf, W. E. (1980). LHRH-systems in the brain

of the golden hamster. *Cell Tissue Res.* **209**, 239-256.

39. Kalra, S. P. and Kalra, P. S. (1989). Do testosterone and estradiol-17 beta enforce inhibition or stimulation of luteinizing hormone-releasing hormone secretion? *Biol. Reprod.* **41**, 559-570.

40. Kevetter, G. A. and Winans, S. S. (1981). Connections of the corticomедial amygdala in the golden hamster. I. Efferents of the "vomeronasal amygdala". *Journal of Comparative Neurology* **197**, 81-98.

41. King, J. C., Kugel, G., Zahniser, D., Woolledge, K., Damassa, D. A., and Alexsavich, B. (1987). Changes in populations of LHRH-immunopositive cell bodies following gonadectomy. *Peptides* **8**, 721-725.

42. Kollack-Walker, S. and Newman, S. W. (1997). Mating-induced expression of c-fos in the male Syrian hamster brain: role of experience, pheromones and ejaculations. *Journal of Neurobiology* **32**, 481-501.

43. Lanciego, J. L., Luquin, M. R., Guillen, J., and Gimenez-Amaya, J. M. (1998). Multiple neuroanatomical tracing in primates. *Brain Res. Brain Res. Protoc.* **2**, 323-332.

44. Lehman, M. N., Goodman, R. L., Karsch, F. J., Jackson, G. L.,

Berriman, S. J., and Jansen, H. T. (1997). The GnRH system of seasonal breeders: anatomy and plasticity. *Brain Res. Bull.* **44**, 445-457.

45. Lehman, M. N. and Silverman, A. J. (1988). Ultrastructure of luteinizing hormone-releasing hormone (LHRH) neurons and their projections in the golden hamster. *Brain Res. Bull.* **20**, 211-221.

46. Levine, J. E., Bauer-Dantoin, A. C., Besecke, L. M., Conaghan, L. A., Legan, S. J., Meredith, J. M., Strobl, F. J., Urban, J. H., Vogelsong, K. M., and Wolfe, A. M. (1991). Neuroendocrine regulation of the luteinizing hormone-releasing hormone pulse generator in the rat. *Recent Prog. Horm. Res.* **47**, 97-151.

47. Levine, J. E. and Ramirez, V. D. (1980). In vivo release of luteinizing hormone-releasing hormone estimated with push-pull cannulae from the mediobasal hypothalami of ovariectomized, steroid-primed rats. *Endocrinology* **107**, 1782-1790.

48. Levine, J. E. and Ramirez, V. D. (1982). Luteinizing hormone-releasing hormone release during the rat estrous cycle and after ovariectomy, as estimated with push-pull cannulae. *Endocrinology* **111**, 1439-1448.

49. Macrides, F., Bartke, A., Fernandez, F., and D'Angelo, W. (1974).

Effects of exposure to vaginal odor and receptive females on plasma testosterone in the male hamster. *Neuroendocrinology* **15**, 355-364.

50. Malik, K. F., Silverman, A. J., and Morrell, J. I. (1991).

Gonadotropin-releasing hormone mRNA in the rat: distribution and neuronal content over the estrous cycle and after castration of males. *Anat. Rec.* **231**, 457-466.

51. Maragos, W. F., Newman, S. W., Lehman, M. N., and Powers, J. B.

(1989). Neurons of origin and fiber trajectory of amygdalofugal projections to the medial preoptic area in Syrian hamsters. *J. Comp Neurol.* **280**, 59-71.

52. Maurer, J. A. and Wray, S. (1997). Luteinizing hormone-releasing

hormone (LHRH) neurons maintained in hypothalamic slice explant cultures exhibit a rapid LHRH mRNA turnover rate. *J. Neurosci.* **17**, 9481-9491.

53. Meek, L. R., Romeo, R. D., Novak, C. M., and Sisk, C. L. (1997).

Actions of testosterone in prepubertal and postpubertal male hamsters: dissociation of effects on reproductive behavior and brain androgen receptor immunoreactivity. *Horm. Behav.* **31**, 75-88.

54. Meredith, M. (1991). Sensory processing in the main and

accessory olfactory systems: comparisons and contrasts. *Journal of*

Steroid Biochemistry and Molecular Biology **39**, 601-614.

55. Meredith, M. (1998). Vomeronasal, olfactory, hormonal convergence in the brain. Cooperation or coincidence? *Ann. N. Y. Acad. Sci.* **855**, 349-361.

56. Meredith, M. and Fewell, G. (2001). Vomeronasal organ: electrical stimulation activates Fos in mating pathways and in GnRH neurons. *Brain Res.* **922**, 87-94.

57. Meredith, M. and Howard, G. (1992). Intracerebroventricular LHRH relieves behavioral deficits due to vomeronasal organ removal. *Brain Res. Bull.* **29**, 75-79.

58. Mitchell, V., Bouret, S., Prevot, V., Jennes, L., and Beauvillain, J. C. (1999). Evidence for expression of galanin receptor Gal-R1 mRNA in certain gonadotropin releasing hormone neurones of the rostral preoptic area. *J. Neuroendocrinol.* **11**, 805-812.

59. Morgan, J. I. and Curran, T. (1991). Stimulus-transcription coupling in the nervous system: Involvement of the inducible proto-oncogenes *fos* and *jun*. *Annual Review of Neuroscience* **14**, 421-451.

60. Morin, L. P. and Wood, R. I. (2001). *Hamster atlas: a stereotaxic atlas of the golden hamster brain*. Academic Press, Inc, San Diego.

61. Ojeda, S. R. and Urbanski, H. F. (1994). Puberty in the rat. In E. Knobil and J. D. Neill (Eds.), *The Physiology of Reproduction*, Vol. 2, pp. 452-485. Raven Press, New York.
62. Parfitt, D. B., Thompson, R. C., Richardson, H. N., Romeo, R. D., and Sisk, C. L. (1999). GnRH mRNA increases with puberty in the male Syrian hamster brain. *J. Neuroendocrinol.* **11**, 621-627.
63. Park, Y., Park, S. D., Cho, W. K., and Kim, K. (1988). Testosterone stimulates LH-RH-like mRNA level in the rat hypothalamus. *Brain Res.* **451**, 255-260.
64. Petersen, S. L., McCrone, S., Keller, M., and Gardner, E. (1991). Rapid increase in LHRH mRNA levels following NMDA. *Endocrinology* **129**, 1679-1681.
65. Petersen, S. L., McCrone, S., Keller, M., and Shores, S. (1995). Effects of estrogen and progesterone on luteinizing hormone-releasing hormone messenger ribonucleic acid levels: consideration of temporal and neuroanatomical variables. *Endocrinology* **136**, 3604-3610.
66. Pfeiffer, C. A. and Johnston, R. E. (1992). Socially stimulated androgen surges in male hamsters: the roles of vaginal secretions, behavioral interactions, and housing conditions. *Horm. Behav.* **26**, 283-293.

67. Pfeiffer, C. A. and Johnston, R. E. (1994). Hormonal and behavioral responses of males to females and female odors-roles of olfaction, the vomeronasal system, and sexual experience. *Physiology and Behavior* **55**, 129-138.
68. Plant, T. M. (1994). Puberty in primates. In E. Knobil and J. D. Neill (Eds.), *The Physiology of Reproduction*, Vol. 2, pp. 453-485. Raven Press, New York.
69. Porkka-Heiskanen, T., Khoshaba, N., Scarbrough, K., Urban, J. H., Vitaterna, M. H., Levine, J. E., Turek, F. W., and Horton, T. H. (1997). Rapid photoperiod-induced increase in detectable GnRH mRNA-containing cells in Siberian hamster. *Am. J. Physiol* **273**, R2032-R2039.
70. Porkka-Heiskanen, T., Urban, J. H., Turek, F. W., and Levine, J. E. (1994). Gene expression in a subpopulation of luteinizing hormone-releasing hormone (LHRH) neurons prior to the preovulatory gonadotropin surge. *J. Neurosci.* **14**, 5548-5558.
71. Prevot, V., Bouret, S., Croix, D., Takumi, T., Jennes, L., Mitchell, V., and Beauvillain, J. C. (2000). Evidence that members of the TGFbeta superfamily play a role in regulation of the GnRH neuroendocrine axis: expression of a type I serine-threonine kinase receptor for TGRbeta and activin in GnRH neurones and hypothalamic

areas of the female rat. *J. Neuroendocrinol.* **12**, 665-670.

72. Rajendren, G. and Gibson, M. J. (2001). A confocal microscopic study of synaptic inputs to gonadotropin-releasing hormone cells in mouse brain: regional differences and enhancement by estrogen. *Neuroendocrinology* **73**, 84-90.

73. Rajendren, G. and Li, X. (2001). Galanin synaptic input to gonadotropin-releasing hormone perikarya in juvenile and adult female mice: implications for sexual maturity. *Brain Res. Dev. Brain Res.* **131**, 161-165.

74. Richardson, H. N., Parfitt, D. B., Thompson, J. T., and Sisk, C. L. Redefining gonadotropin releasing hormone (GnRH) cell groups in the male syrian hamster: testosterone regulates GnRH mRNA in the tenia tecta. *J. Neuroendocrinol.* 2002.

Ref Type: In Press

75. Richardson, H. N., Romeo, R. D., and Sisk, C. L. (1999). Regional changes in GnRH immunoreactivity with puberty in the male Syrian hamster. *Brain Res.* **817**, 232-235.

76. Romeo, R. D., Cook-Wiens, E., Richardson, H. N., and Sisk, C. L. (2001). Dihydrotestosterone activates sexual behavior in adult male hamsters but not in juveniles. *Physiol Behav.* **73**, 579-584.

77. Romeo, R. D., Parfitt, D. B., Richardson, H. N., and Sisk, C. L. (1998). Pheromones elicit equivalent levels of Fos-immunoreactivity in prepubertal and adult male Syrian hamsters. *Horm. Behav.* **34**, 48-55.

78. Romeo, R. D., Richardson, H. N., and Sisk, C. L. Puberty and the maturation of the male brain and sexual behavior: a recasting of behavioral potentials. *Neuroscience and Biobehavioral Reviews* . 2002.
Ref Type: In Press

79. Ronchi, E., Aoki, C., Krey, L. C., and Pfaff, D. W. (1992a). Immunocytochemical study of GnRH and GnRH-associated peptide in male Syrian hamsters as a function of photoperiod and gonadal alterations. *Neuroendocrinology* **55**, 134-145.

80. Ronchi, E., Krey, L. C., and Pfaff, D. W. (1992b). Steady state analysis of hypothalamic GnRH mRNA levels in male Syrian hamsters: influences of photoperiod and androgen. *Neuroendocrinology* **55**, 146-155.

81. Ronnekleiv, O. K. and Resko, J. A. (1990). Ontogeny of gonadotropin-releasing hormone containing neurons in early fetal development of rhesus macaques. *Endocrinology* **126**, 498-511.

82. Rubin, B. S. and King, J. C. (1994). The number and distribution of detectable luteinizing hormone (LH)-releasing hormone cell bodies

changes in association with the preovulatory LH surge in the brains of young but not middle-aged female rats. *Endocrinology* **134**, 467-474.

83. Rugarli, E. I. (1999). Kallmann syndrome and the link between olfactory and reproductive development. *Am. J. Hum. Genet.* **65**, 943-948.

84. Schwanzel-Fukuda, M. and Pfaff, D. W. (1989). Origin of luteinizing hormone-releasing hormone neurons. *Nature* **338**, 161-163.

85. Selmanoff, M., Shu, C., Petersen, S. L., Barraclough, C. A., and Zoeller, R. T. (1991). Single cell levels of hypothalamic messenger ribonucleic acid encoding luteinizing hormone-releasing hormone in intact, castrated, and hyperprolactinemic male rats. *Endocrinology* **128**, 459-466.

86. Shivers, B. D., Harlan, R. E., Morrel, J. I., and Pfaff, D. W. (1983). Immunocytochemical localization of luteinizing hormone-releasing hormone in male and female rat brains. *Neuroendocrinology* **36**, 1-12.

87. Silverman, A. J., Livne, I., and Witkin, J. W. (1994). The gonadotropin-releasing hormone (GnRH), neuronal systems: Immunocytochemistry and in situ hybridization. In E. Knobil and J. D. Neill (Eds.), *The Physiology of Reproduction*, Vol. 1, pp. 1683-1709.

Raven Press, New York.

88. Sim, J. A., Skynner, M. J., Pape, J. R., and Herbison, A. E. (2000). Late postnatal reorganization of GABA(A) receptor signalling in native GnRH neurons. *Eur. J. Neurosci.* **12**, 3497-3504.

89. Sisk, C. L. (1987). Evidence that a decrease in testosterone negative feedback mediates the pubertal increase in luteinizing hormone pulse frequency in male ferrets. *Biol. Reprod.* **37**, 73-81.

90. Sisk, C. L., Richardson, H. N., Chappell, P. E., and Levine, J. E. (2001). In vivo gonadotropin-releasing hormone secretion in female rats during peripubertal development and on proestrus. *Endocrinology* **142**, 2929-2936.

91. Sisk, C. L. and Turek, F. W. (1983a). Developmental time course of pubertal and photoperiodic changes in testosterone negative feedback on gonadotropin secretion in the golden hamster. *Endocrinology* **112**, 1208-1216.

92. Sisk, C. L. and Turek, F. W. (1983b). Gonadal growth and gonadal hormones do not participate in the development of responsiveness to photoperiod in the golden hamster. *Biol. Reprod.* **29**, 439-445.

93. Spratt, D. P. and Herbison, A. E. (1997). Regulation of preoptic area gonadotrophin-releasing hormone (GnRH) mRNA expression by

gonadal steroids in the long-term gonadectomized male rat. *Brain Res. Mol. Brain Res.* **47**, 125-133.

94. Swann, J. and Fiber, J. M. (1997). Sex differences in function of a pheromonally stimulated pathway: role of steroids and the main olfactory system. *Brain Res. Bull.* **44**, 409-413.

95. Swann, J. M. and Newman, S. W. (1992). Testosterone regulates substance P within neurons of the medial nucleus of the amygdala, the bed nucleus of the stria terminalis and the medial preoptic area of the male golden hamster. *Brain Res.* **590**, 18-28.

96. Tang, Y. P., Kashon, M. L., and Sisk, C. L. (1997). Brain region-specific regulation of luteinizing hormone-releasing hormone messenger ribonucleic acid in the male ferret: interactions between pubertal maturation and testosterone. *Endocrinology* **138**, 4740-4747.

97. Tang, Y. P. and Sisk, C. L. (1992). LHRH in the ferret: pubertal decrease in the number of immunopositive arcuate neurons. *Peptides* **13**, 241-247.

98. Terasawa, E. (2001). Luteinizing hormone-releasing hormone (LHRH) neurons: mechanism of pulsatile LHRH release. *Vitam. Horm.* **63**, 91-129.

99. Terasawa, E. and Fernandez, D. L. (2001). Neurobiological

mechanisms of the onset of puberty in primates. *Endocr. Rev.* **22**, 111-151.

100. Urbanski, H. F., Doan, A., and Pierce, M. (1991). Immunocytochemical investigation of luteinizing hormone-releasing hormone neurons in Syrian hamsters maintained under long or short days. *Biol. Reprod.* **44**, 687-692.
101. Urbanski, H. F., Doan, A., Pierce, M., Fahrenbach, W. H., and Collins, P. M. (1992). Maturation of the hypothalamo-pituitary-gonadal axis of male Syrian hamsters. *Biol. Reprod.* **46**, 991-996.
102. van der Beek, E. M., van Oudheusden, H. J., Buijs, R. M., van der Donk, H. A., Van den Hurk, R., and Wiegant, V. M. (1994). Preferential induction of c-fos immunoreactivity in vasoactive intestinal polypeptide-innervated gonadotropin-releasing hormone neurons during a steroid-induced luteinizing hormone surge in the female rat. *Endocrinology* **134**, 2636-2644.
103. Vazquez-Martinez, R., Shorte, S. L., Boockfor, F. R., and Frawley, L. S. (2001). Synchronized exocytotic bursts from gonadotropin-releasing hormone-expressing cells: dual control by intrinsic cellular pulsatility and gap junctional communication. *Endocrinology* **142**, 2095-2101.

104. Watanabe, G. and Terasawa, E. (1989). In vivo release of luteinizing hormone releasing hormone increases with puberty in the female rhesus monkey. *Endocrinology* **125**, 92-99.
105. Wiemann, J. N., Clifton, D. K., and Steiner, R. A. (1990). Gonadotropin-releasing hormone messenger ribonucleic acid levels are unaltered with changes in the gonadal hormone milieu of the adult male rat. *Endocrinology* **127**, 523-532.
106. Wirsig-Wiechmann, C. R. (1993). Nervus terminalis lesions: I. No effect on pheromonally induced testosterone surges in the male hamster. *Physiol Behav.* **53**, 251-255.
107. Witkin, J. W. (1999). Synchronized neuronal networks: the GnRH system. *Microsc. Res. Tech.* **44**, 11-18.
108. Witkin, J. W. and Silverman, A. J. (1985). Synaptology of luteinizing hormone-releasing hormone neurons in rat preoptic area. *Peptides* **6**, 263-271.
109. Wood, R. I., Brabec, R. K., Swann, J. M., and Newman, S. W. (1992). Androgen and estrogen concentrating neurons in chemosensory pathways of the male Syrian hamster brain. *Brain Res.* **596**, 89-98.
110. Wood, R. J. and Coolen, L. M. (1997). Integration of chemosensory and hormonal cues is essential for sexual behavior in the

male Syrian hamster: role of the medial amygdaloid nucleus.

Neuroscience **78**, 1027-1035.

111. Wray, S., Nieburgs, A., and Elkabes, S. (1989). Spatiotemporal cell expression of luteinizing hormone-releasing hormone in the prenatal mouse: evidence for an embryonic origin in the olfactory placode. *Brain Res. Dev. Brain Res.* **46**, 309-318.

112. Wray, S., Zoeller, R. T., and Gainer, H. (1989). Differential effects of estrogen on luteinizing hormone-releasing hormone gene expression in slice explant cultures prepared from specific rat forebrain regions. *Mol. Endocrinol.* **3**, 1197-1206.

113. Wu, T. J., Segal, A. Z., Miller, G. M., Gibson, M. J., and Silverman, A. J. (1992). FOS expression in gonadotropin-releasing hormone neurons: enhancement by steroid treatment and mating. *Endocrinology* **131**, 2045-2050.

114. Wysocki, C. J. and Lepri, J. J. (1991). Consequences of removing the vomeronasal organ. *J. Steroid Biochem. Mol. Biol.* **39**, 661-669.

MICHIGAN STATE UNIVERSITY LIBRARIES



3 1293 02334 2235